

中間質量ブラックホールからの重力波 GW from merging Intermediate-Mass BHs



真貝寿明 (大阪工業大)

[http://www.oit.ac.jp/~shinkai/](http://www.oit.ac.jp/is/~shinkai/)

Supermassive BHs

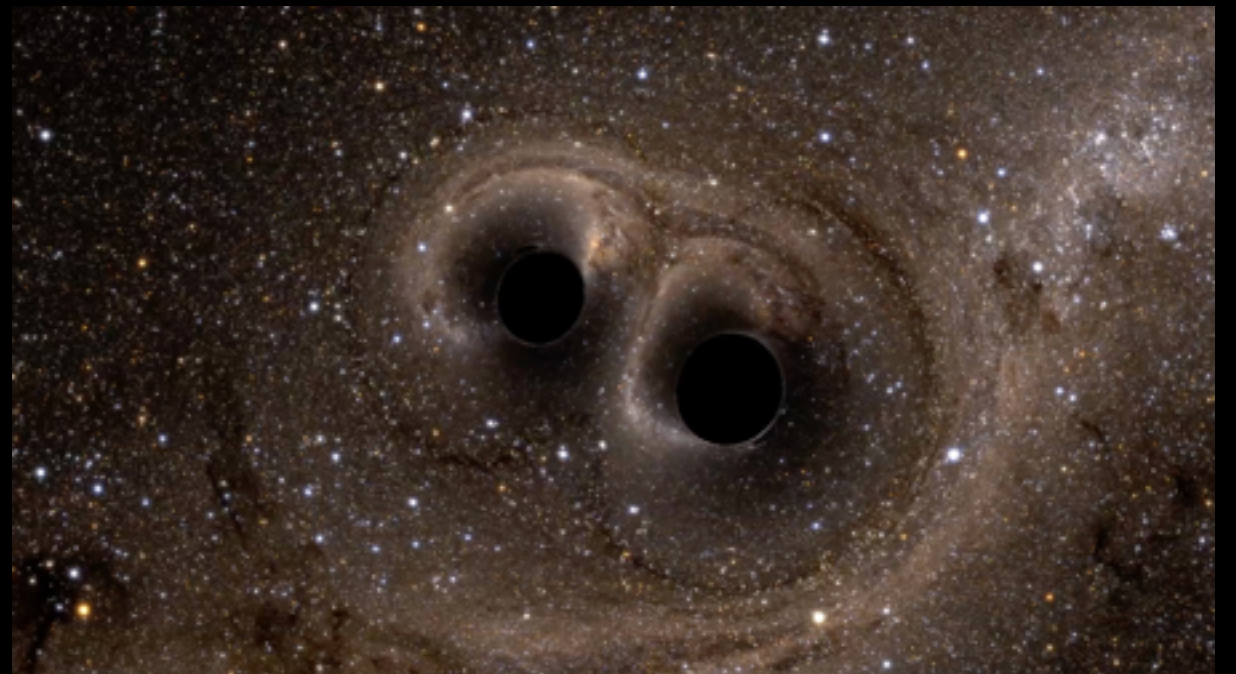
$$10^5 M_{\odot} \sim 10^{10} M_{\odot}$$

Intermediate-Mass BHs

$$10^2 M_{\odot} \sim 10^5 M_{\odot}$$

(Stellar-Mass) BHs

$$10 M_{\odot} \sim 100 M_{\odot}$$



真貝・神田・戎崎, ApJ, 835 (2017) 276 [arXiv:1610.09505]

contents

1. Gravitational Waves

Detectors, GW events

2. Models of SMBH

hierarchical growth model, or others

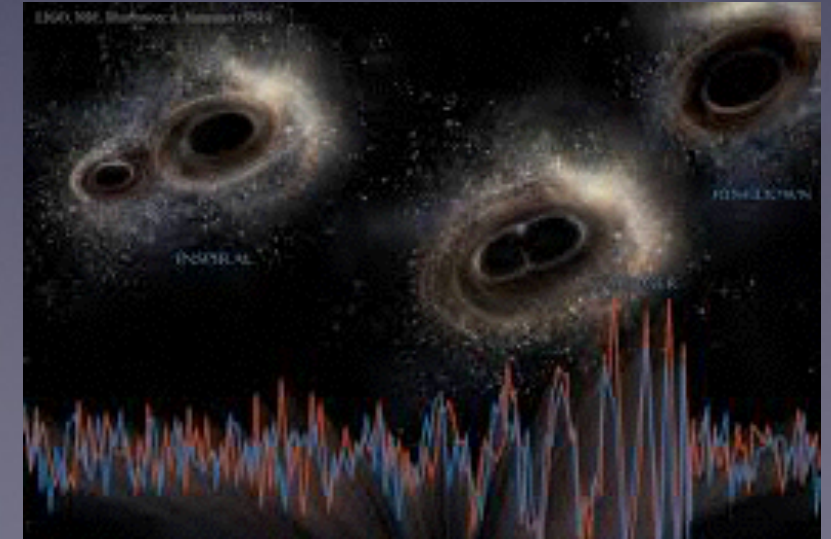
3. Counting BHs

How many BHs in a galaxy?

How many galaxies in the Universe?

4. Event Rates at aLIGO/KAGRA/DECIGO/LISA

How many BH mergers in the Universe?



contents

1. Gravitational Waves

Detectors, GW events

2. Models of SMBH

hierarchical growth model, or others

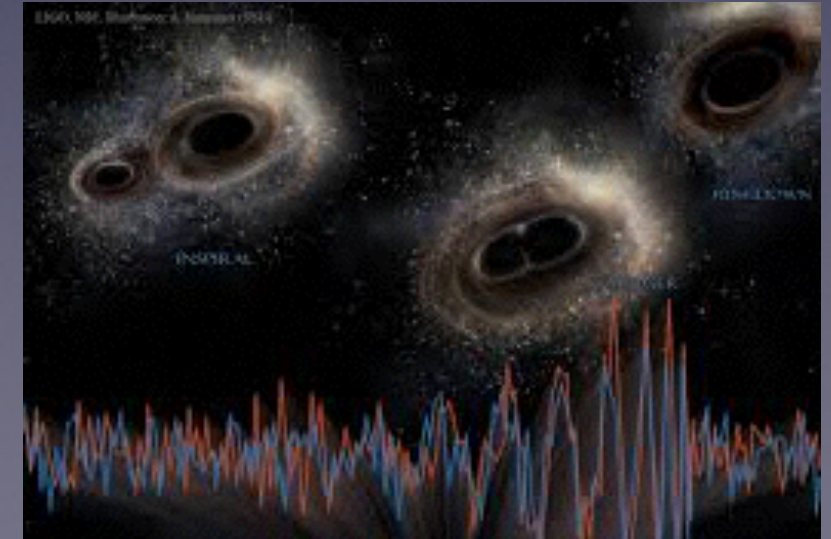
3. Counting BHs

How many BHs in a galaxy?

How many galaxies in the Universe?

4. Event Rates at aLIGO/KAGRA/DECIGO/LISA

How many BH mergers in the Universe?



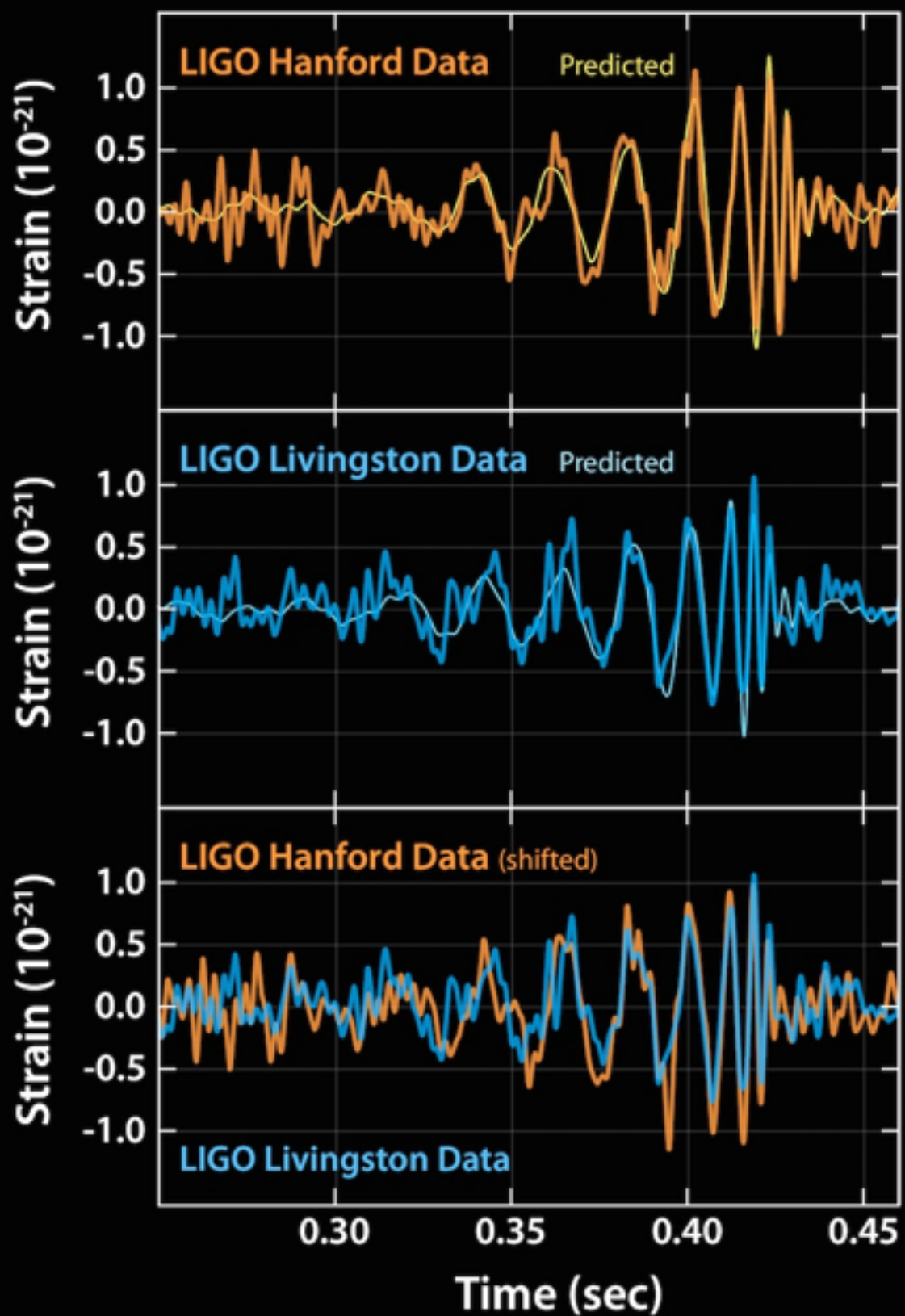
2016年2月、LIGOが重力波を初めて検出した、と発表した



四国新聞だけ
ちがった... 残念 (笑)

2016年2月, LIGOが重力波を初めて検出した, と発表した

2015年9月14日



2016年2月、LIGOが重力波を初めて検出した、と発表した

毎日新聞 2016/2/13

「窮理」 2016/8

2017年1月センター試験 国語 小林博司「科学コミュニケーション」

第1問

の都合で本文の段落に 1 ～ 13 の番号を付してある。また、表記を一部改めている。(配点 50)

1 現代社会は科学技術に依存した社会である。近代科学の成立期とされる十六世紀、十七世紀においては、そもそも「科学」という名称で認知されるような知的活動は存在せず、伝統的な自然哲学の一環としての、一部の好事家による楽しみの側面が強かつた。しかし、十九世紀になると、科学研究は「科学者」という職業的専門家によって各種高等教育機関で営まれる知識生産へと変容し始める。既存の知識の改訂と拡大のみを生業とする集団を社会に組み込むことになったのである。さらに二十世紀になり、国民国家の競争の時代になると、科学は技術的な威力と結びつくことによって、この競争の重要な戦力としての力を発揮し始める。二度にわたる世界大戦が科学・技術の社会における位置づけを決定的にしていったのである。

2 第二次世界大戦以後、科学技術という営みの存在は膨張を続ける。^(注1) ブライスによれば、科学技術という営みは十七世紀以来、十五年で^(ア)バイソウするという速度で膨張しており、二十世紀後半の科学技術の存在はGNPの二バーセント強の投資を要求するまでになつてきているのである。現代の科学技術は、かつてのような思弁的、宇宙論的伝統に基づく自然哲学的性格を失い、A 先進国^(注2)の社会体制を維持する重要な装置となつてきている。

3 十九世紀から二十世紀前半にかけては科学という営みの規模は小さく、にもかかわらず技術と結びつき始めた科学・技術は社会の諸問題を解決する能力を持つていた。「もつと科学を」というスローガンが説得力を持ち得た所以である。しかし二十世紀後半の科学・技術は両面価値的存在になり始める。現代の科学・技術では、自然の仕組みを解明し、宇宙を説明するという営みの比重が下がり、実験室の中に天然では生じない条件を作り出し、そのもとでさまざまな人工物を作り出すなど、自然に入りし、操作する能力の開発に重点が移動している。その結果、永らく人類を脅かし苦しめてきた病や災害といった自然の脅威を制御できるようになつてきたが、同時に、科学・技術の作り出した人工物が人類にさまざまな災いをもたらし始めてもいるのである。科学・技術が恐るべき速度で生み出す新知識が、われわれの日々の生活に商品や製品として放出されてくる。い

わゆる「環境ホルモン」や地球環境問題、先端医療、情報技術などがその例である。B こうして「もつと科学を」というスローガンの説得力は低下し始め、「科学が問題ではないか」という新たな意識が社会に生まれ始めているのである。

4 しかし、科学者は依然として「もつと科学を」という発想になじんでおり、このような「科学が問題ではないか」という問い合わせを、科学に対する無知や誤解から生まれた情緒的反発とみなしがちである。ここからは、素人の一般市民への科学教育の充実や、科学啓蒙プログラムの展開という発想しか生まれないのである。

5 このような状況に一石を投じたのが科学社会学者のコリンズとビンチの『ゴレム』である。ゴレムとはユダヤの神話に登場する怪物である。人間が水と土から創り出した怪物で、魔術的力量を備え、日々その力を増加させつつ成長する。人間の命令に従い、人間の代わりに仕事をし、外敵から守ってくれる。しかしこの怪物は不器用で危険な存在でもあり、適切に制御しなければ主人を破壊する威力を持つている。コリンズとビンチは、現代では、科学が、全面的に善なる存在か全面的に悪なる存在かのどちらかのイメージに引き裂かれているという。そして、このような分裂したイメージを生んだ理由は、科学が実在と直結した無謬^(注3)の知識という神のイメージで捉えられており、科学が自らを実態以上に美化することによって過大な約束をし、それが必ずしも実現しないことが幻滅を生み出したからだという。つまり、全面的に善なる存在というイメージが科学者から振りまかれ、他方、チエルノブイリ事故や狂牛病に象徴されるような事件によって科学への幻滅が生じ、一転して全面的に悪なる存在というイメージに変わったのである。

6 コリンズとビンチの処方箋は、科学者が振りまいした当初の「実在と直結した無謬の知識という神のイメージ」を科学の実態に即した「不確実で失敗しがちな向こう見ずでへまをする巨人のイメージ」、つまり C ゴレムのイメージに取りかえることを主張したのである。そして、科学史から七つの具体的な実験をめぐる論争を取り上げ、近年の科学社会学研究に基づくケーススタディーを提示し、科学上の論争の終結がおよそ科学哲学者が想定するような論理的、方法論的決着ではなく、さまざまなヨウインが絡んで生じていることを明らかにしたのである。

7 彼らが扱ったケーススタディーの一例を挙げよう。一九六九年にウェーバーが、十二年の歳月をかけて開発した実験装置を

2017年1月センター試験 国語 小林博司「科学コミュニケーション」

(ウ)

- 3 ヤツカイ
——
① ② ③ ④ ⑤

- 4 ヤツコウ
——
① ② ③ ④ ⑤

(エ)

- 4 センコク
——
① ② ③ ④ ⑤

- 4 コクジ
——
① ② ③ ④ ⑤

- 7 ウエーバー——ジョセフ・ウェーバー(一九一九—二〇〇〇)。物理学者。
8 重力波——時空のゆがみが波となつて光速で伝わる現象。一九一六年にアインシュタインがその存在を予言していた。
9 重力波の存在は明確に否定された——ウェーバーによる検出の事実は証明されなかつたが、二〇一六年、アメリカの研究チームが直接検出に成功したと発表した。

10

- コリンズとビンチは、このようなケーススタディーをもとに、「もつと科学を」路線を批判するのである。民主主義国家の

用いて、重力波の測定に成功したと発表した。これをきっかけに、追試をする研究者があらわれ、重力波の存在をめぐって論争となつたのである。この論争において、実験はどのような役割を果たしていたかという点が興味深い。追試実験から、ウェーバーの結果を否定するようなデータを手に入れた科学者は、それを発表するかいなかという選択の際に(ウ)ヤツカイな問題を抱え込むのである。否定的な結果を発表することは、ウェーバーの実験が誤りであり、このような大きな値の重力波は存在しないという主張をすることになる。しかし、実は批判者の追試実験の方に不備があり、本当はウェーバーの検出した重力波が存在するということが明らかになれば、この追試実験の結果によって彼は自らの実験能力の低さを公表することになる。

8

- 学生実験の場合には、実験をする前におおよそどのような結果になるかがわかつており、それと食い違えば実験の失敗がセンエコクされる。しかし現実の科学では必ずしもそうはことが進まない。重力波の場合、どのような結果になれば実験は成功といえるかがわからないのである。重力波が検出されれば、実験は成功なのか、それとも重力波が検出されなければ、実験は成功なのか。しかしまさに争点は、重力波が存在するかどうかであり、そのための実験なのである。何が実験の成功といえ

る結果なのかを、前もってることはできない。重力波が存在するかどうかを知るために、「優れた検出装置を作らなければならぬ。しかし、その装置を使って適切な結果を手に入れなければ、装置が優れたものであつたかどうかはわからない。しかし、優れた装置がなければ、何が適切な結果かということはわからない……」。コリンズとビンチはこのような循環を「実験家の悪循環」と呼んでいる。

9

- 重力波の論争に関しては、このような悪循環が生じ、その存在を完全に否定する実験的研究は不可能であるにもかかわらず(存在・非存在の可能性がある)、結局、有力科学者の否定的発言をきっかけにして、科学者の意見が雪崩を打つて否定論に傾き、それ以後、重力波の存在は明確に否定されたのであつた。つまり、論理的には重力波の存在もしくは非存在を実験によつて決着をつけられていなかつたが、科学者共同体の判断は、非存在の方向で収束したということである。

タディーを提示し、科学上の論争の絆縫かおよそ科学哲学者が想定するような論理的方法論的決着ではなく、さまざまな三ウイインが絡んで生じていることを明らかにしたのである。

7

- 彼らが扱つたケーススタディーの一例を挙げよう。一九六九年にウェーバーが、十二年の歳月をかけて開発した実験装置を

2016.2.29配信



絶対に役立つ中学受験専門プロ家庭教師からの必勝アドバイス！

入試で狙われそうな今月の理科トピックス

今月は、記事の数が多かった宇宙のお話の特集です。

“インシュタインの最後の宿題”と“H2Aロケット30号機で6世代目のX線天文衛星「ひとみ」を打ち上げ”それに“太陽系第9番目の惑星発見か?”について取り上げます。

< インシュタインの最後の宿題 >

今月11日、米国重力波観測所LIGOのリーダーであるデビッド・ライツ氏は、重力波の観測に成功したと発表しました。この発見は100年にインシュタインによって存在が予言されていた重力波が確認されたものです。これはノーベル賞級の快挙です。

『重力波ってなに？』

皆さんはセルロイドの下敷きを髪の毛でこすると髪の毛や軽い紙やほこりが下敷きに引き寄せられてくっつく遊びをしたことありますよね。これは電気（静電気）の力ですが、砂場で遊んだ磁石が砂鉄や他の磁石とくっつくのは磁気の力（磁力）です。他に物体が引き寄せあう力には重力があります。リンゴが地面に落ちるのを見てアイザック・ニュートンが発見したと言われる万有引力の法則がありますが、これは物体同士の引き合う力

これらの予言が次々と観測で証明され、最後まで残ったのが重力波の証明だったので、最後の宿題と言われてきました。

『なぜ重力波の発見が困難なのでしょうか？』

重力波による空間の伸び縮みは3~4kmの長さに対し1兆分の1の更に1万分の1mm（1京分の1）が変化するのを観測しようと科学者は頑張ってきたのです。つまり陽子の大きさの1万分の1の長さが変化する程度といえば、その変化の小ささがお判りになるでしょうか。そのため、観測技術が追いつかなかったのです。

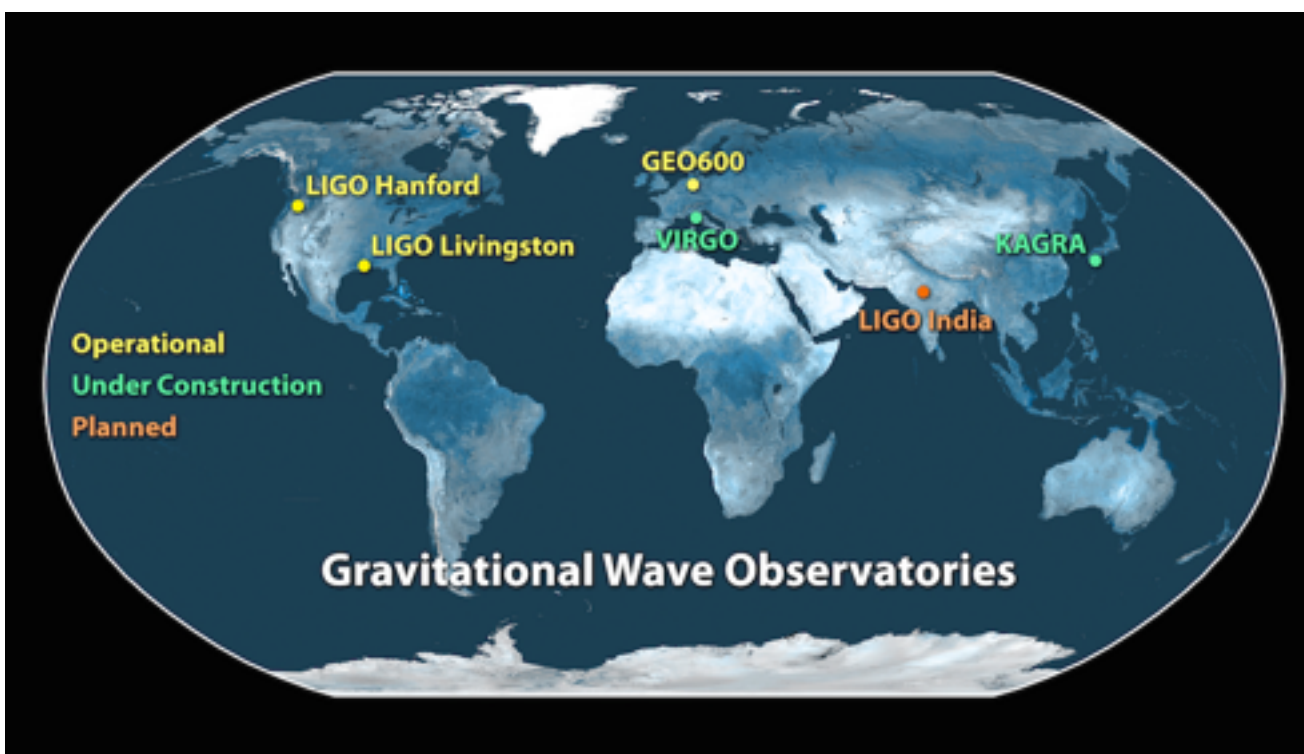
どうやって測るのでしょうか？

L型の同じ長さのトンネルに真空にしたパイプの両端に鏡を向かい合わせ、そこに光を何度も反射させ時間を図ります。重力波が来ると空間が歪み、トンネルの片方が伸び片方が縮みます。光の速さは約秒速30万kmと一定なので、到達時間に差が生じます。時間差が起ったら重力波が観測できたことになります。日本では1999年東京都三鷹市の国立天文台構内にTAMA300という観測装置を建設しましたが、近くの調布のサッカー場で観戦者の飛び跳ねる振動が観測に影響したそうです。観測装置はそんなに敏感にできているのです。

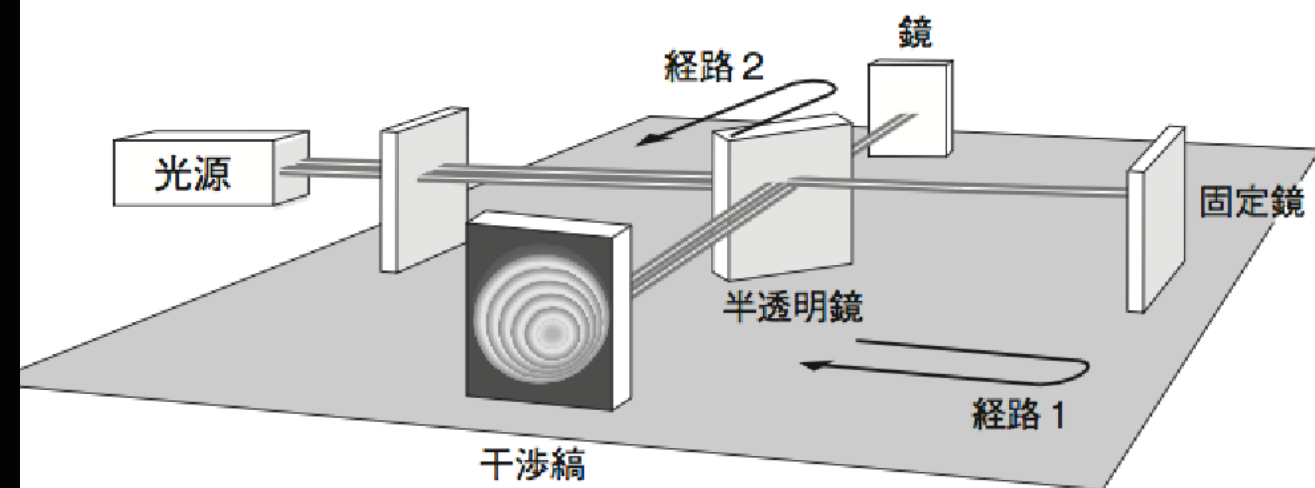
その様な経験から現在は岐阜県飛騨市山中にパイプ長3kmの観測装置「かぐら」を建設中で、来年度から本格運用に入る予定です。

LIGO (ライゴ：レーザー干渉計重力波天文台)

Laser Interferometer Gravitational-Wave Observatory (1992年予算承認)



<https://mediaassets.caltech.edu/gwave>



LIGO: The Laser Interferometer Gravitational-Wave Observatory

Alex Abramovici, William E. Althouse, Ronald W. P. Drever,
Yekta Gürsel, Seiji Kawamura, Frederick J. Raab,
David Shoemaker, Lisa Sievers, Robert E. Spero,
Kip S. Thorne, Rochus E. Vogt, Rainer Weiss,
Stanley E. Whitcomb, Michael E. Zucker

The goal of the Laser Interferometer Gravitational-Wave Observatory (LIGO) Project is to detect and study astrophysical gravitational waves and use data from them for research in physics and astronomy. LIGO will support studies concerning the nature and nonlinear dynamics of gravity, the structures of black holes, and the equation of state of nuclear matter. It will also measure the masses, birth rates, collisions, and distributions of black holes and neutron stars in the universe and probe the cores of supernovae and the very early universe. The technology for LIGO has been developed during the past 20 years. Construction will begin in 1992, and under the present schedule, LIGO's gravitational-wave searches will begin in 1998.

Einstein's general relativity theory describes gravity as due to a curvature of space-time (1). When the curvature is weak, it produces the familiar Newtonian gravity that governs the solar system. When

The authors are the members of the LIGO Science Steering Group. A. Abramovici, W. E. Althouse (Chief Engineer), R. W. P. Drever, S. Kawamura, F. J. Raab, L. Sievers, R. E. Spero, K. S. Thorne, R. E. Vogt (Director), S. E. Whitcomb (Deputy Director), and M. E. Zucker are with the California Institute of Technology, Pasadena, CA 91125. Y. Gürsel is at the Jet Propulsion Laboratory, Pasadena, CA 91109. D. Shoemaker and R. Weiss are at the Massachusetts Institute of Technology, Cambridge, MA 02129.

SCIENCE • VOL. 256 • 17 APRIL 1992

325

the curvature is strong, however, it should behave in a radically different, highly nonlinear way. According to general relativity, the nonlinearity creates black holes (curvature produces curvature without the aid of any matter), governs their structure, and holds them together against disruption (2). Inside a black hole, the curvature should nonlinearly amplify itself to produce a space-time singularity (2), and near some singularities the nonlinearity should force the curvature to evolve chaotically (3). When an object's curvature varies rapidly (for example, because of pulsations, colli-

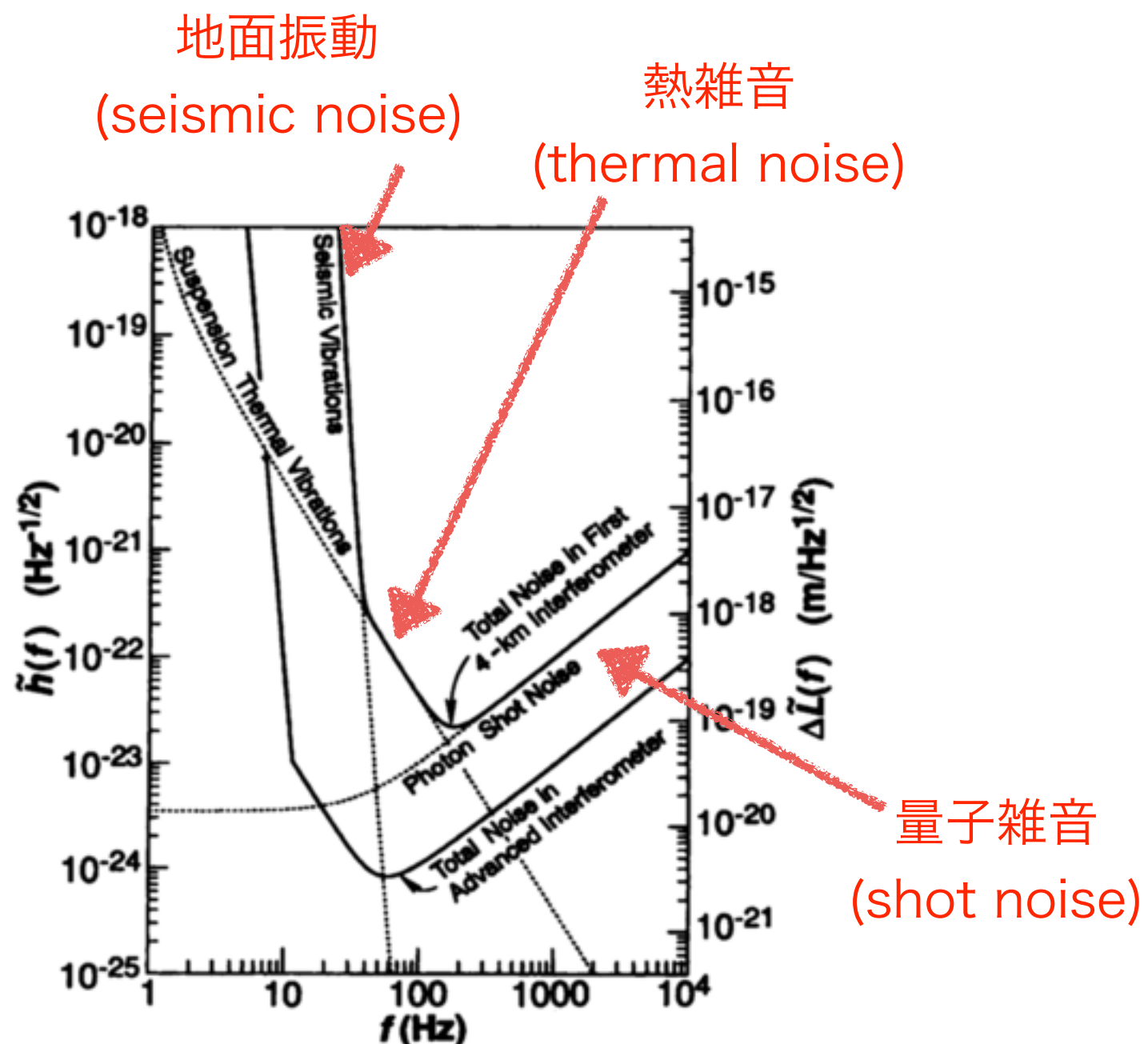


Fig. 7. The expected total noise in each of LIGO's first 4-km interferometers (upper solid curve) and in a more advanced interferometer (lower solid curve). The dashed curves show various contributions to the first interferometer's noise.

KAGRA (かぐら：大型低温重力波望遠鏡)

Kamioka Gravitational wave detector, (Large-scale Cryogenic Gravitational wave Telescope)

大型低温重力波望遠鏡



望遠鏡の大きさ：基線長 3km

望遠鏡を神岡鉱山内に建設

地面振動が小さい岐阜県飛騨市にある神岡鉱山

鏡をマイナス250度 (20K) まで冷却

熱雑音を小さくするため

鏡の材質としてサファイア

光学特性に優れ、低温に冷却すると熱伝導や機械的損失が少なくなる

天文宇宙検定



受験のご案内



公式テキスト



天文宇宙クイズ

[ホーム](#) > 2014年度 第4回天文宇宙検定 解答速報

● 解答速報



2014年度 第4回天文宇宙検定 解答速報

1級

問題と解答

2014年6月、日本が岐阜県に建設している重力波干渉計KAGRA（かぐら）のトンネルが貫通し、マスコミに公開された。KAGRAは、一边が3kmもあるレーザー干渉計だが、岐阜県神岡鉱山跡の山中にわざわざ建設した理由は何か。

- ①近くにはスーパーカミオカンデというニュートリノ観測装置があり、実験装置の調整にニュートリノを使うから
- ②山の中だと地面の振動が少なく、干渉計装置のゆれを押さえることができるから
- ③山の中だと温度調整が少なくて済むので、レーザー光源のメンテナンスに都合がよいから
- ④強力なレーザー光の発生や、真空ポンプの稼働で、騒音が激しいから

signal = gw + noise

$$s(t) = h(t) + n(t)$$

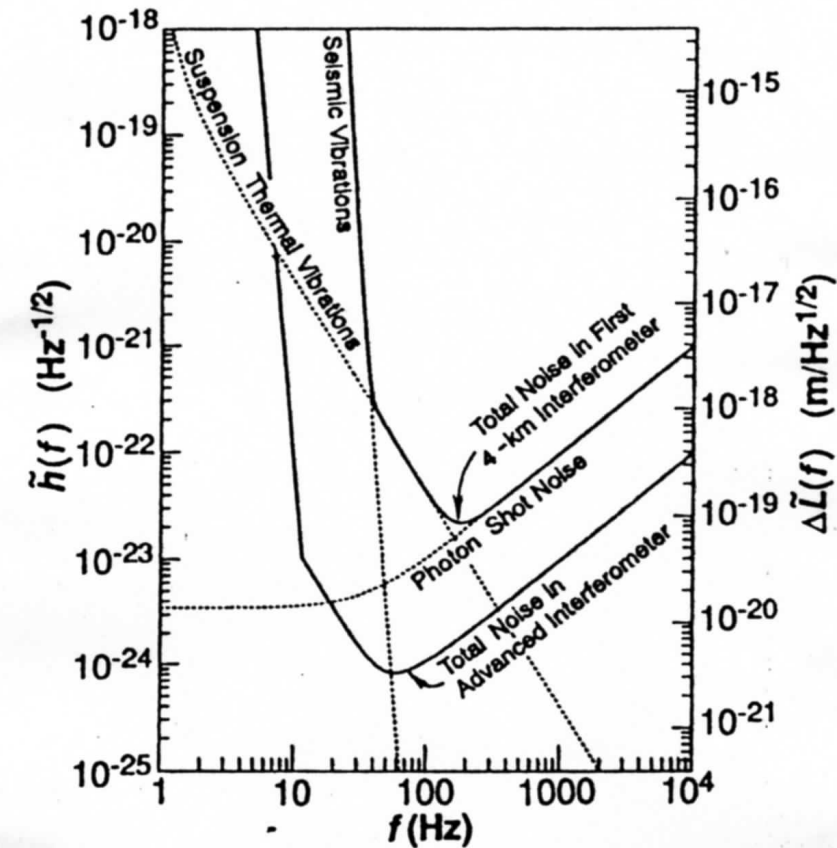
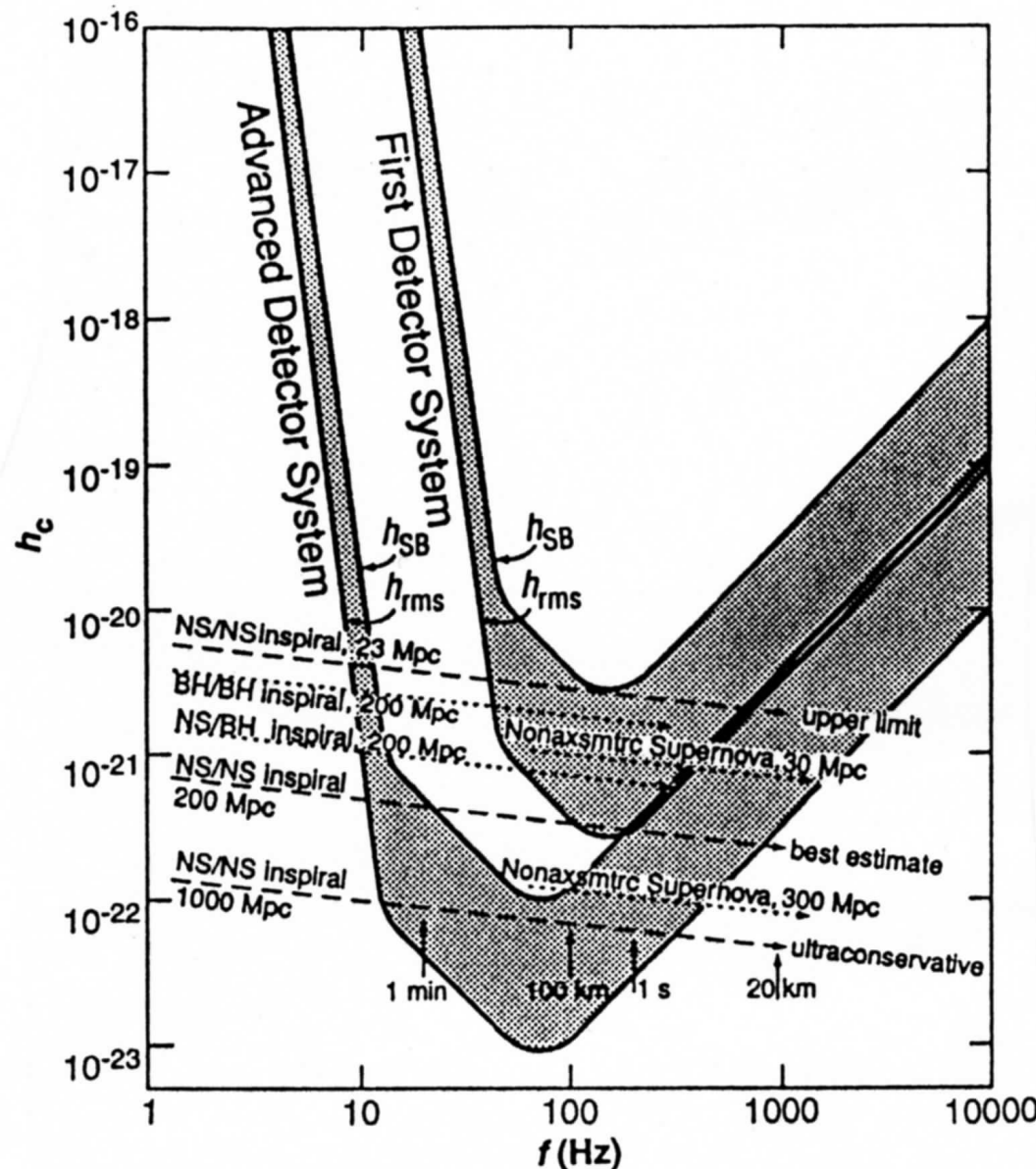


Fig. 7. The expected total noise in each of LIGO's first 4-km interferometers (upper solid curve) and in a more advanced interferometer (lower solid curve). The dashed curves show various contributions to the first interferometer's noise.

spectral density [sec]

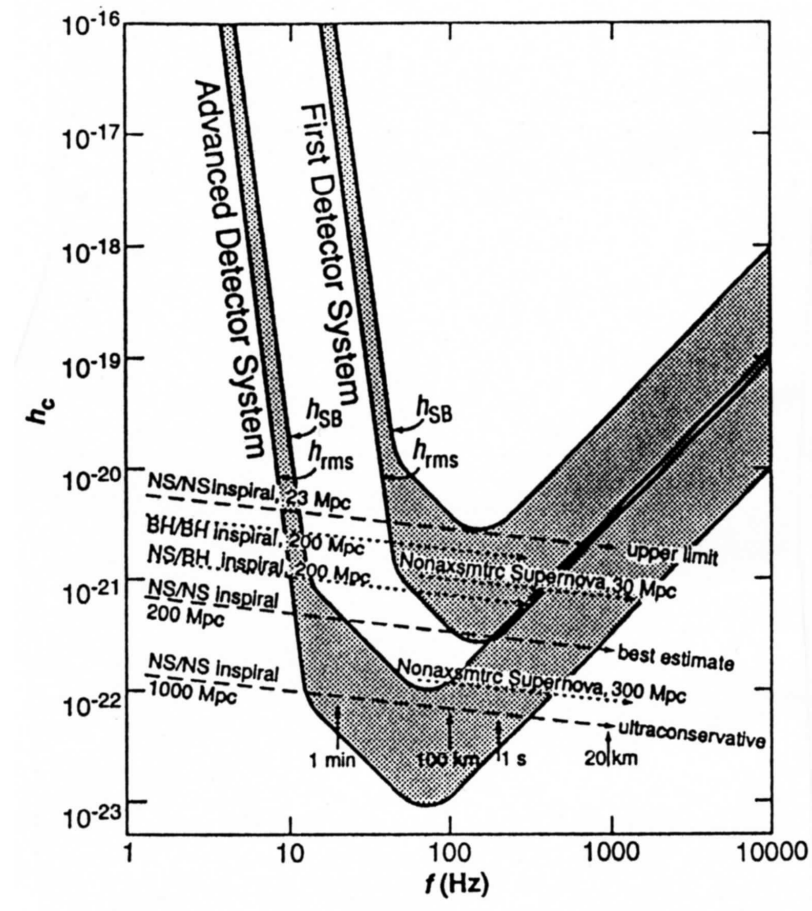
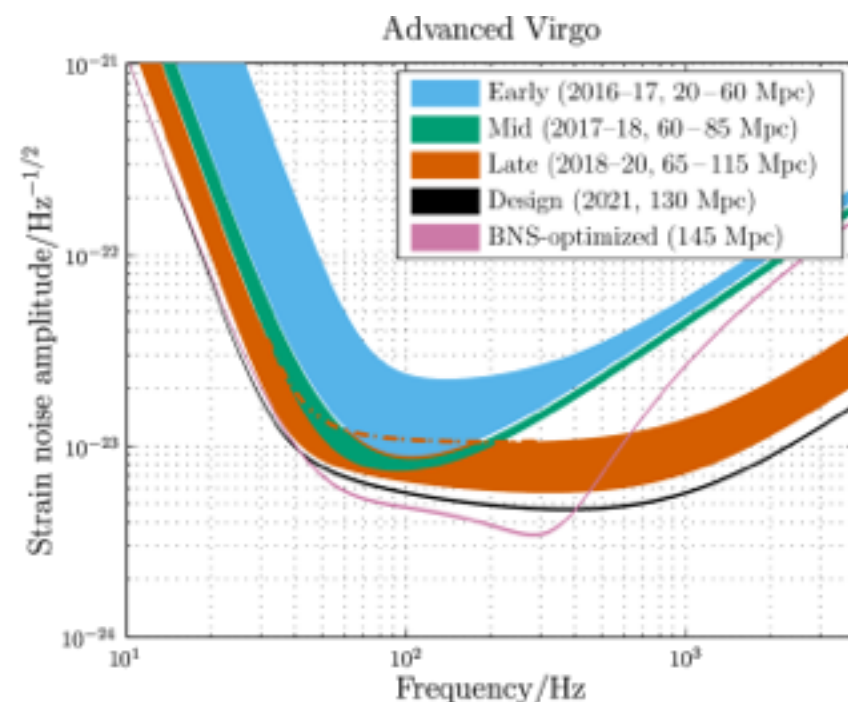
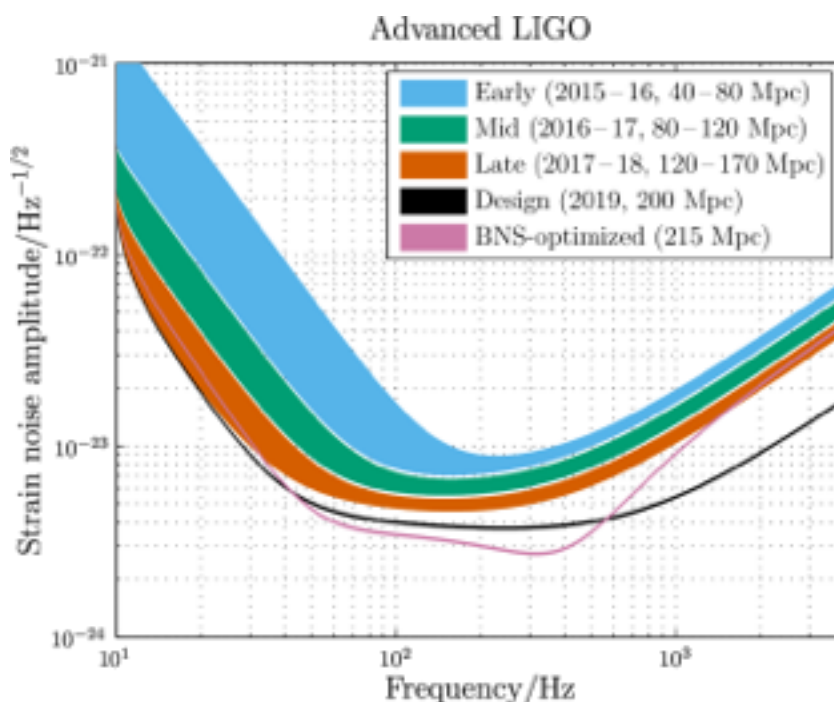
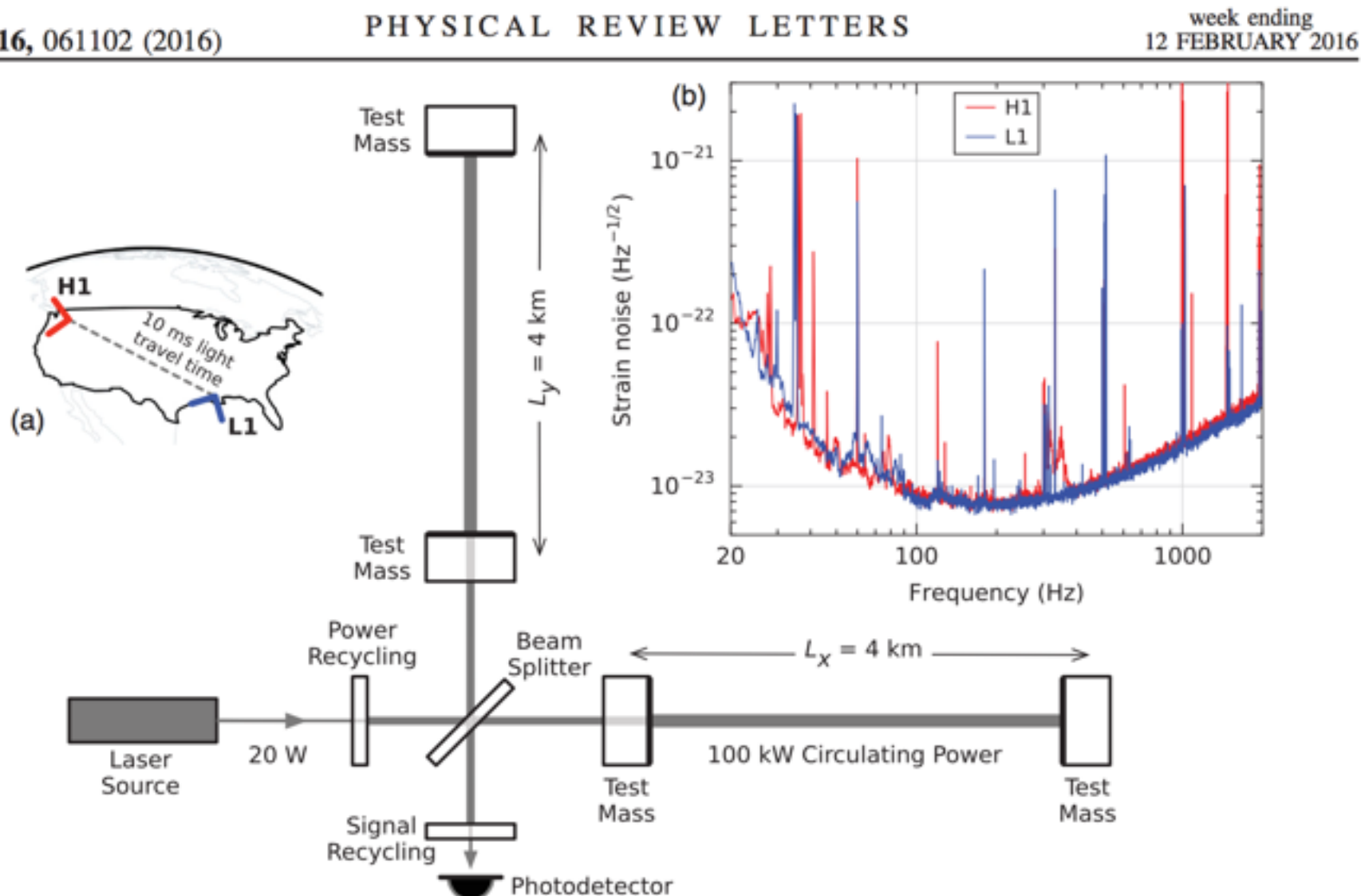
$$S_n(f) = 2 \int C_n(\tau) e^{i2\pi f\tau} d\tau$$

$$C_n(\tau) = \overline{n(t)n(t+\tau)}$$

$$h_n(f) = \sqrt{f S_n(f)} \rightarrow \sqrt{S_n(f)}$$

$$\overline{n(t)} = \lim_{T \rightarrow \infty} \frac{1}{2T} \int_{-T}^{+T} n(t) dt$$

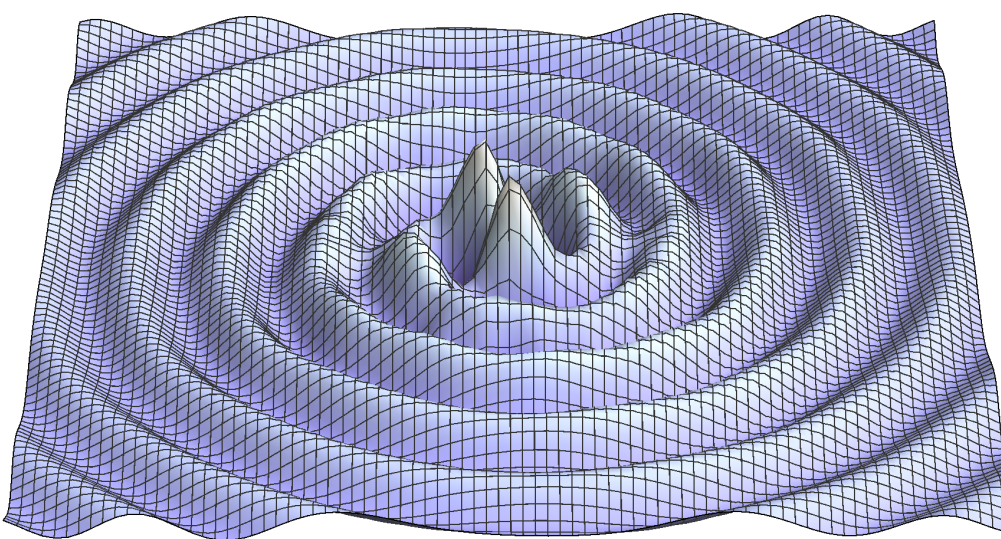
strain noise



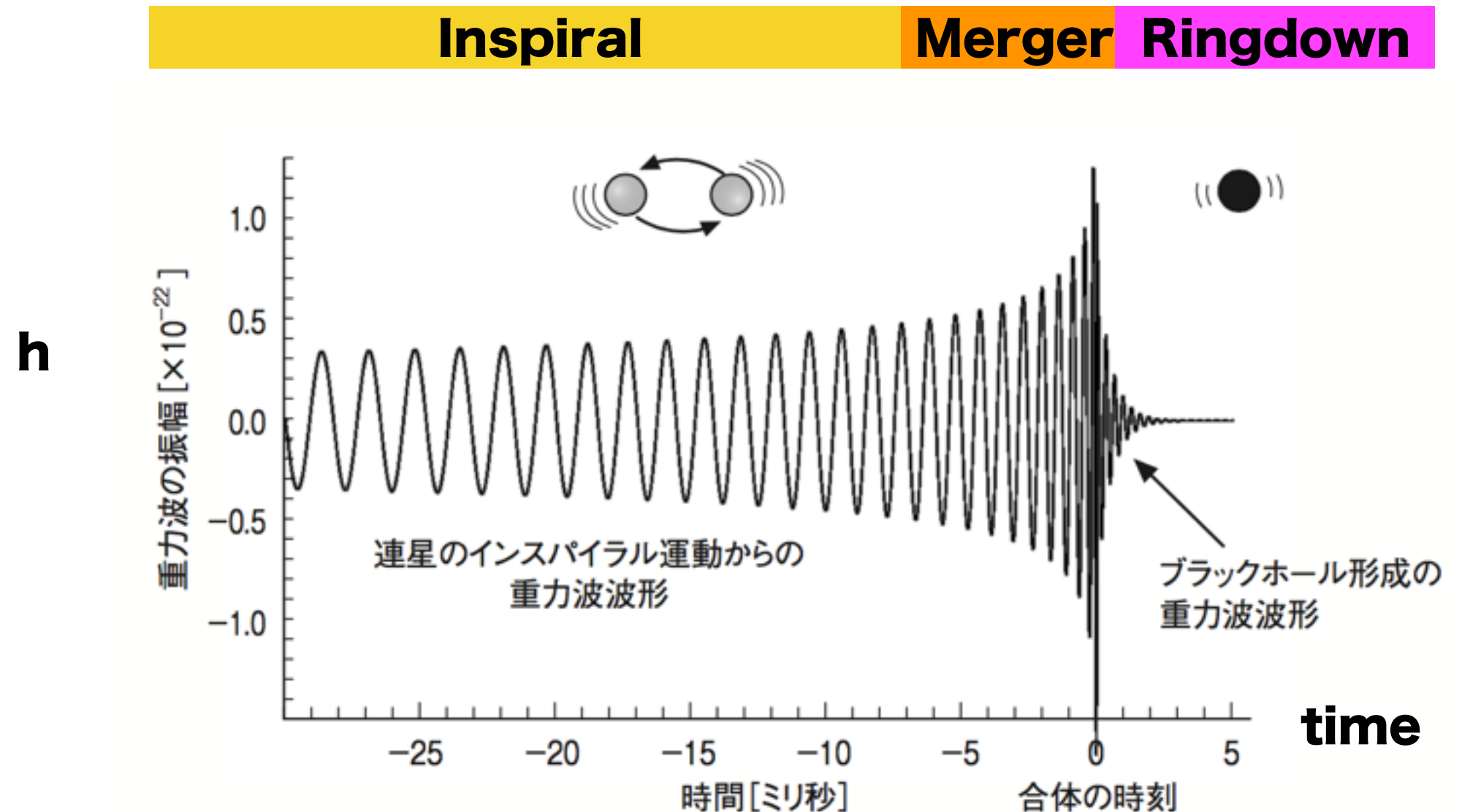
**2015/9/16–2016/1/15
Observational run 1**

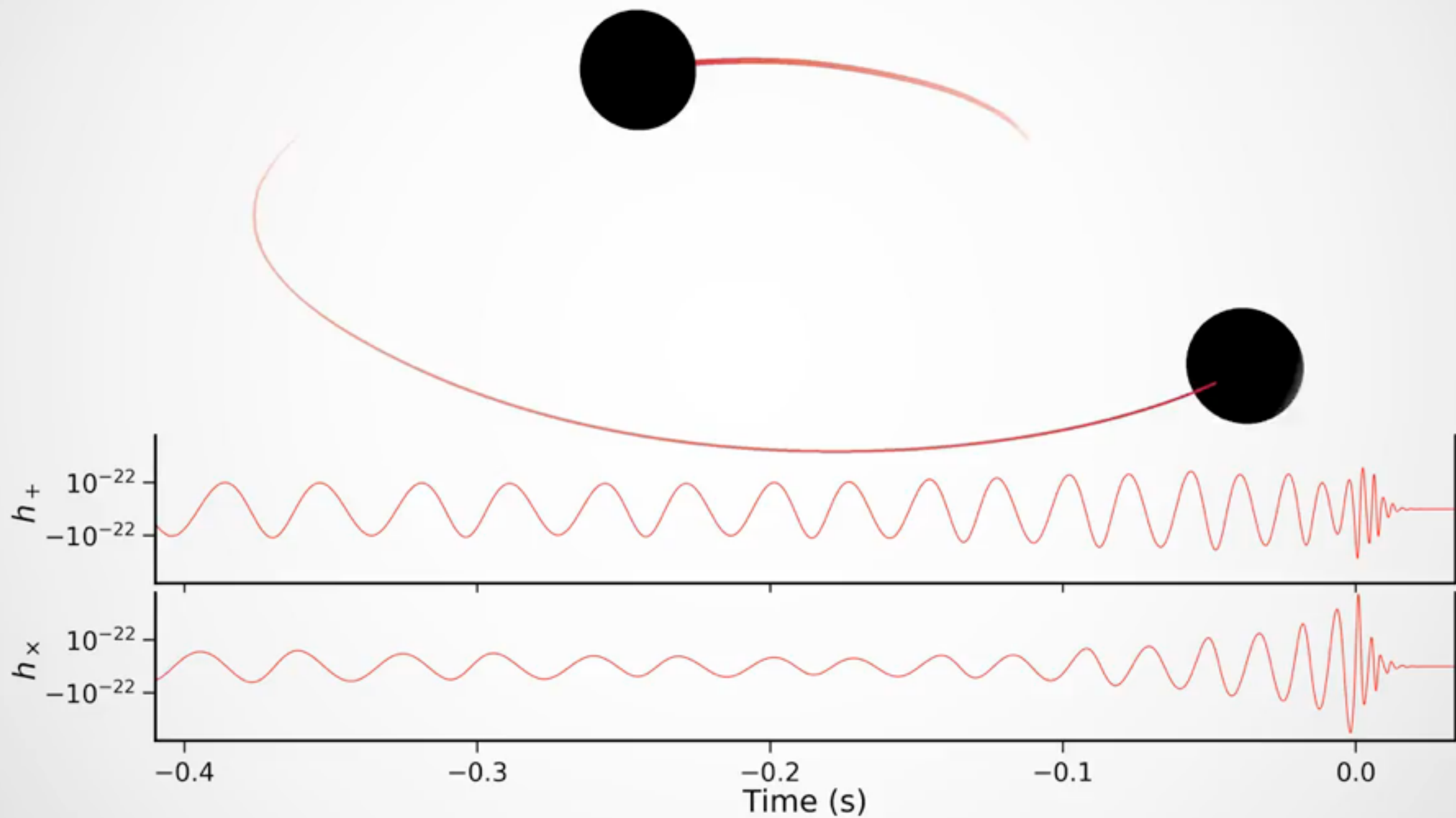
**2016/11/30—
Observational run 2**

1. Gravitational Wave >> Expected Waveform



NS-NS
NS-BH
BH-BH





Animation of the inspiral and collision of two black holes consistent with the masses and spins of GW170104. The top part of the movie shows the black hole horizons (surfaces of "no return"). The initial two black holes orbit each other, until they merge and form one larger remnant black hole. The shown black holes are spinning, and angular momentum is exchanged among the two black holes and with the orbit. This results in a quite dramatic change in the orientation of the orbital plane, clearly visible in the movie. Furthermore, the spin-axes of the black holes change, as visible through the colored patch on each black hole horizon, which indicates the north pole.

The lower part of the movie shows the two distinct gravitational waves (called 'polarizations') that the merger is emitting into the direction of the camera. The modulations of the polarizations depend sensitively on the orientation of the orbital plane, and thus encode information about the orientation of the orbital plane and its change during the inspiral. Presently, LIGO can only measure one of the polarizations and therefore obtains only limited information about the orientation of the binary. This disadvantage will be remedied with the advent of additional gravitational wave detectors in Italy, Japan and India.

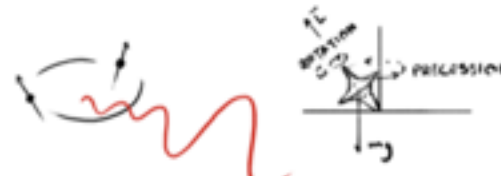
Finally, the slowed-down replay of the merger at the end of the movie makes it possible to observe the distortion of the newly formed remnant black hole, which decays quickly. Furthermore, the remnant black hole is "kicked" by the emitted gravitational waves, and moves upward. (Credit: A. Babul/H. Pfeiffer/CITA/SXS.) - See more at: <http://ligo.org/detections/GW170104.php#sthash.NZPaW2LT.dpu>

The waveform explained

[BLACK HOLE]

A BLACK HOLE IS ONE OF THE SIMPLEST OBJECTS IN THE UNIVERSE. IT HAS ONLY TWO CHARACTERISTICS: ITS MASS (WHICH DETERMINES ITS SIZE), AND ITS SPIN (HOW MUCH SPACETIME SWIRLS AROUND).

WHEN YOU HAVE TWO BLACK HOLES IN A BINARY SYSTEM, THINGS GET MORE COMPLICATED. WE NOW HAVE THE MASSES AND SPINS OF BOTH BLACK HOLES. THE SPINS STAY THE SAME SIZE DURING THE ORBIT, BUT THEIR DIRECTIONS WOBBLE AROUND IN A PROCESS CALLED PRECESSION. THE GRAVITATIONAL WAVES REACHING EARTH FROM THE BINARY ALSO DEPEND ON WHERE THE BINARY IS AND WHICH WAY IT IS ORIENTATED.



[SPIN]

AS THE BLACK HOLES ORBIT EACH OTHER, THEIR SPINS CHANGE DIRECTION. THIS ALSO CAUSES THE ORBIT TO TOGGLE BACKWARDS AND FORWARDS A LITTLE. THIS PRECESSION LEAVES AN IMPRINT ON THE GRAVITATIONAL WAVES: THEY BECOME LOUDER AND QUIETER AS THE SPINS WOBBLE AROUND. THE PRECESSION DEPENDS ON DIRECTIONS OF THE TWO SPINS, COMPARED TO EACH OTHER AND COMPARED TO THAT OF THE ORBIT. THE SPIN OF THE MORE MASSIVE BLACK HOLE HAS A LARGER EFFECT THAN THAT OF THE SMALLER ONE.

WE DON'T SEE MUCH SIGN OF PRECESSION IN GW150914. THIS MAY BE BECAUSE SPINS ARE SMALL, ITS INCLINATION MEANS THE WOBBLES AREN'T VISIBLE, OR A COMBINATION OF BOTH. SINCE THE INSPIRAL IS SHORT, WE WOULD NOT EXPECT TO SEE A LARGE EFFECT IN ANY CASE.

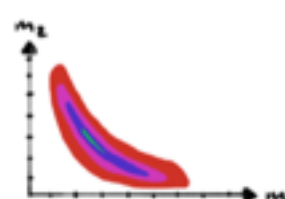


[REDSHIFT]

THE EXPANSION OF THE UNIVERSE AFFECTS GRAVITATIONAL WAVES IN A COUPLE OF WAYS. AS THE UNIVERSE EXPANDS, IT STRETCHES THE WAVES TRAVELLING THROUGH IT. THIS IS WELL KNOWN IN ASTRONOMY AND IS CALLED REDSHIFT, AS IT MAKES VISIBLE LIGHT MORE RED. TO HAVE A LARGE EFFECT, THE WAVES MUST HAVE TRAVELED A LONG WAY.

THE FIRST EFFECT IS THAT THE FREQUENCY OF THE WAVE CHANGES. THIS HAS THE SAME IMPACT AS CHANGING THE MASSES: THINGS FURTHER AWAY APPEAR MORE MASSIVE. THE SECOND EFFECT IS TO CHANGE THE AMPLITUDE, WHICH IS THE SAME AS CHANGING THE DISTANCE. WE OFTEN TALK ABOUT THE LUMINOSITY DISTANCE, WHICH ABSORBS THIS EFFECT, BUT ISN'T THE SAME AS IF WE MEASURED THE DISTANCE TO THE SOURCE USING A TAPE MEASURE.

IF WE GET ENOUGH MEASUREMENTS OF HOW GRAVITATIONAL WAVES ARE REDSHIFTED, WE COULD POSSIBLY LEARN SOMETHING ABOUT HOW THE UNIVERSE IS EXPANDING.



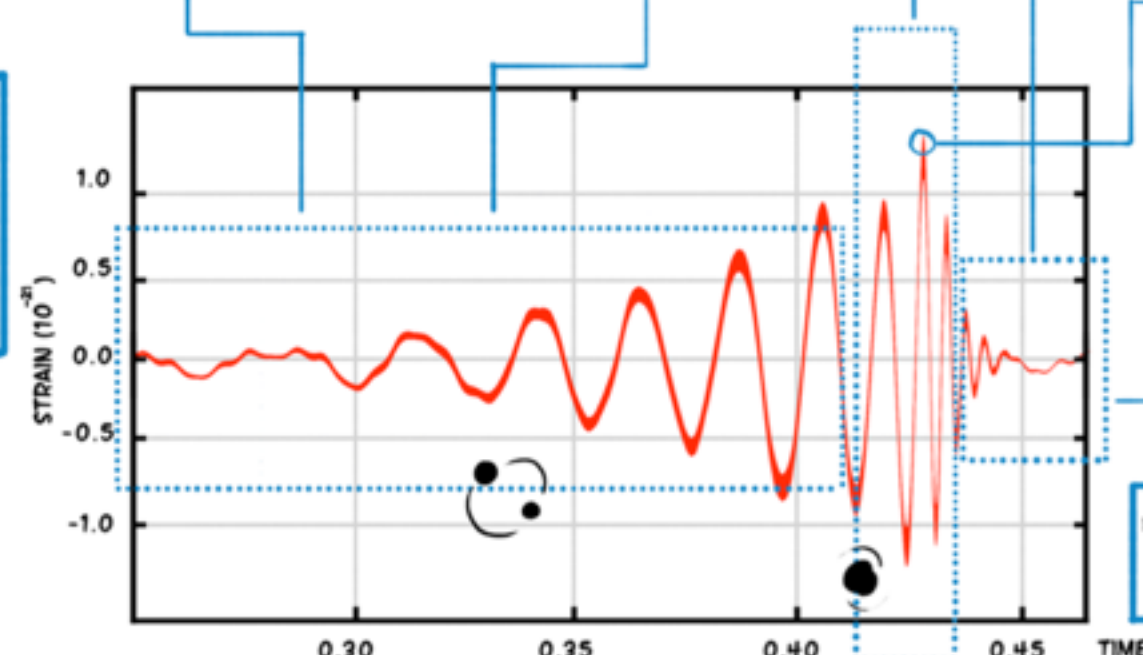
THE WAY THE SIGNAL CHANGES DURING THE INSPIRAL IS PRIMARILY FIXED BY A COMBINATION OF THE BLACK HOLE MASSES WE CALL THE CHIRP MASS. IF WE SEE LOTS OF CYCLES OF INSPIRAL, WE CAN MEASURE THE CHIRP MASS REALLY WELL (BETTER THAN A FRACTION OF A PERCENT). WHEN THINKING ABOUT WHAT WE CAN LEARN FROM GRAVITATIONAL WAVES, PEOPLE OFTEN FIRST THINK ABOUT THE CHIRP MASS.

[STAGES]

ONE OF THE REASONS WE DIVIDE UP THE GRAVITATIONAL WAVE SIGNAL IS BECAUSE DIFFERENT TECHNIQUES CAN BE USED TO CALCULATE THE WAVES AT DIFFERENT POINTS. THE EARLY INSPIRAL CAN BE CALCULATED USING POST-NEWTONIAN THEORY (THIS STARTS WITH NEWTON'S THEORY OF GRAVITY AND ADDS LITTLE EXTRA BITS TO ACCOUNT FOR HOW THINGS CHANGE IN GENERAL RELATIVITY). THE RINGDOWN CAN BE CALCULATED USING BLACK HOLE PERTURBATION THEORY (THIS STARTS WITH THE FINAL SHAPE OF THE BLACK HOLE, AND SEES HOW IT REACTS TO SMALL CHANGES). THE MERGER CAN ONLY BE CALCULATED USING NUMERICAL RELATIVITY (SIMULATIONS OF THE FULL EQUATIONS OF GENERAL RELATIVITY WHICH TAKE LOTS OF COMPUTING POWER). THIS HAS ONLY BEEN POSSIBLE IN THE LAST 10 YEARS, SO THE MERGER WAS THE LAST PART OF THE PUZZLE.

IF WE HAD A BINARY CONTAINING NEUTRON STARS INSTEAD OF BLACK HOLES, THE INSPIRAL WOULD BE MUCH THE SAME, BUT THERE WOULD NOT BE THE SAME MERGER AND RINGDOWN. THE SIGNAL WOULD BE MUCH MESSIER, POSSIBLY FEATURING NEUTRON STARS BEING RIPPED APART, BEFORE COLLIDING AND COLLAPSING TO A FINAL BLACK HOLE.

- INSPIRAL**
- MERGER**
- RINGDOWN**



THE WAY THE BINARY IS FACING THE EARTH DETERMINES THE GRAVITATIONAL WAVES WE SEE. IF IT IS EDGE ON, THE SIGNAL IS QUIETER, BUT IT IS EASIER TO SPOT SMALL CHANGES CAUSED BY THE BLACK HOLES' SPINS. IF IT IS FACING US, THE SIGNAL IS LOUDER, BUT IT'S HARDER TO TELL IF THE ORBIT WOBBLES BECAUSE OF PRECESSION. WE HAVE A GREATER CHANCE OF DETECTING A FACE-ON BINARY BECAUSE THEY CAN BE DETECTED FROM FURTHER AWAY.

[AMPLITUDE]

THE SIZE OF THE SIGNAL, ITS AMPLITUDE, DEPENDS ON HOW FAR AWAY THE BINARY IS. IF THE DISTANCE WERE TWICE AS BIG, THE AMPLITUDE WOULD BE HALF. THE QUITER A SIGNAL IS, THE HARDER IT IS TO DETECT, AND THE LESS WE CAN LEARN ABOUT ITS PROPERTIES.

HEAVIER SYSTEMS PRODUCE LOUDER GRAVITATIONAL WAVES AS THERE IS MORE MASS MOVING AROUND TO CREATE THE WAVES.

THE SIGNAL AMPLITUDE DEPENDS UPON THE WAY THE BINARY IS FACING (ITS INCLINATION), AND ITS POSITION IN THE SKY. THE DETECTORS ARE NOT EQUALLY SENSITIVE TO GRAVITATIONAL WAVES FROM ALL DIRECTIONS (THE SIGNAL IS LOUDEST WHEN THE SOURCE IS DIRECTLY ABOVE OR BELOW A DETECTOR).

$$h(t) = \frac{Gm\pi^2}{c^4 r} \sin(\omega t)$$

[RINGDOWN]

THE RINGDOWN PART OF THE SIGNAL COMES FROM THE FINAL BLACK HOLE, SO IT DEPENDS UPON ITS MASS AND SPIN. THE FINAL MASS IS ALMOST THE SAME AS THE TOTAL MASS OF THE TWO INITIAL BLACK HOLES (SOME ENERGY IS LOST, CARRIED AWAY BY THE GRAVITATIONAL WAVES). THE FINAL SPIN DEPENDS UPON THE SPIN OF THE INITIAL BLACK HOLES AND HOW THEY WERE ORBITING AROUND EACH OTHER WHEN THEY MERGED.

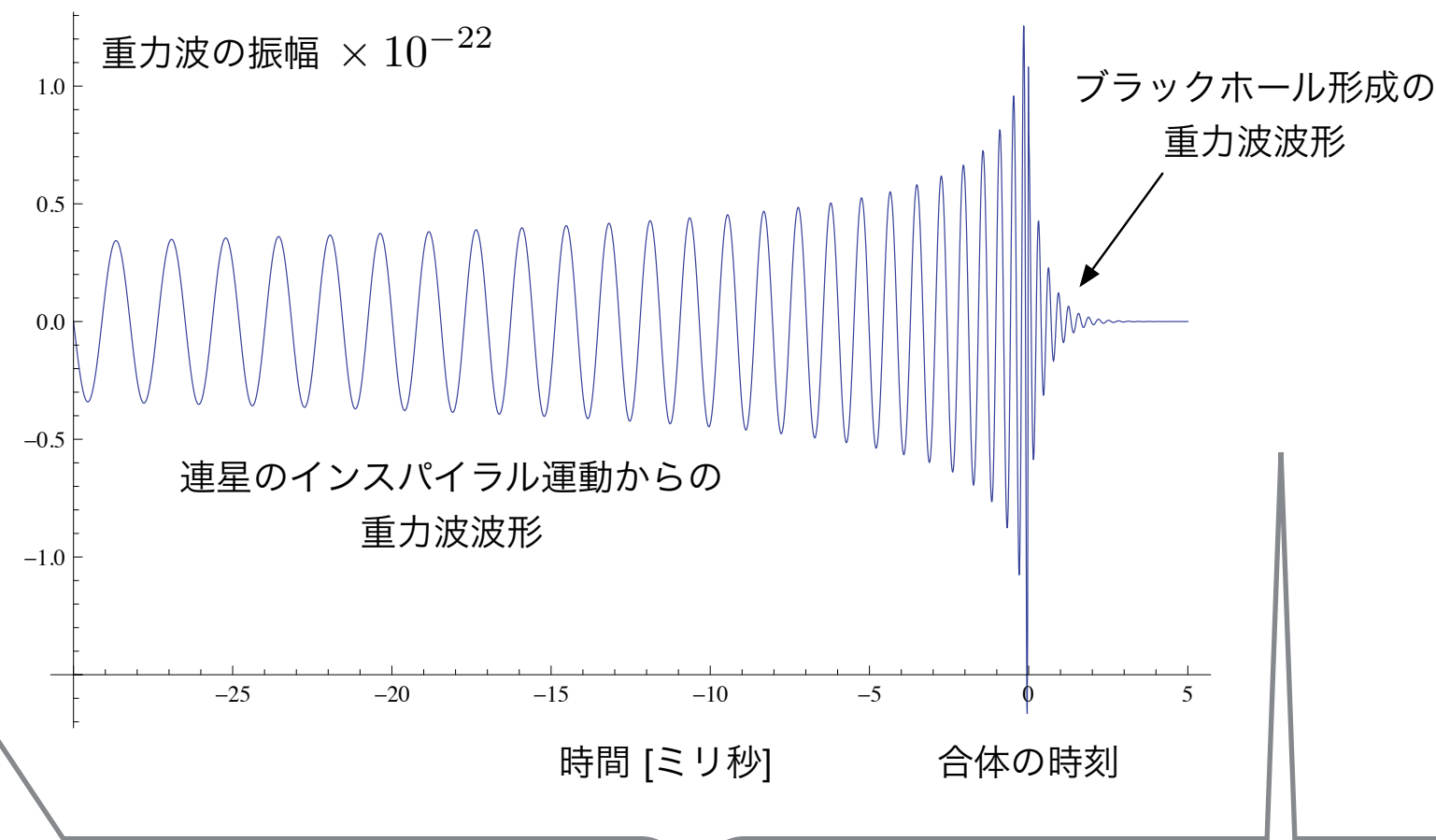
[SKY]

WITH MULTIPLE DETECTORS, WE CAN WORK OUT WHICH DIRECTION THE GRAVITATIONAL WAVES CAME FROM BY LOOKING AT THE TIMES WHEN THE SIGNALS ARRIVED AT EACH DETECTOR. THIS IS SIMILAR TO HOW YOU CAN LOCATE THE SOURCE OF A SOUND USING YOUR EARS.

WE CAN GET SOME EXTRA INFORMATION ABOUT THE DIRECTION FROM HOW LOUD EACH SIGNAL IS (SINCE EACH OF THE DETECTORS HAS ITS BEST SENSITIVITY IN A DIFFERENT DIRECTION), AND WHERE THE WAVE IS IN ITS CYCLE.



1. Gravitational Wave >> Expected Amplitude



$$f_{\text{insp}} = \frac{1}{\pi} \sqrt{\frac{GM_T}{a^3}} \\ \approx 11.4 \left(\frac{a}{R_{\text{grav}}} \right)^{-3/2} \left(\frac{2 \times 10^3 M_\odot}{M_T} \right) \text{ Hz},$$

$$h_{\text{insp}} = \sqrt{\frac{32}{5}} \pi^{2/3} G^{5/3} c^{-4} M_1 M_2 M_T^{-1/3} f^{2/3} R^{-1},$$

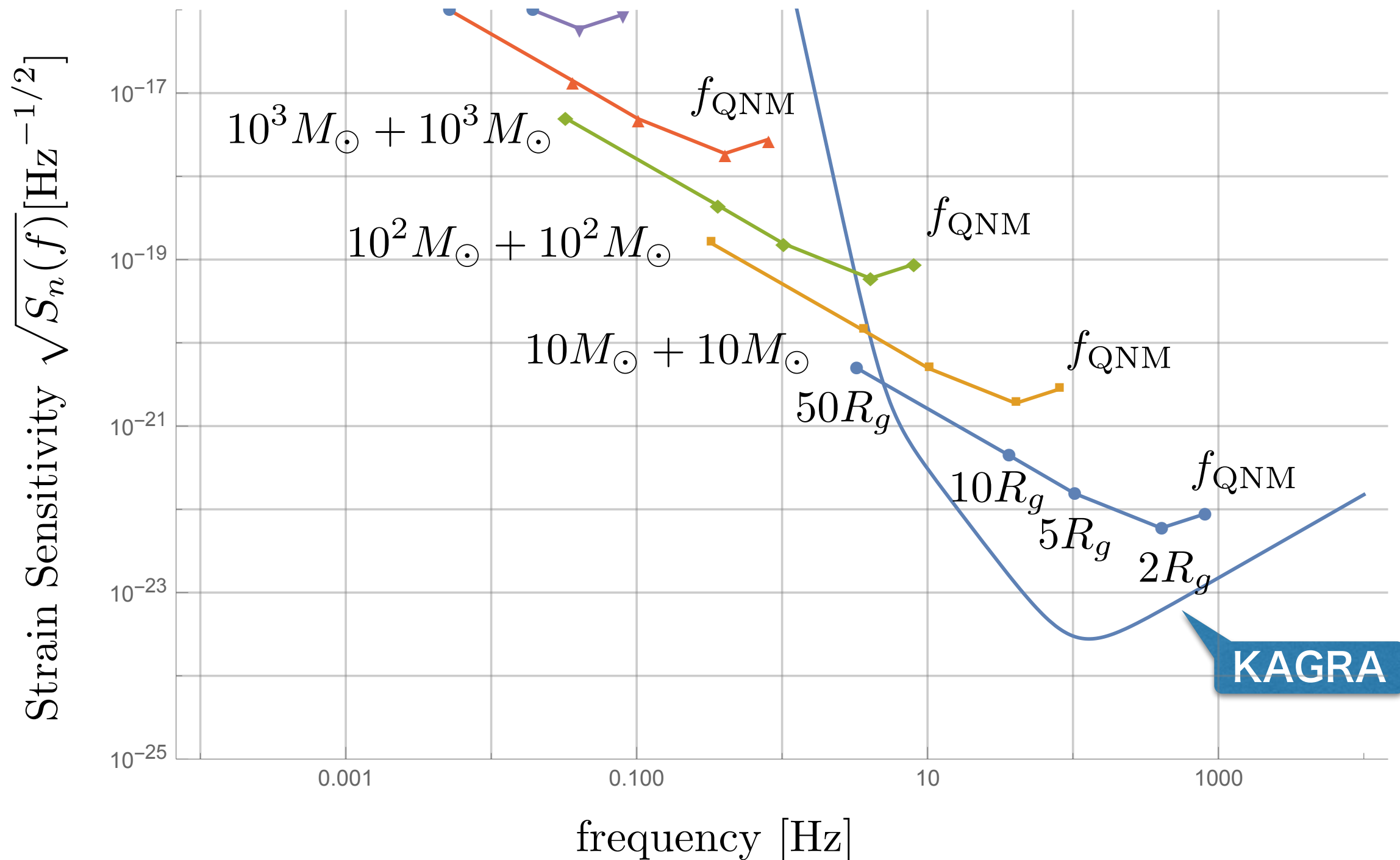
$$\approx 1.49 \times 10^{-21} \left(\frac{M_1}{10^3 M_\odot} \right) \left(\frac{M_2}{10^3 M_\odot} \right) \\ \times \left(\frac{M_T}{2 \times 10^3 M_\odot} \right)^{-1/3} \left(\frac{f}{1 \text{ Hz}} \right)^{2/3} \left(\frac{R}{4 \text{ Gpc}} \right)^{-1}.$$

$$f_{\text{QNM}} \approx \frac{lc^3}{\sqrt{27} GM_T} \sim 39.1 \left(\frac{2 \times 10^3 M_\odot}{M_T} \right) \text{ Hz},$$

$$h_{\text{coal}} \approx 5.45 \times 10^{-21} \left(\frac{\epsilon}{0.01} \right)^{1/2} \left(\frac{4 \text{ Gpc}}{R} \right) \left(\frac{\mu}{\sqrt{2} \times 10^3 M_\odot} \right)$$

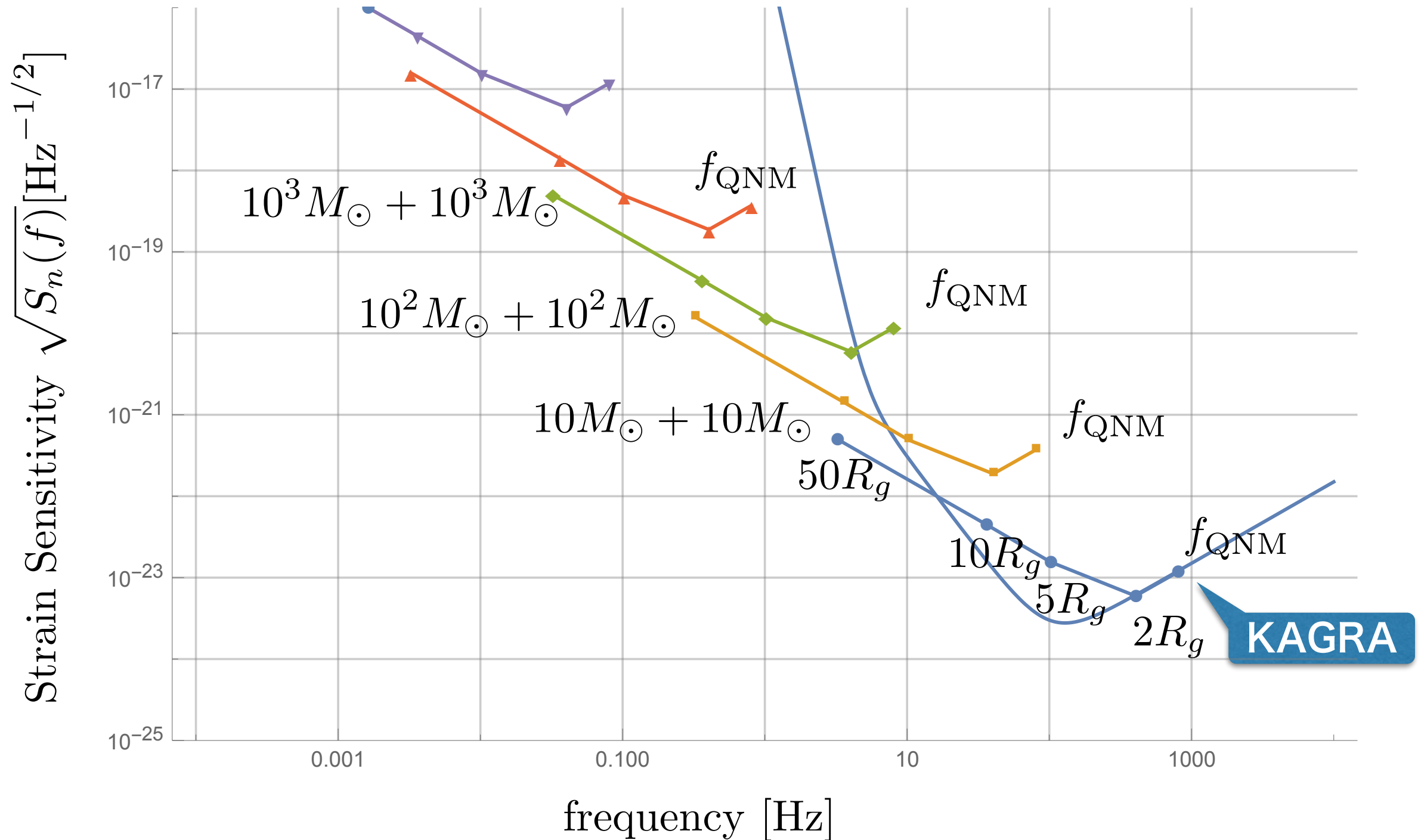
1. Gravitational Wave >> Expected Events

Typical frequency of BH-BH binary merger @ 100Mpc



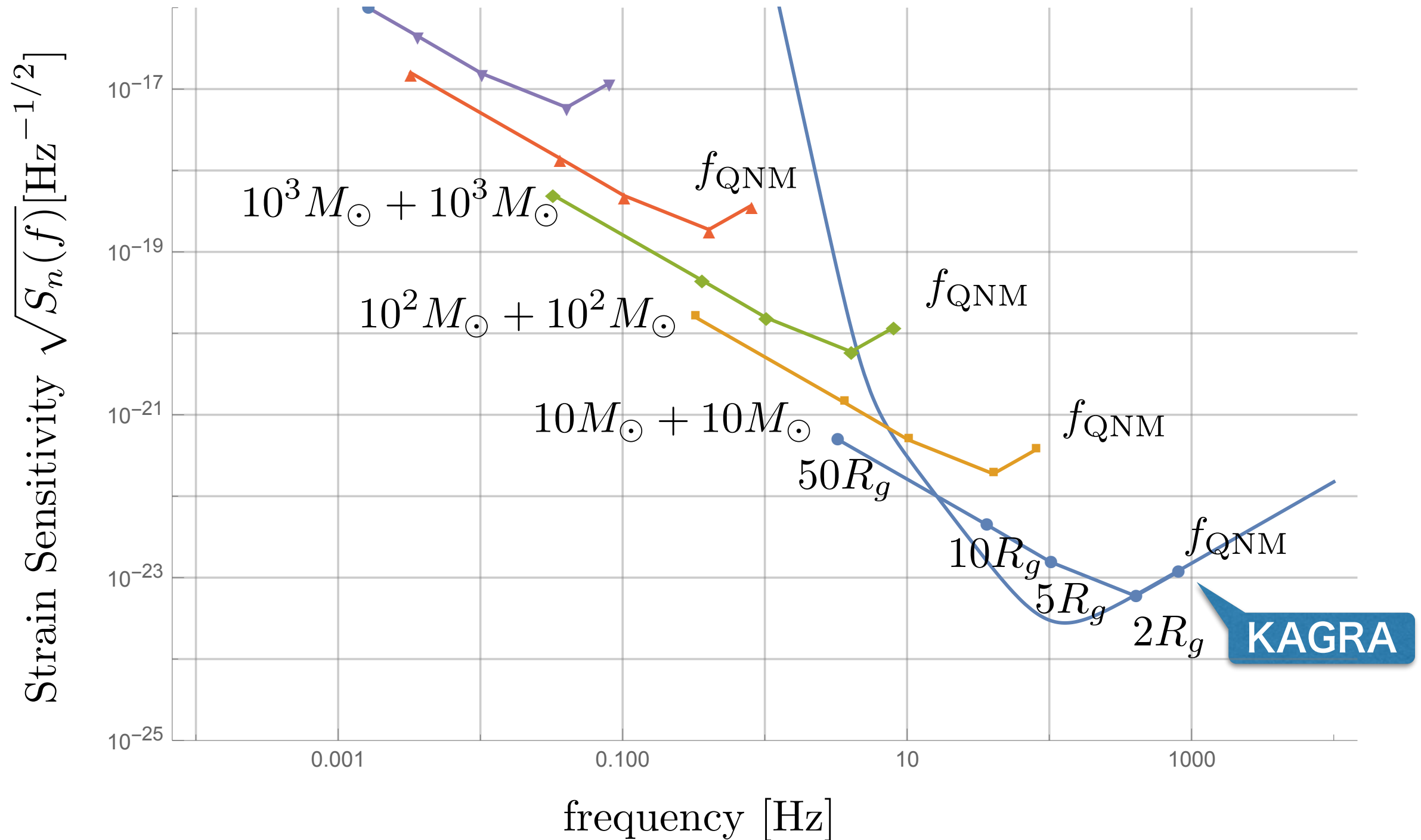
1. Gravitational Wave >> Expected Events

Typical frequency of BH-BH binary merger @ 1000Mpc



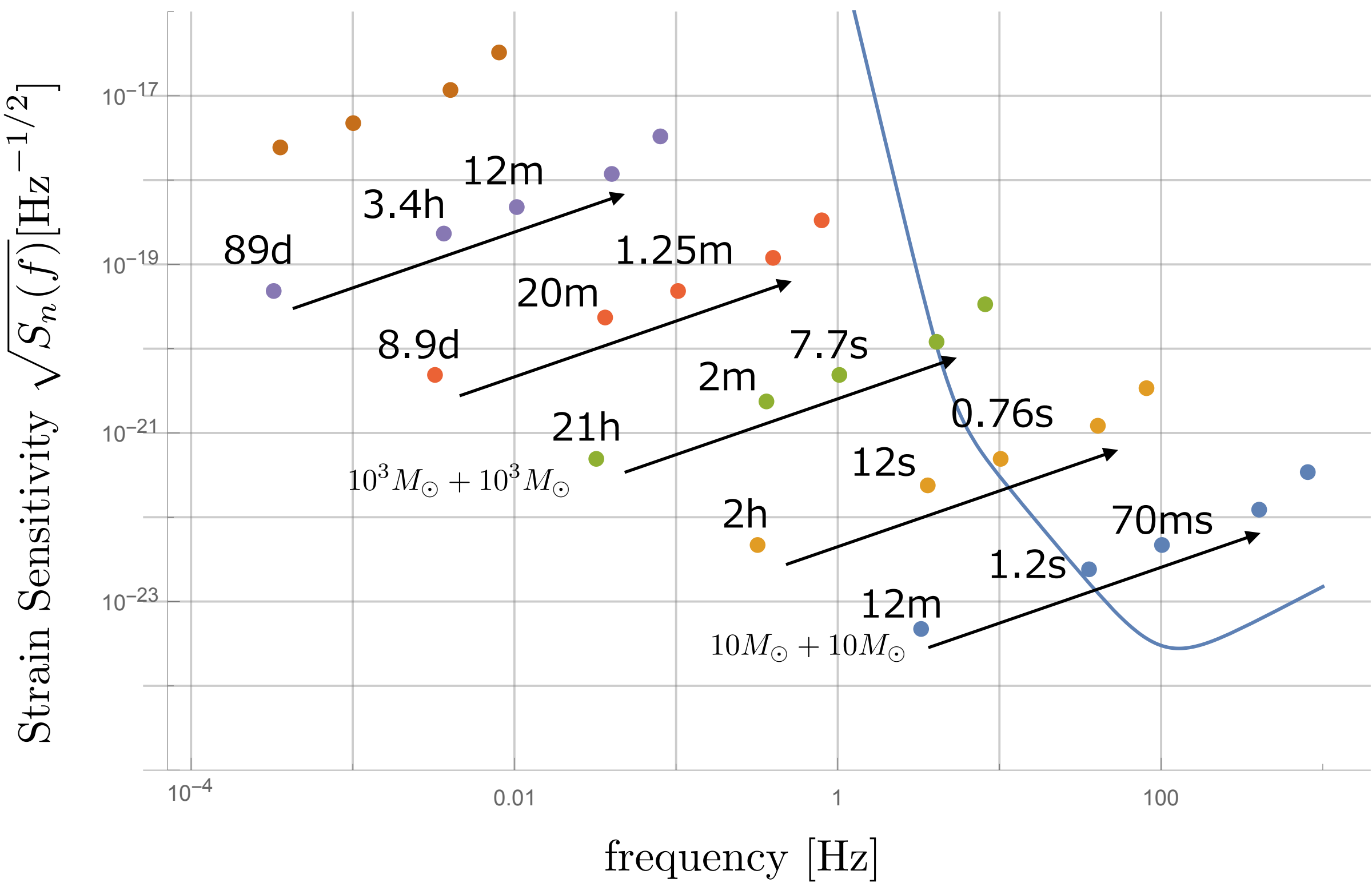
1. Gravitational Wave >> Expected Events

Typical frequency of BH-BH binary merger @ 1000Mpc

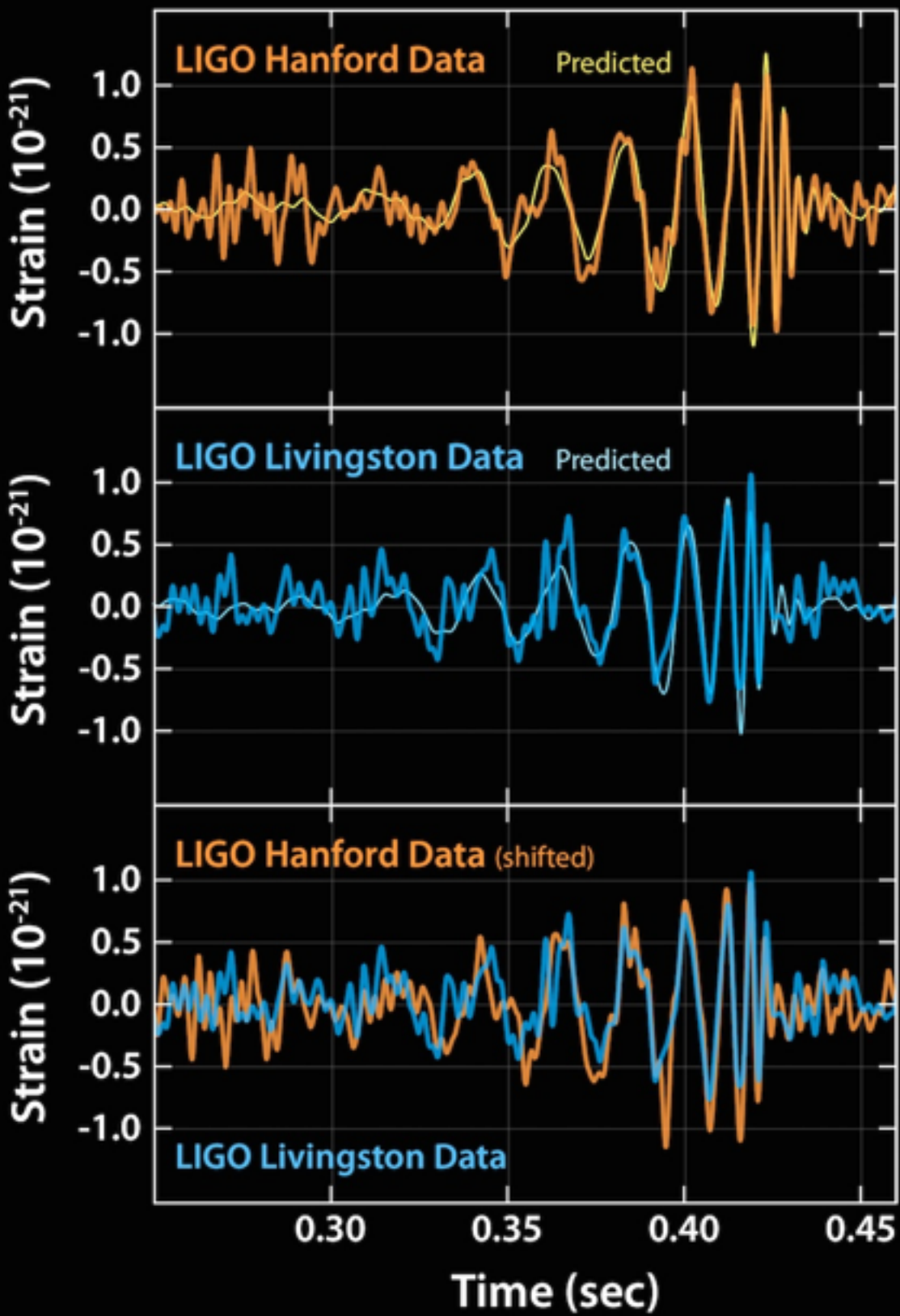


1. Gravitational Wave >> Expected Events

Typical merger duration of BH-BH binary merger @ 1000Mpc



GW150914



GW150914: FACTSHEET

BACKGROUND IMAGES: TIME-FREQUENCY TRACE (TOP) AND TIME-SERIES (BOTTOM) IN THE TWO LIGO DETECTORS; SIMULATION OF BLACK HOLE HORIZONS (MIDDLE-TOP), BEST FIT WAVEFORM (MIDDLE-BOTTOM)

first direct detection of gravitational waves (GW) and first direct observation of a black hole binary

observed by	LIGO L1, H1	duration from 30 Hz	~ 200 ms
source type	black hole (BH) binary	# cycles from 30 Hz	~10
date	14 Sept 2015	peak GW strain	1×10^{-21}
time	09:50:45 UTC	peak displacement of interferometers arms	$\pm 0.002 \text{ fm}$
likely distance	0.75 to 1.9 Gly 230 to 570 Mpc	frequency/wavelength at peak GW strain	150 Hz, 2000 km
redshift	0.054 to 0.136	peak speed of BHs	~ 0.6 c
signal-to-noise ratio	24	peak GW luminosity	$3.6 \times 10^{56} \text{ erg s}^{-1}$
false alarm prob.	< 1 in 5 million	radiated GW energy	$2.5\text{-}3.5 M_{\odot}$
false alarm rate	< 1 in 200,000 yr	remnant ringdown freq.	~ 250 Hz
Source Masses M_{\odot}		remnant damping time	~ 4 ms
total mass	60 to 70	remnant size, area	180 km, $3.5 \times 10^5 \text{ km}^2$
primary BH	32 to 41	consistent with general relativity?	passes all tests performed
secondary BH	25 to 33	graviton mass bound	< $1.2 \times 10^{-22} \text{ eV}$
remnant BH	58 to 67	coalescence rate of binary black holes	2 to 400 $\text{Gpc}^{-3} \text{ yr}^{-1}$
mass ratio	0.6 to 1	online trigger latency	~ 3 min
primary BH spin	< 0.7	# offline analysis pipelines	5
secondary BH spin	< 0.9	CPU hours consumed	~ 50 million (=20,000 PCs run for 100 days)
remnant BH spin	0.57 to 0.72	papers on Feb 11, 2016	13
signal arrival time delay	arrived in L1 7 ms before H1	# researchers	~ 1000, 80 institutions in 15 countries
likely sky position	Southern Hemisphere		
likely orientation resolved to	face-on/off ~600 sq. deg.		

Detector noise introduces errors in measurement. Parameter ranges correspond to 90% credible bounds.

Acronyms: L1=LIGO Livingston, H1=LIGO Hanford; Gly=giga lightyear= $9.46 \times 10^{12} \text{ km}$; Mpc=mega parsec=3.2 million lightyear, Gpc= 10^3 Mpc , fm=femtometer= 10^{-15} m , M_{\odot} =1 solar mass= $2 \times 10^{30} \text{ kg}$

36Msun + 29 Msun
のBHが合体して 62 Msun
(3 Msun分の質量が消失)

13億光年先
(400 ± 170 Mpc)
($z=0.054$ — 0.136)

重力波が検出された！
重力波が検出できた！
BHが存在した！
BH連星が存在した！
相対論が第0近似で正しい！

GW150914: FACTSHEET

BACKGROUND IMAGES: TIME-FREQUENCY TRACE (TOP) AND TIME-SERIES (BOTTOM) IN THE TWO LIGO DETECTORS; SIMULATION OF BLACK HOLE HORIZONS (MIDDLE-TOP), BEST FIT WAVEFORM (MIDDLE-BOTTOM)

first direct detection of gravitational waves (GW) and first direct observation of a black hole binary

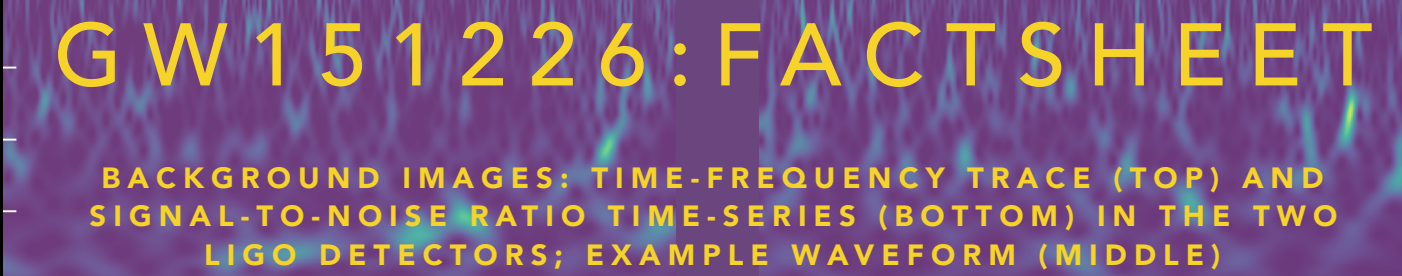
observed by	LIGO L1, H1	duration from 30 Hz	~ 200 ms
source type	black hole (BH) binary	# cycles from 30 Hz	~ 10
date	14 Sept 2015	peak GW strain	1×10^{-21}
time	09:50:45 UTC	peak displacement of interferometers arms	± 0.002 fm
likely distance	0.75 to 1.9 Gly 230 to 570 Mpc	frequency/wavelength at peak GW strain	150 Hz, 2000 km
redshift	0.054 to 0.136	peak speed of BHs	~ 0.6 c
signal-to-noise ratio	24	peak GW luminosity	3.6×10^{56} erg s ⁻¹
false alarm prob.	< 1 in 5 million	radiated GW energy	2.5-3.5 M \odot
false alarm rate	< 1 in 200,000 yr	remnant ringdown freq.	~ 250 Hz
Source Masses M \odot		remnant damping time	~ 4 ms
total mass	60 to 70	remnant size, area	180 km, 3.5×10^5 km ²
primary BH	32 to 41	consistent with general relativity?	passes all tests performed
secondary BH	25 to 33	graviton mass bound	< 1.2×10^{-22} eV
remnant BH	58 to 67	coalescence rate of binary black holes	2 to 400 Gpc ⁻³ yr ⁻¹
mass ratio	0.6 to 1	online trigger latency	~ 3 min
primary BH spin	< 0.7	# offline analysis pipelines	5
secondary BH spin	< 0.9	CPU hours consumed	~ 50 million (=20,000 PCs run for 100 days)
remnant BH spin	0.57 to 0.72	papers on Feb 11, 2016	13
signal arrival time delay	arrived in L1 7 ms before H1	# researchers	~ 1000 , 80 institutions in 15 countries
likely sky position	Southern Hemisphere		
likely orientation resolved to	face-on/off ~ 600 sq. deg.		

Detector noise introduces errors in measurement. Parameter ranges correspond to 90% credible bounds.
Acronyms: L1=LIGO Livingston, H1=LIGO Hanford; Gly=giga lightyear= 9.46×10^{12} km; Mpc=mega parsec=3.2 million lightyear, Gpc= 10^3 Mpc, fm=femtometer= 10^{-15} m, M \odot =1 solar mass= 2×10^{30} kg

GW151226

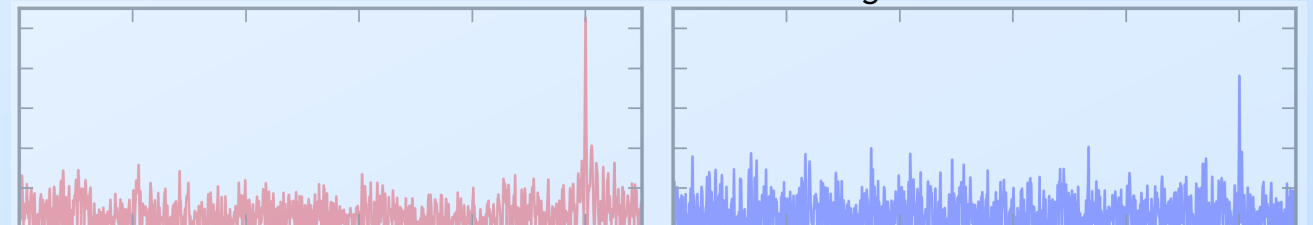
14Msun + 7.5 Msun
のBHが合体して 21 Msun
(1 Msun分の質量が消失)

15億光年先
(440 ± 190 Mpc)
($z=0.05$ — 0.13)

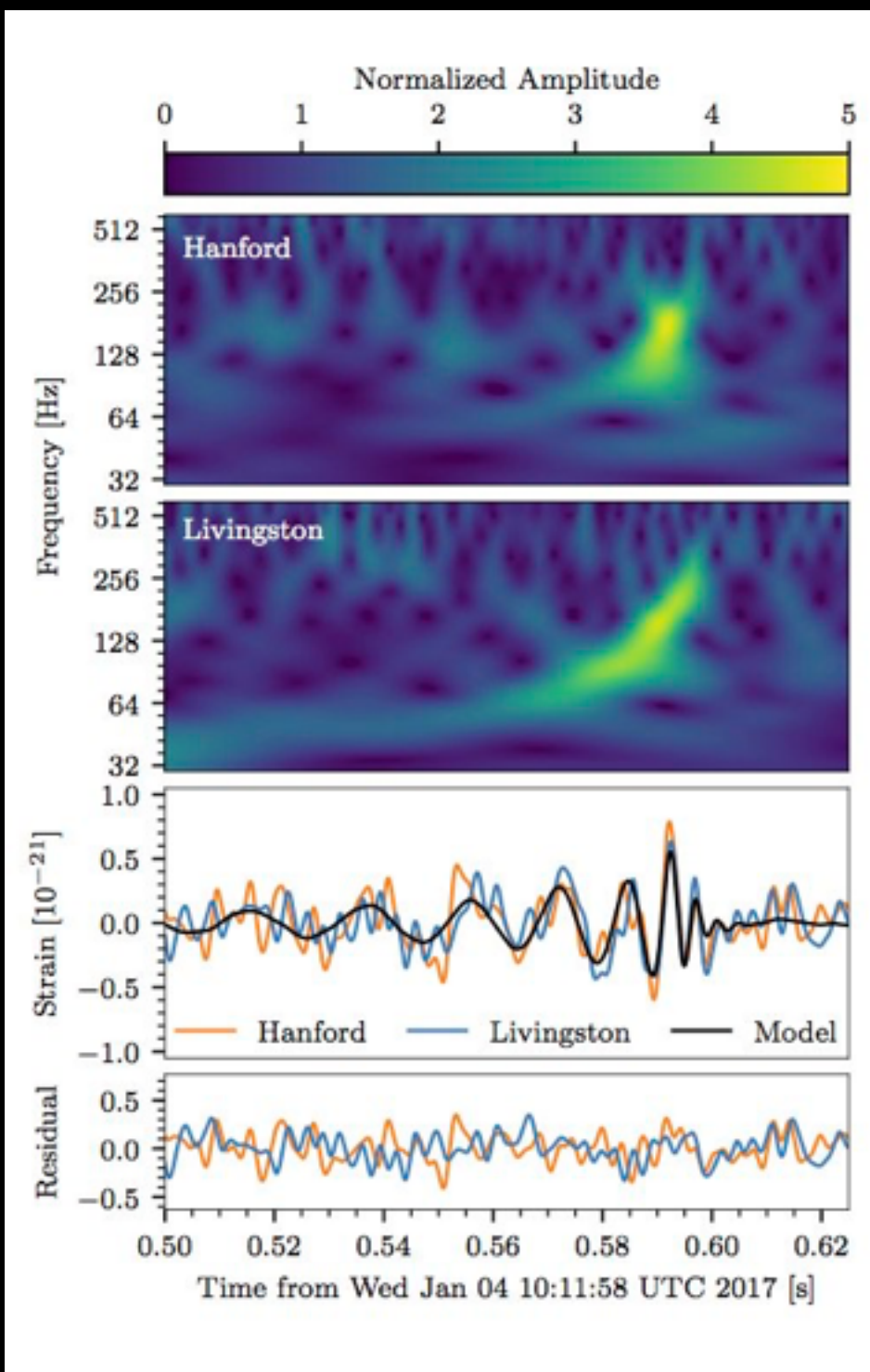


observed by	LIGO L1, H1	duration from 35 Hz	~ 1 s
source type	black hole (BH) binary	# cycles from 35 Hz	~ 55
date	26 Dec 2015	signal arrival time delay	arrived in H1 1 ms after L1
time	03:38:53 UTC		
distance	250 to 620 Mpc	peak GW strain	$\sim 3.4 \times 10^{-22}$
redshift	0.05 to 0.13	peak displacement of interferometers arms	$\sim \pm 0.7$ am
signal-to-noise ratio	13	frequency/wavelength at peak GW strain	420 Hz, 710 km
false alarm prob.	~ 1 in 10 million	peak speed of BHs	~ 0.6 c
Source Masses M_\odot		peak GW luminosity	2 to 4×10^{56} erg s $^{-1}$
total mass	20 to 28	radiated GW energy	0.8 – 1.1 M_\odot
primary BH	11 to 23	remnant ringdown freq.	~ 750 Hz
secondary BH	5 to 10	remnant damping time	0.00 – ~ 1.3 ms
remnant BH	19 to 27	remnant size, area	60 km, 3.5×10^4 km 2
(Reconstructed (template))		online trigger latency	~ 67 s
mass ratio	> 0.28	# offline analysis pipelines	2
spin of one of the black holes	> 0.2		
remnant BH spin	0.7 to 0.8		
resolved to	~850 sq. deg.		

Parameter ranges correspond to 90% credible bounds. Acronyms: L1/H1=LIGO Livingston/Hanford; Mpc=mega parsec=3.2 million lightyear, am=attometer= 10^{-18} m, M_\odot =1 solar mass= 2×10^{30} kg



GW170104



GW170104: FACTSHEET

Background Images: time-frequency trace (top), H1 and L1 time series and maximum-likelihood binary black hole model (middle top), residuals between data and best-fit model (middle bottom), reconstructed waveforms from wavelet and binary black hole analyses (bottom)

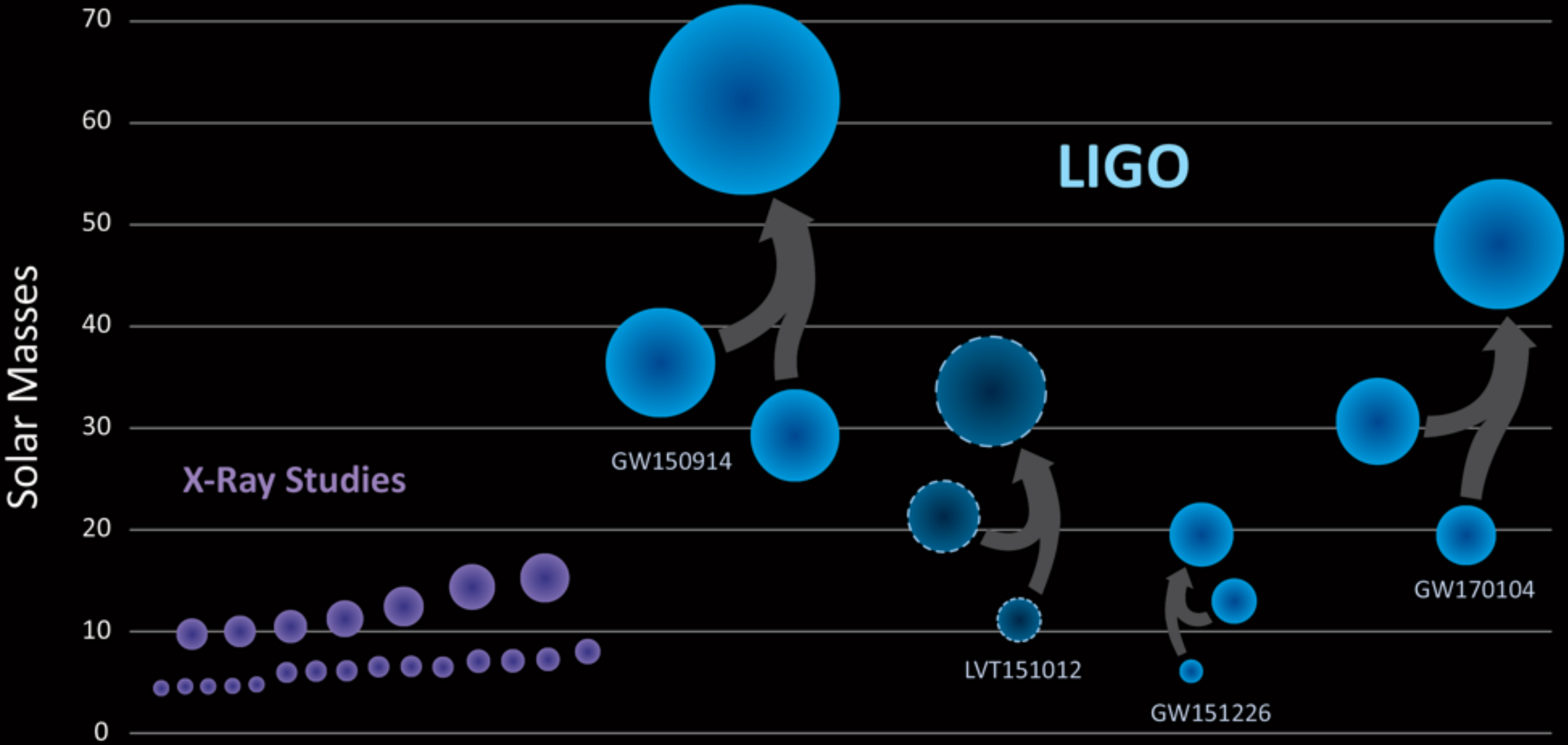
observed by	LIGO L1, H1	duration from 30 Hz	~ 0.25 to 0.31 s
source type	black hole (BH) binary	# of cycles from 30 Hz	~ 14 to 16
date	04 Jan 2017	signal arrival time delay	arrived at H1 3 ms before L1
time	10:11:58.6 UTC	credible region sky area	1200 sq. deg.
signal-to-noise ratio	13	peak GW strain	$\sim 5 \times 10^{-22}$
false alarm rate	< 1 in 70,000 years	peak displacement of interferometer arm	$\sim \pm 1$ am
probability of astrophysical origin	> 0.99997	frequency at peak GW strain	160 to 199 Hz
distance	1.6 to 4.3 billion light-years	wavelength at peak GW strain	1510 to 1880 km
redshift	0.10 to 0.25	peak GW luminosity	1.8 to 3.8×10^{56} erg s $^{-1}$
total mass	46 to 57 M $_{\odot}$	radiated GW energy	1.3 to 2.6 M $_{\odot}$
primary BH mass	25 to 40 M $_{\odot}$	remnant ringdown freq.	297 to 373 Hz
secondary BH mass	13 to 25 M $_{\odot}$	remnant damping time	2.5 to 3.2 ms
mass ratio	0.36 to 0.94	consistent with general relativity?	passes all tests performed
remnant BH mass	44 to 54 M $_{\odot}$	graviton mass combined bound	$\leq 7.7 \times 10^{-23}$ eV/c 2
remnant BH spin	0.39 to 0.7	evidence for dispersion of GWs	none
remnant size (effective radius)	123 to 150 km		
remnant area	1.9 to 2.8×10^5 km 2		
effective spin parameter	-0.42 to 0.09		
effective precession spin parameter	unconstrained		

Parameter ranges correspond to 90% credible intervals.

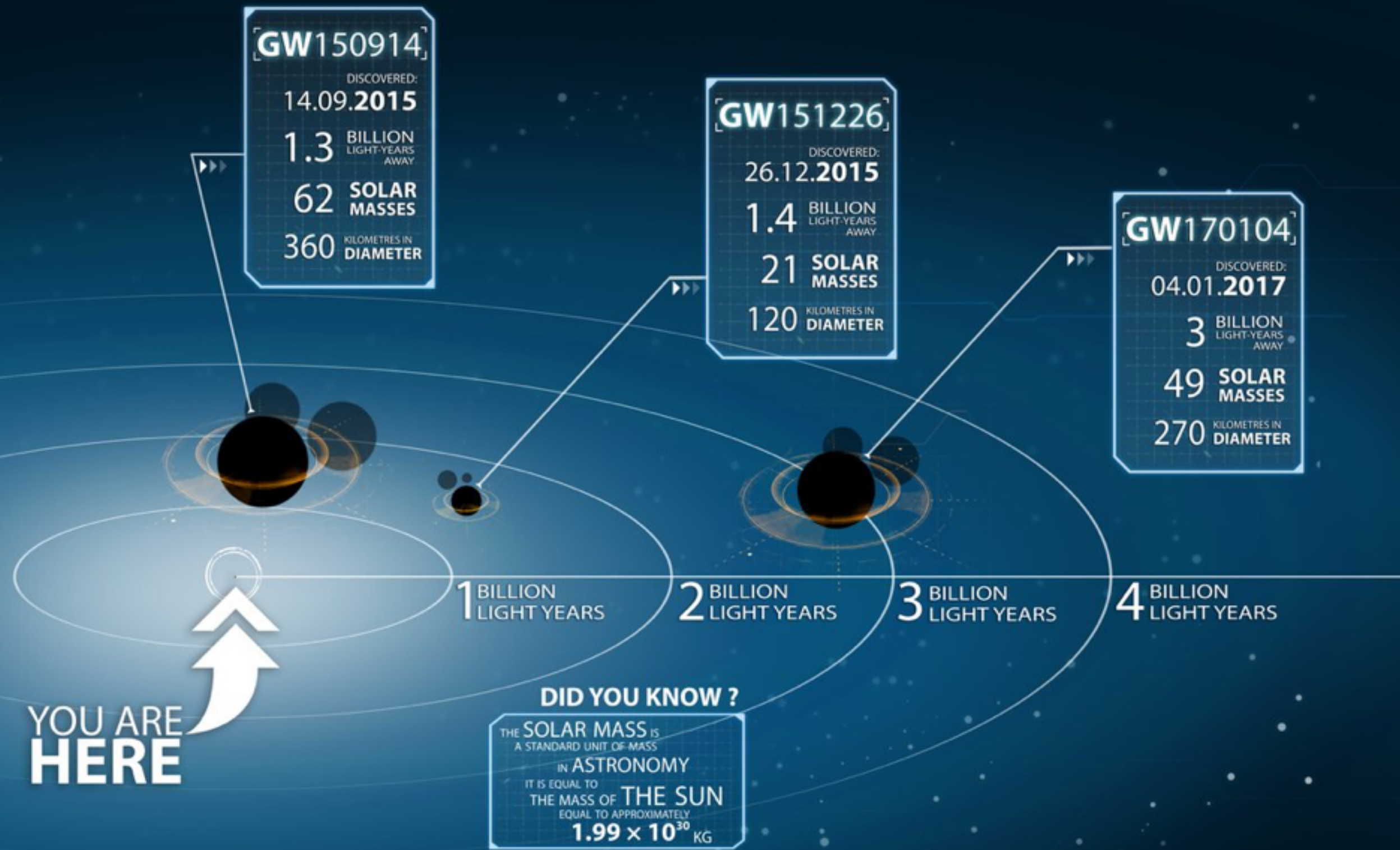
Acronyms:

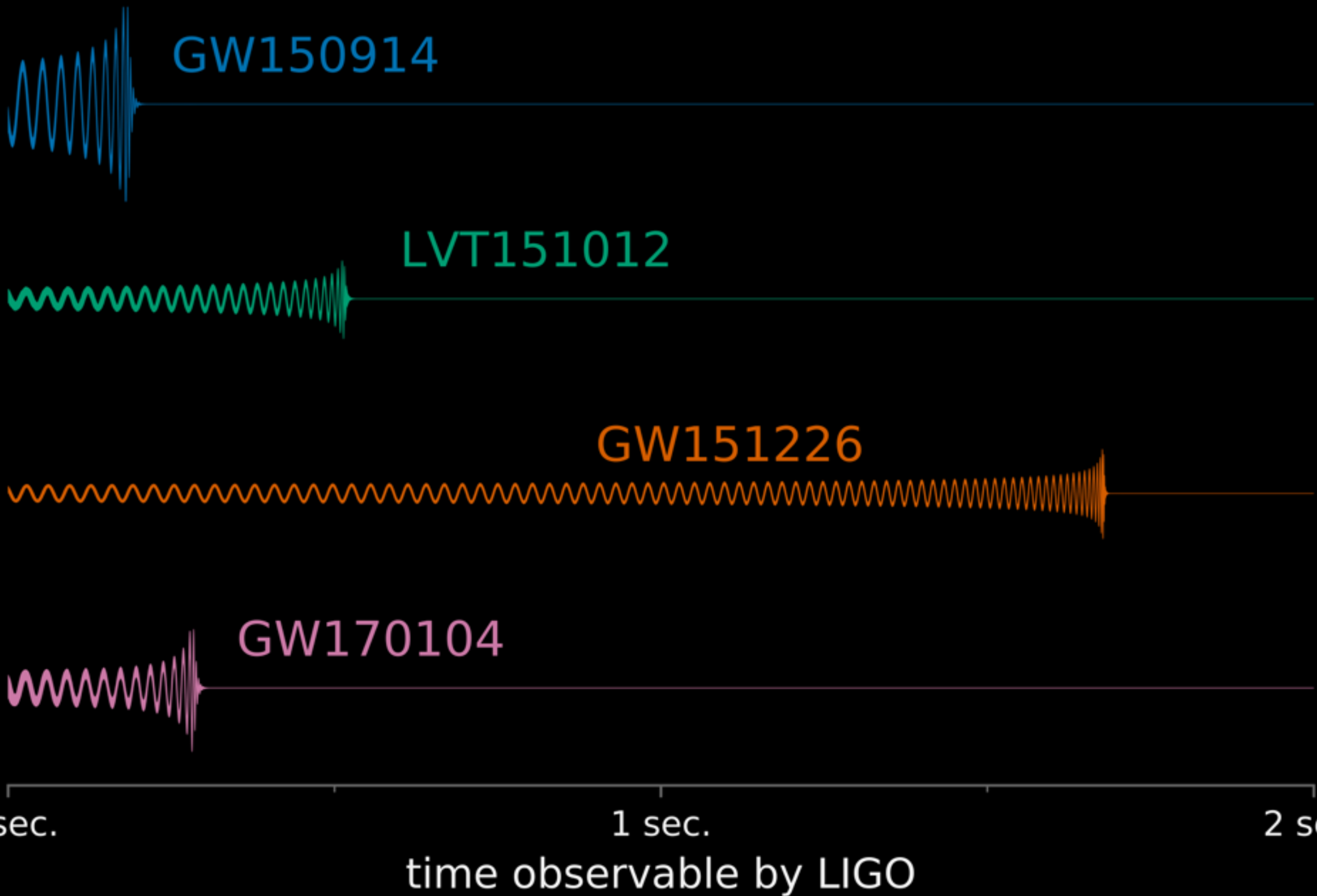
L1/H1=LIGO Livingston/Hanford, am=attometer= 10^{-18} m, M $_{\odot}$ =1 solar mass= 2×10^{30} kg

Black Holes of Known Mass



LIGO'S GRAVITATIONAL-WAVE DETECTIONS

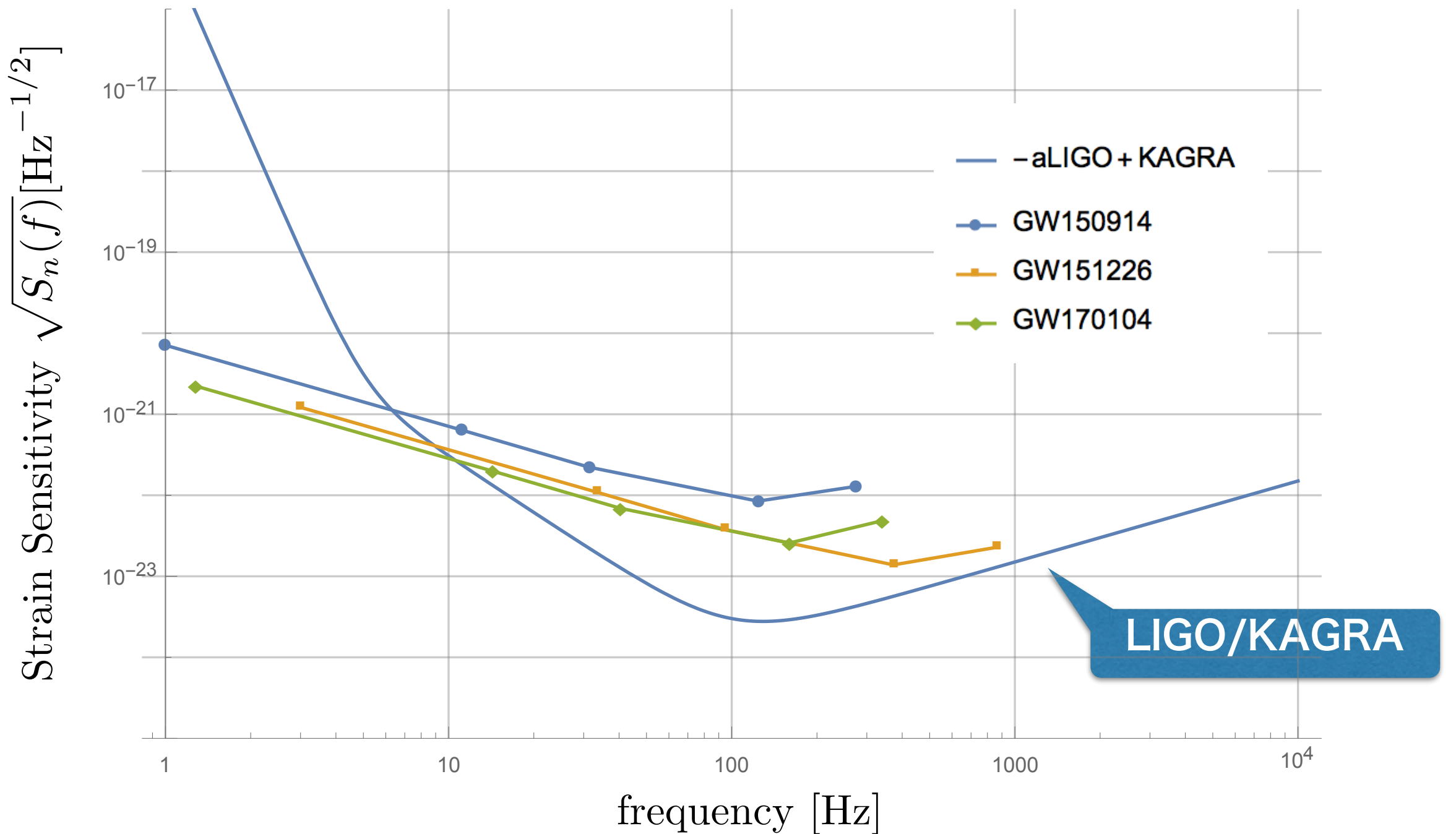


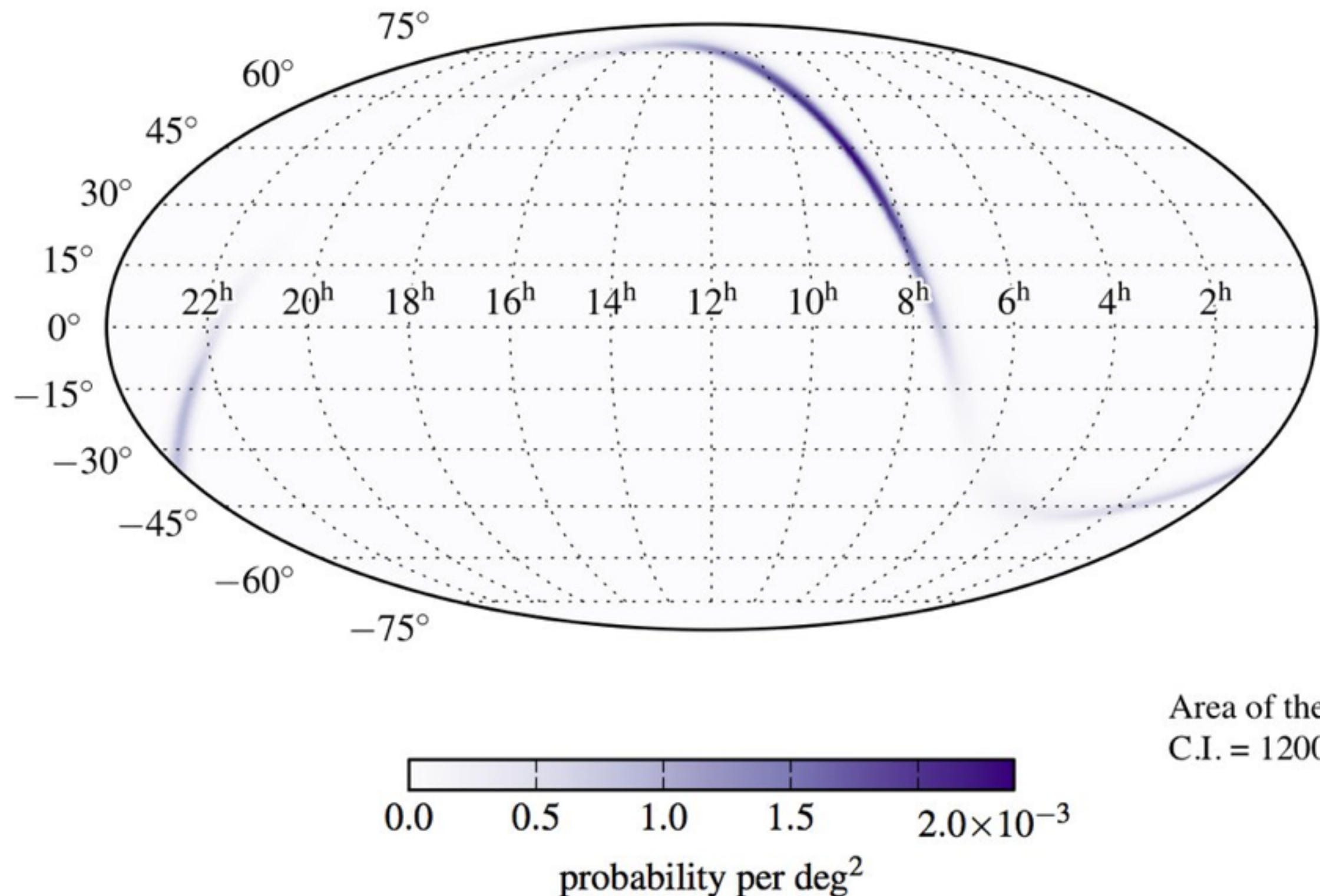


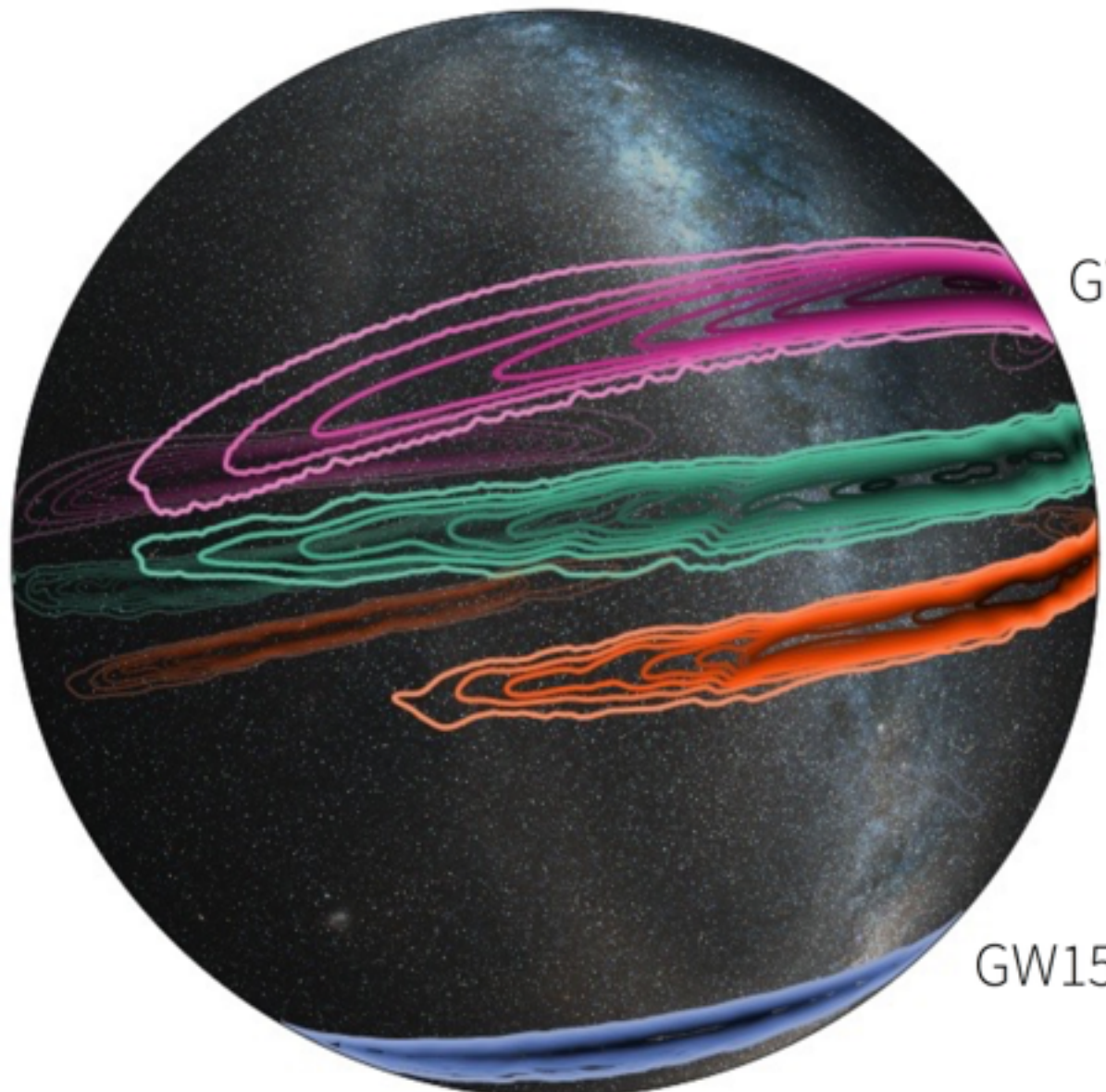
Comparison of gravitational-wave signal templates from recent LIGO observations. This figure shows reconstructions of the three confident and one candidate (LVT151012) gravitational wave signals detected by LIGO to date, including the most recent detection GW170104. Each row shows the signal arriving at the Hanford detector as a function of time. The thickness of the curves indicates the 90% confidence interval on the model parameters. Only the portion of each signal that LIGO was sensitive to is shown here (the final seconds leading up to the black hole merger). [Credit: LIGO/B. Farr (U. Chicago)] - See more at: <http://ligo.org/detections/GW170104.php#sthash.QTJlckcl.dpuf>

1. Gravitational Wave >> Expected Events

Observed BH-BH binary mergers







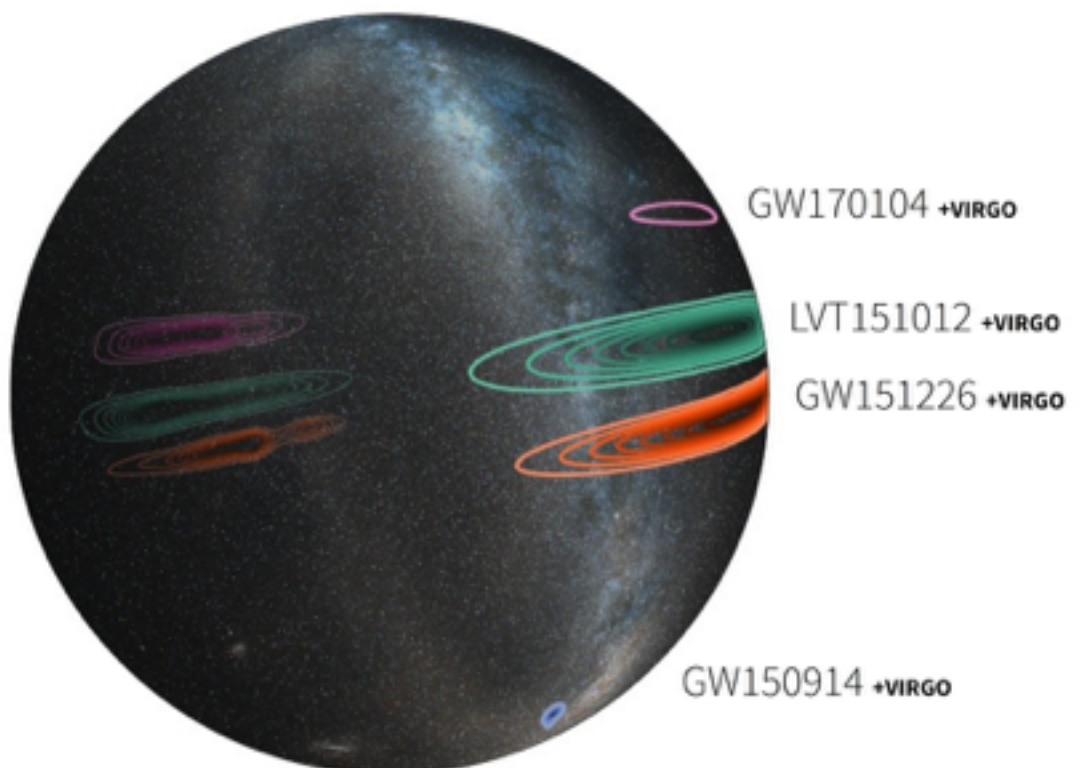
GW170104

LVT151012

GW151226

GW150914

Sky Map of LIGO's Black-Hole Mergers. This three-dimensional projection of the Milky Way galaxy onto a transparent globe shows the probable locations of the three confirmed LIGO black-hole merger events—GW150914 (blue), GW151226 (orange), and the most recent detection GW170104 (magenta)—and a fourth possible detection, at lower significance (LVT151012, green). The outer contour for each represents the 90 percent confidence region; the innermost contour signifies the 10 percent confidence region. [Image credit: LIGO/Caltech/MIT/Leo Singer (Milky Way image: Axel Mellinger)] - See more at: <http://ligo.org/detections/GW170104.php#sthash.pwWdVLL4.dpuf>



Forecasting LIGO Detections in the Three-Detector Era. This map illustrates how the addition of the Virgo detector, scheduled to come online this summer, could improve the localization of sources of gravitational waves. The map shows the estimated locations of the four black-hole merger events detected by LIGO to date (including one event seen at lower significance), after including hypothetical Virgo data. Outer contours represent the 90 percent confidence region; innermost contours signify the 10 percent confidence region. [Image credit: LIGO/Caltech/MIT/Leo Singer (Milky Way image: Axel Mellinger)] - See more at: <http://ligo.org/detections/GW170104.php#sthash.NZPaW2LT.dpuf>

		M1+M2=Mf, Mdiff/Mtotal a_final	Mpc z	SNR	deg^2
GW150914	PRL116, 061102 (2016/2/11)	36.2+29.1=62.3+3.0 4.59% 0.68	410Mpc 0.09	24	600
LVT151012	(2016/2/11)	23+13=35+1.5 2.78% 0.66			
GW151226	PRL116, 241103 (2016/6/15)	14.2+7.5=20.8+0.9 4.15% 0.74	440Mpc 0.09	13	850
GW170104	PRL118, 221101 (2017/6/1)	31.2+19.4=48.7+1.9 3.75% 0.64	880Mpc 0.18	13	1300

<https://losc.ligo.org/events/GW150914/>

<https://losc.ligo.org/events/LVT151012/>

<https://losc.ligo.org/events/GW151226/>

<https://losc.ligo.org/events/GW170104/>

APPENDIX B: SIMULATION RANKINGS

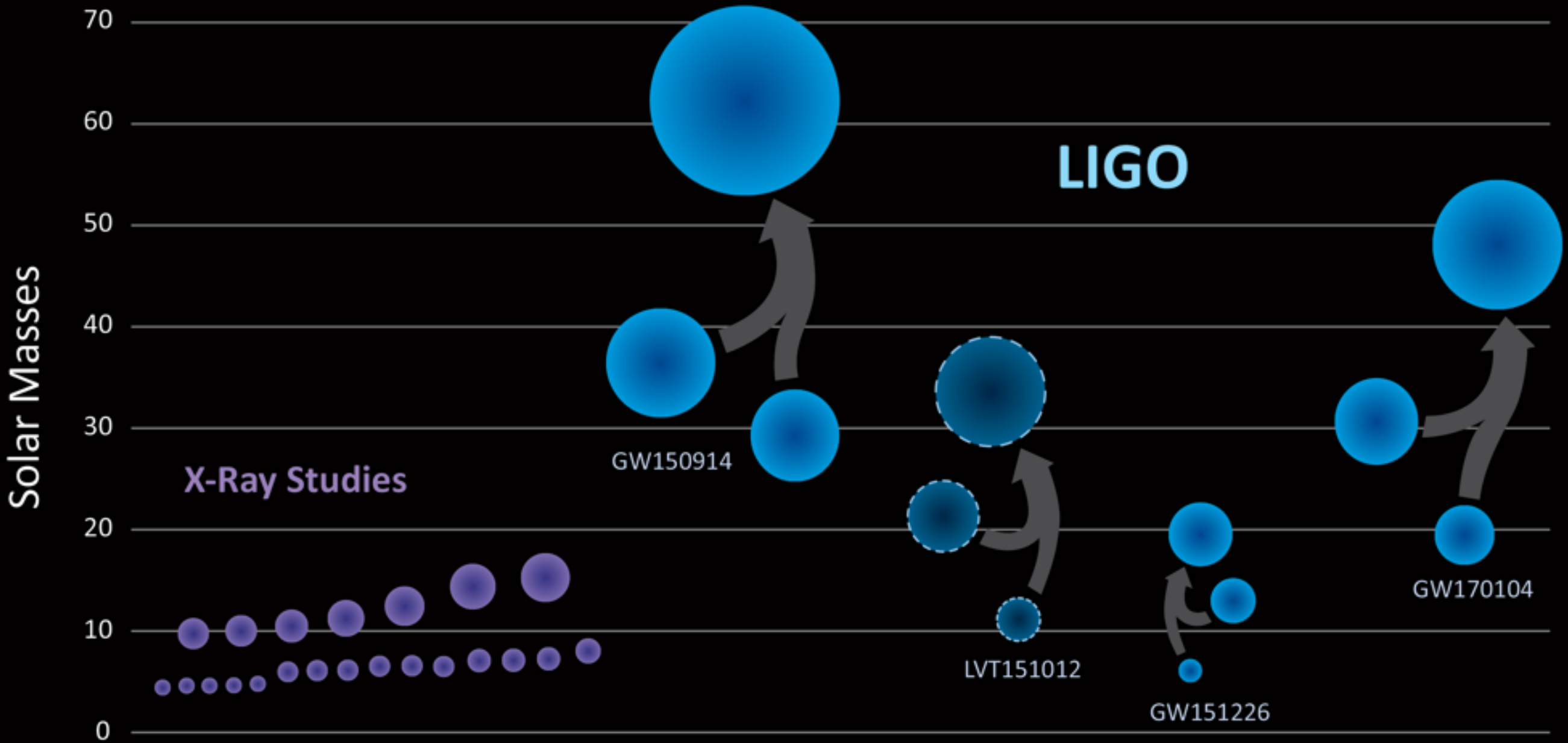
In this appendix, we enumerate the simulations used in this work, ordered by one measure of their similarity with the data ($\ln L$, in Table III). For nonprecessing binaries, Fig. 6 provides a visual illustration of some trends in $\ln L$ versus mass ratio and the two component spins.

TABLE III. *Peak Marginalized $\ln L$ I: Consistency between simulations:* Peak value of the marginalized log likelihood $\ln L$ [Eq. (7)] evaluated using a lower frequency $f_{\text{low}} = 30$ Hz and all modes with $l \leq 2$; the simulation key, described in Table II [an asterisk (*) denotes a new simulation motivated by GW150914, and a (+) denotes one of the simulations reported in [LVC-detect](#) [1]]; the *initial* spins of the simulation (using – to denote zero, to enhance readability); the initial χ_{eff} ; the total (redshifted) mass of the best fit; and the starting frequency (in Hz) of the best fit. Though omitting information accessible to the longest simulations, this choice of low-frequency cutoff eliminates systematic biases associated with simulation duration, which differs across our archive, as seen by the last column.

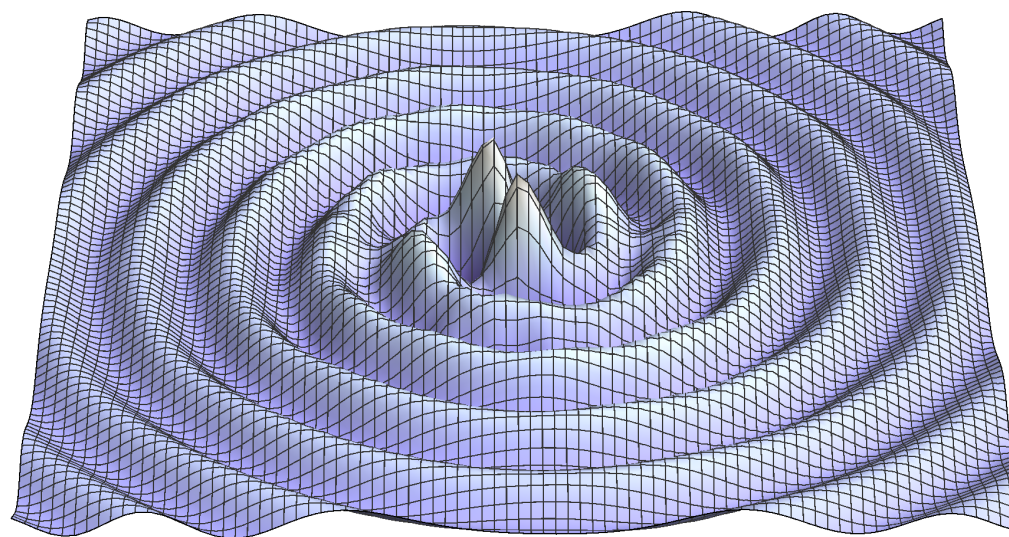
$\ln L$	Key	q	$\chi_{1,x}$	$\chi_{1,y}$	$\chi_{1,z}$	$\chi_{2,x}$	$\chi_{2,y}$	$\chi_{2,z}$	χ_{eff}	M_z/M_\odot	$f_{\text{start}}(\text{Hz})$
272.2	SXS:BBH:0310(*)	1.221	0.00	73.0	15.1
272.1	D12_q1.00_a-0.25_0.25_n100(*)	1.0	0.250	-0.250	-0.00	73.2	20.5
272.1	SXS:BBH:0002[S]	1.0	0.00	73.2	10.0
271.8	D11_q0.75_a0.0_0.0_n100(*)	1.333	-0.00	72.1	23.1
271.8	SXS:BBH:0305(*+)	1.221	0.330	-0.440	-0.02	74.2	14.8
271.6	SXS:BBH:0218	1.0	-0.500	0.500	0.00	73.3	10.6
271.6	SXS:BBH:0198	1.202	0.00	73.4	12.7
271.6	SXS:BBH:0307(*)	1.228	0.320	-0.580	-0.08	70.0	17.0
271.6	GT:BBH:476	1.0	-0.200	-0.200	-0.20	67.9	24.3
271.6	S0_D10.04_q1.3333_a0.45_-0.80_n100	1.334	0.450	-0.801	-0.09	71.9	27.9
271.5	D12.00_q0.85_a0.0_0.0_n100(*)	1.176	-0.00	73.0	20.6
271.5	D12.25_q0.82_a-0.44_0.33_n100(*+)	1.22	0.330	-0.440	-0.02	72.9	20.2
271.5	SXS:BBH:0312(*)	1.203	0.390	-0.480	-0.00	73.9	14.8
271.4	SXS:BBH:0127	1.34	0.010	-0.077	-0.017	-0.061	-0.065	-0.179	-0.09	71.5	14.3
271.4	SXS:BBH:0115	1.07	0.019	0.013	-0.204	0.243	-0.067	0.291	0.04	74.1	13.8
271.3	SXS:BBH:0213	1.0	-0.800	0.800	0.00	73.2	11.7
271.3	UD_D10.01_q1.00_a0.4_n100	1.0	0.400	-0.400	-0.00	73.4	26.7
271.2	D12_q1.00_a-0.25_0.00_n100(*)	1.0	-0.250	-0.12	69.4	21.8
271.2	SXS:BBH:0222	1.0	-0.300	-0.15	69.1	12.3
271.2	SXS:BBH:0217	1.0	-0.600	0.600	0.00	73.2	11.9

Black Holes of Known Mass

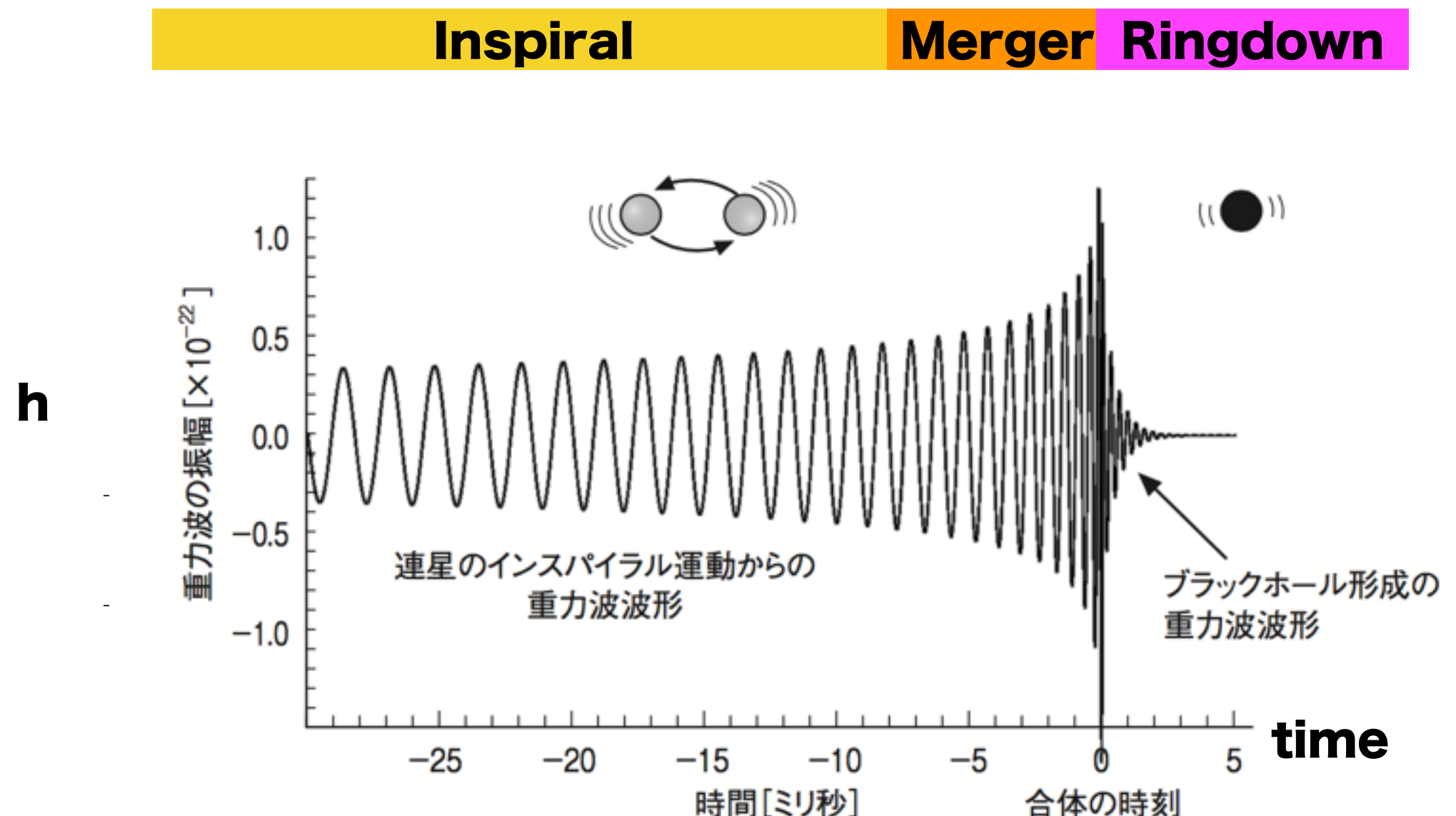
why not more?



1. Gravitational Wave >> Expected Waveform

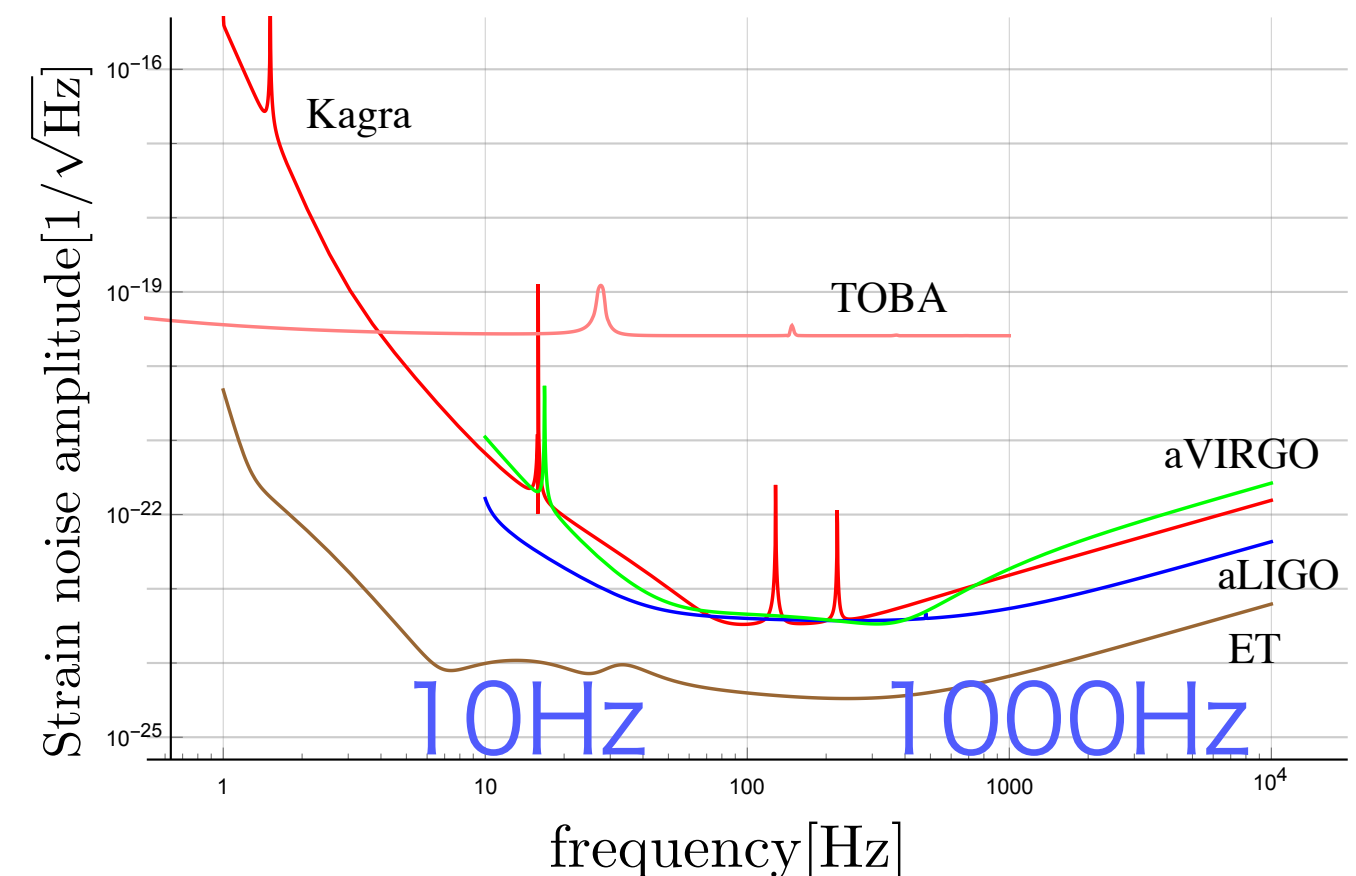
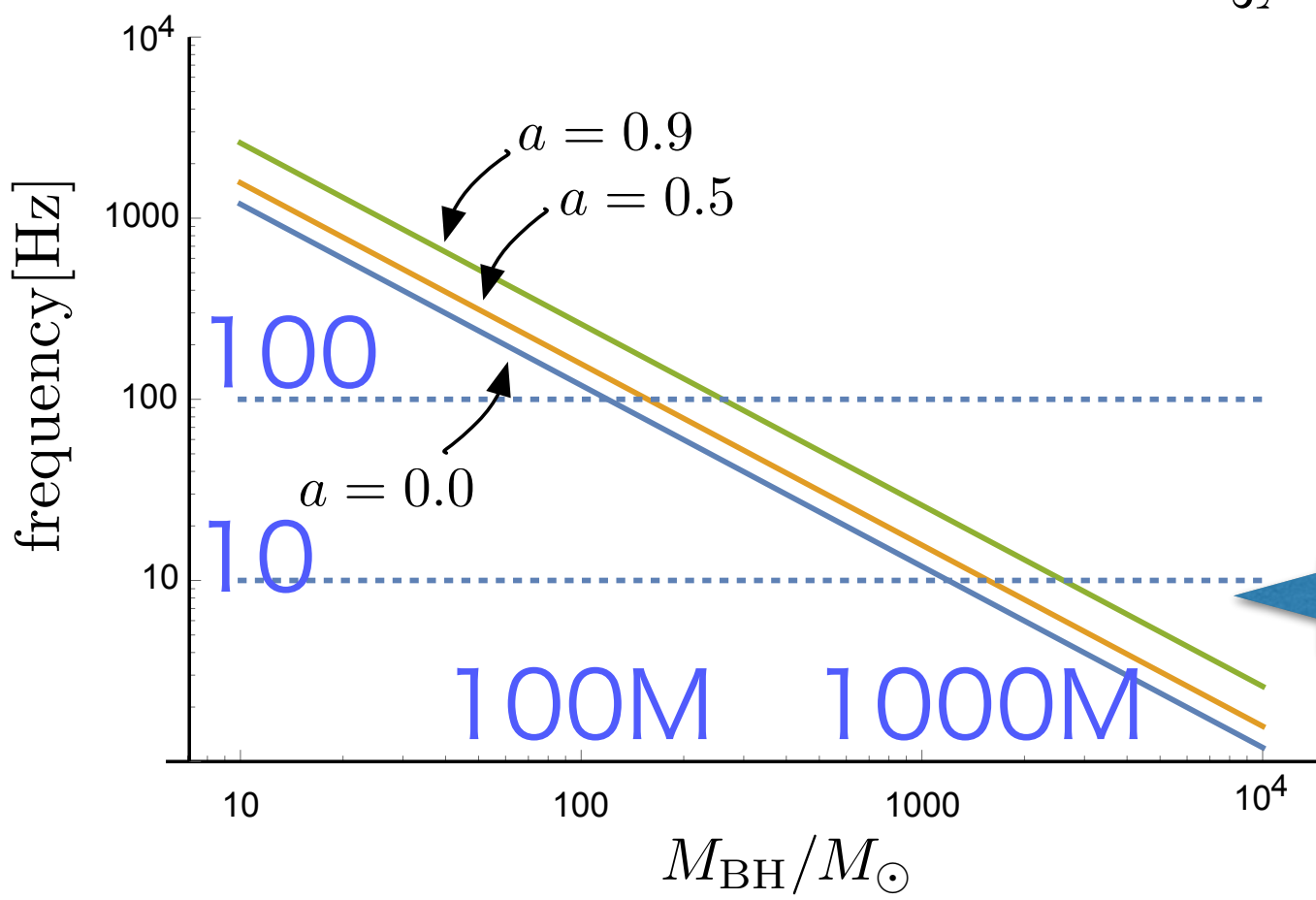


NS-NS
NS-BH
BH-BH



IMBH ringdown freq. is detectable at LIGO/KAGRA

BH quasi-normal freq.
(ringdown freq.)



$$f_{\text{qnm}} = \frac{c^3}{2\pi G M_T} (1 - 0.63(1 - a)^{0.3})$$

BH $< 2000M_{\odot}$ can be a target

contents

1. Gravitational Waves

Detectors, GW events

2. Models of SMBH

hierarchical growth model, or others

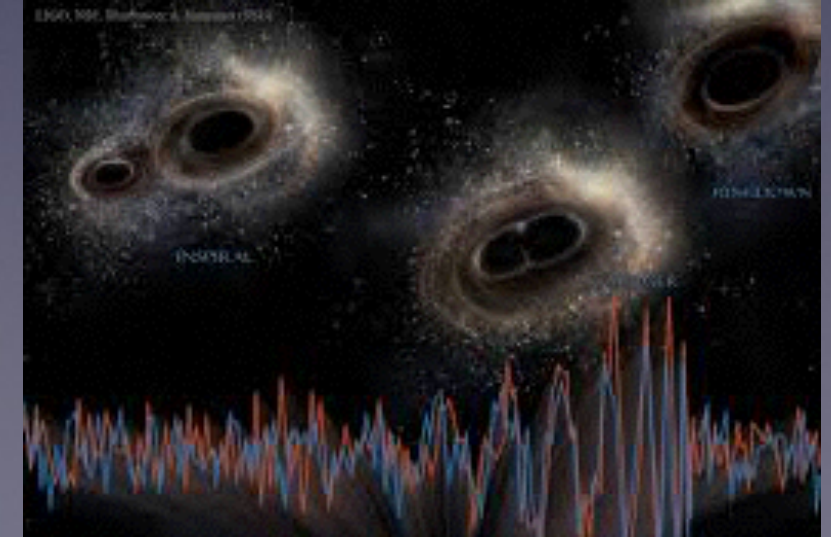
3. Counting BHs

How many BHs in a galaxy?

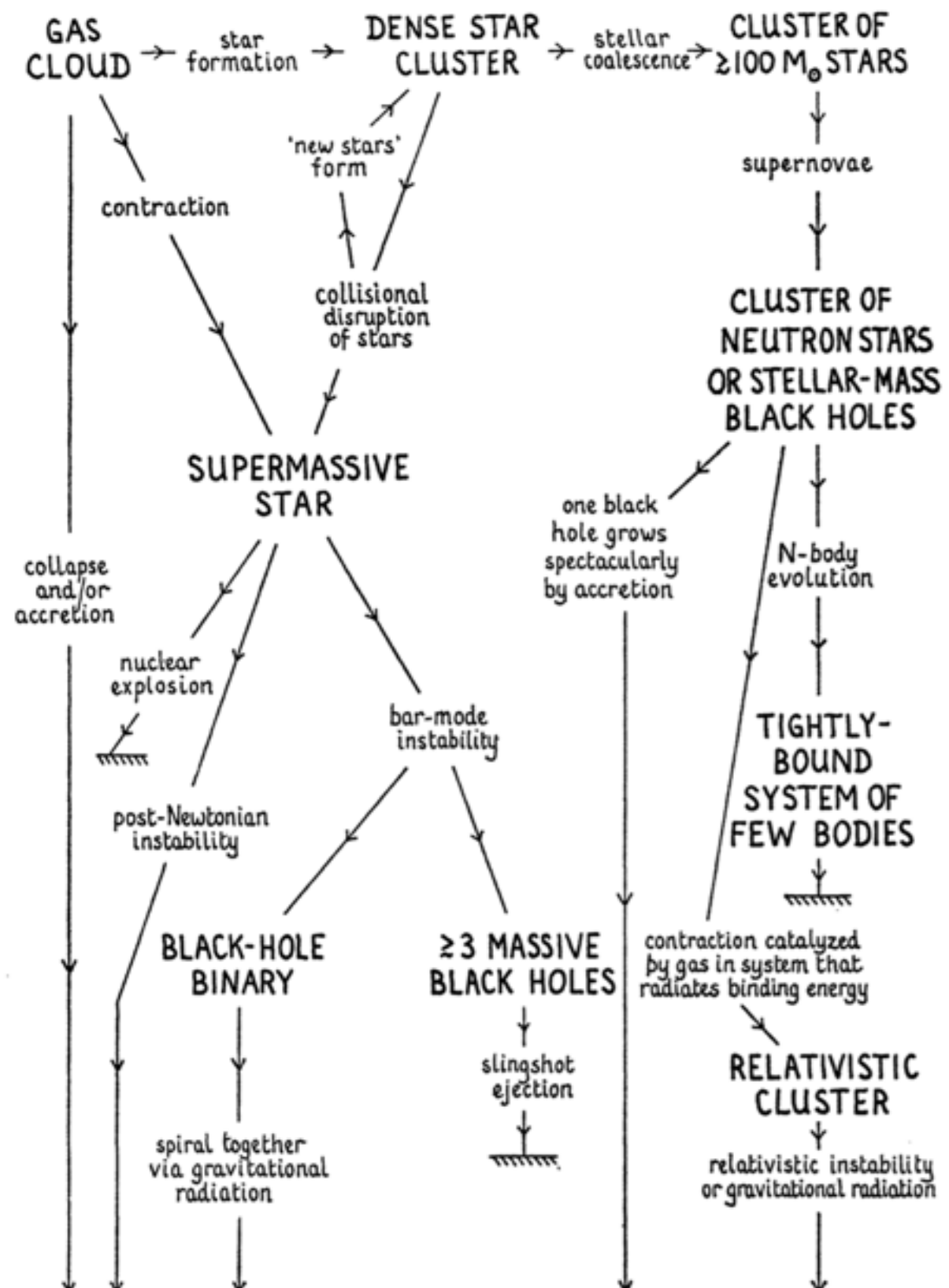
How many galaxies in the Universe?

4. Event Rates at aLIGO/KAGRA/DECIGO/LISA

How many BH mergers in the Universe?



2. Models of SMBH



massive black hole

2. Models of SMBH

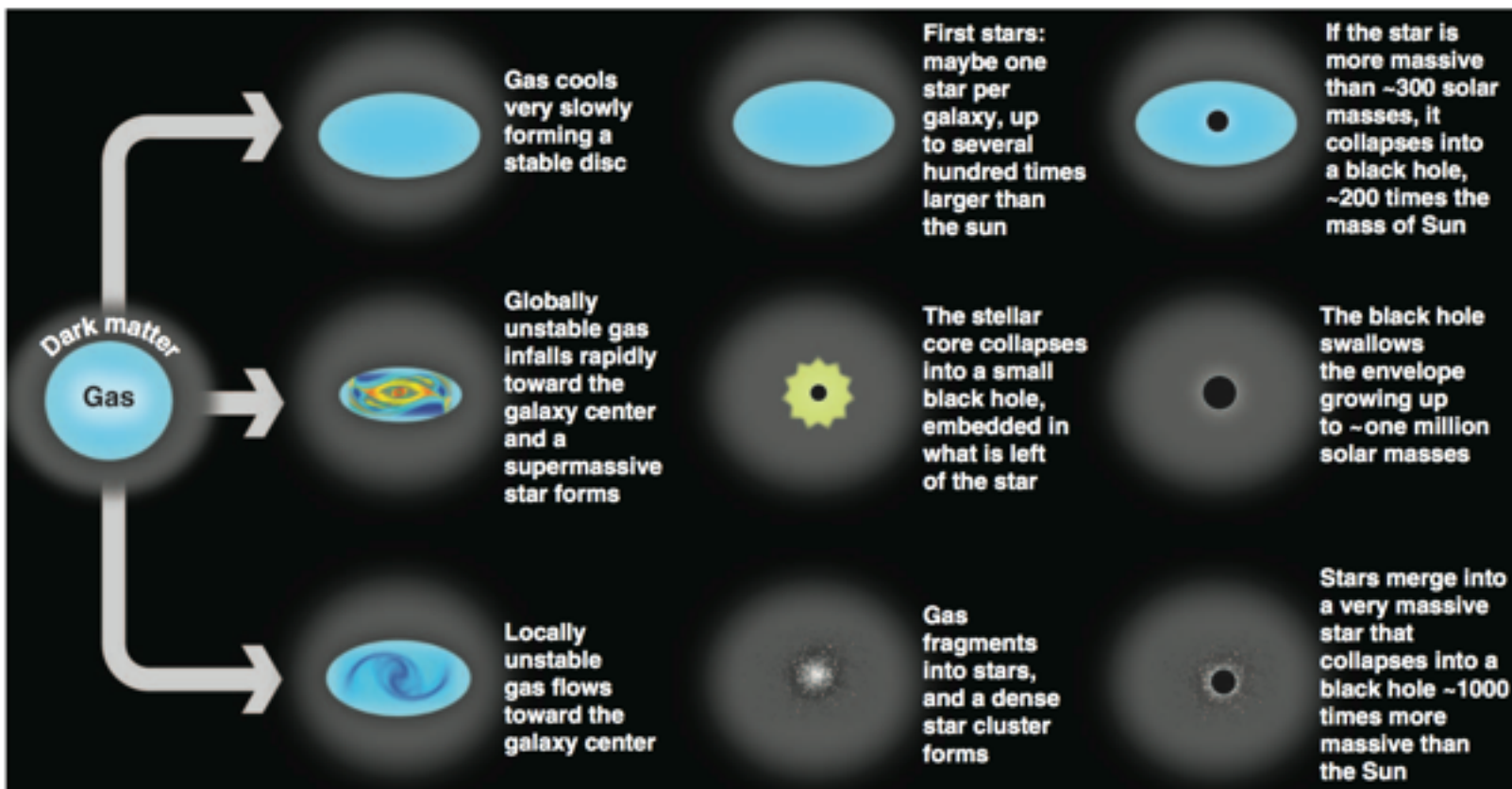


Fig. 1. Illustration showing three pathways to MBH formation that can occur in a distant galaxy (56). The starting point is a primeval galaxy, composed of a dark matter halo and a central condensation of gas. Most of this gas will eventually form stars and contribute to making galaxies as we know them. However, part of this gas has also gone into making a MBH, probably following one of these routes.

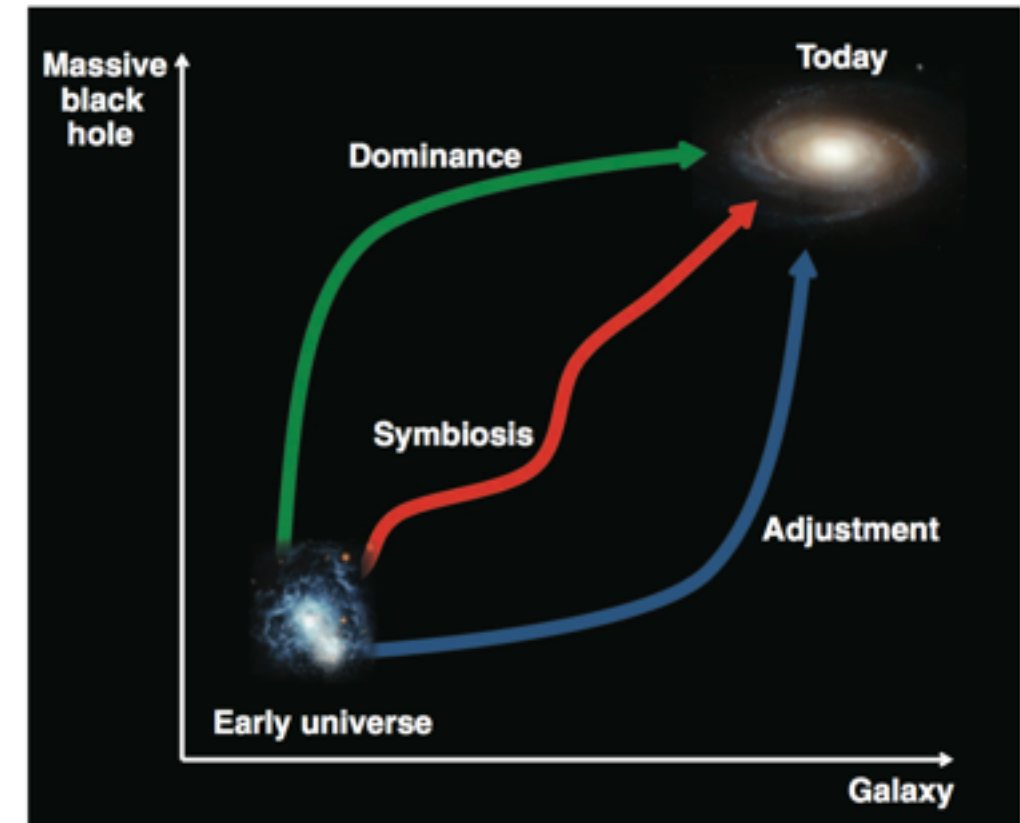


Fig. 3. Possible routes to MBH and galaxy coevolution, starting from black holes forming in distant galaxies in the early universe. [Image credits: NASA, European Space Agency (ESA), A. Aloisi (Space Telescope Science Institute and ESA, Baltimore, MD), and The Hubble Heritage Team (Space Telescope Science Institute/Association of Universities for Research in Astronomy)]

REVIEW

The Formation and Evolution of Massive Black Holes

M. Volonteri^{1,2}

The past 10 years have witnessed a change of perspective in the way astrophysicists think about massive black holes (MBHs), which are now considered to have a major role in the evolution of galaxies. This appreciation was driven by the realization that black holes of millions of solar masses and above reside in the center of most galaxies, including the Milky Way. MBHs also powered active galactic nuclei known to exist just a few hundred million years after the Big Bang. Here, I summarize the current ideas on the evolution of MBHs through cosmic history, from their formation about 13 billion years ago to their growth within their host galaxies.

Volonteri, Science 337 (2012) 544

2. Models of SMBH

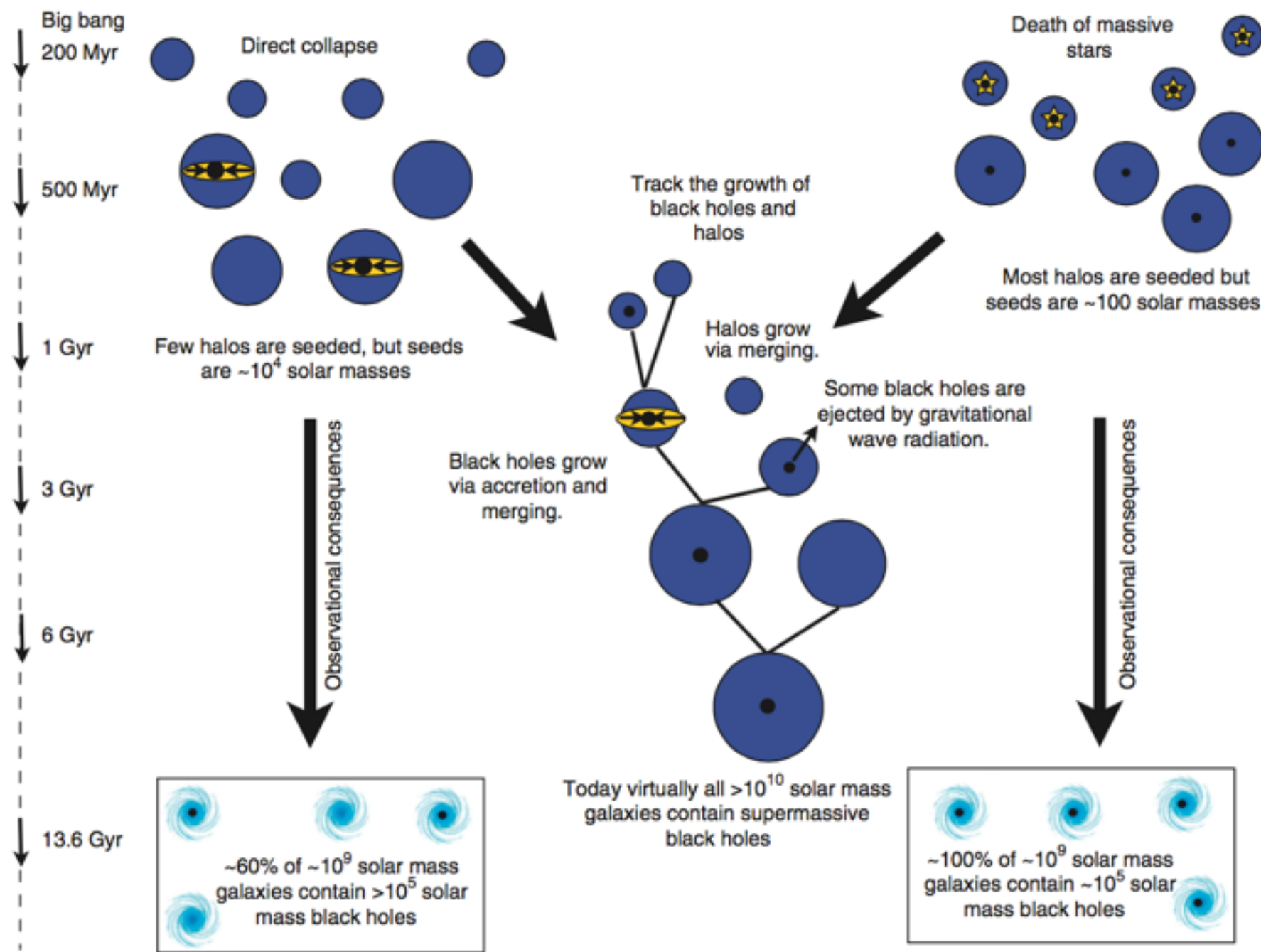
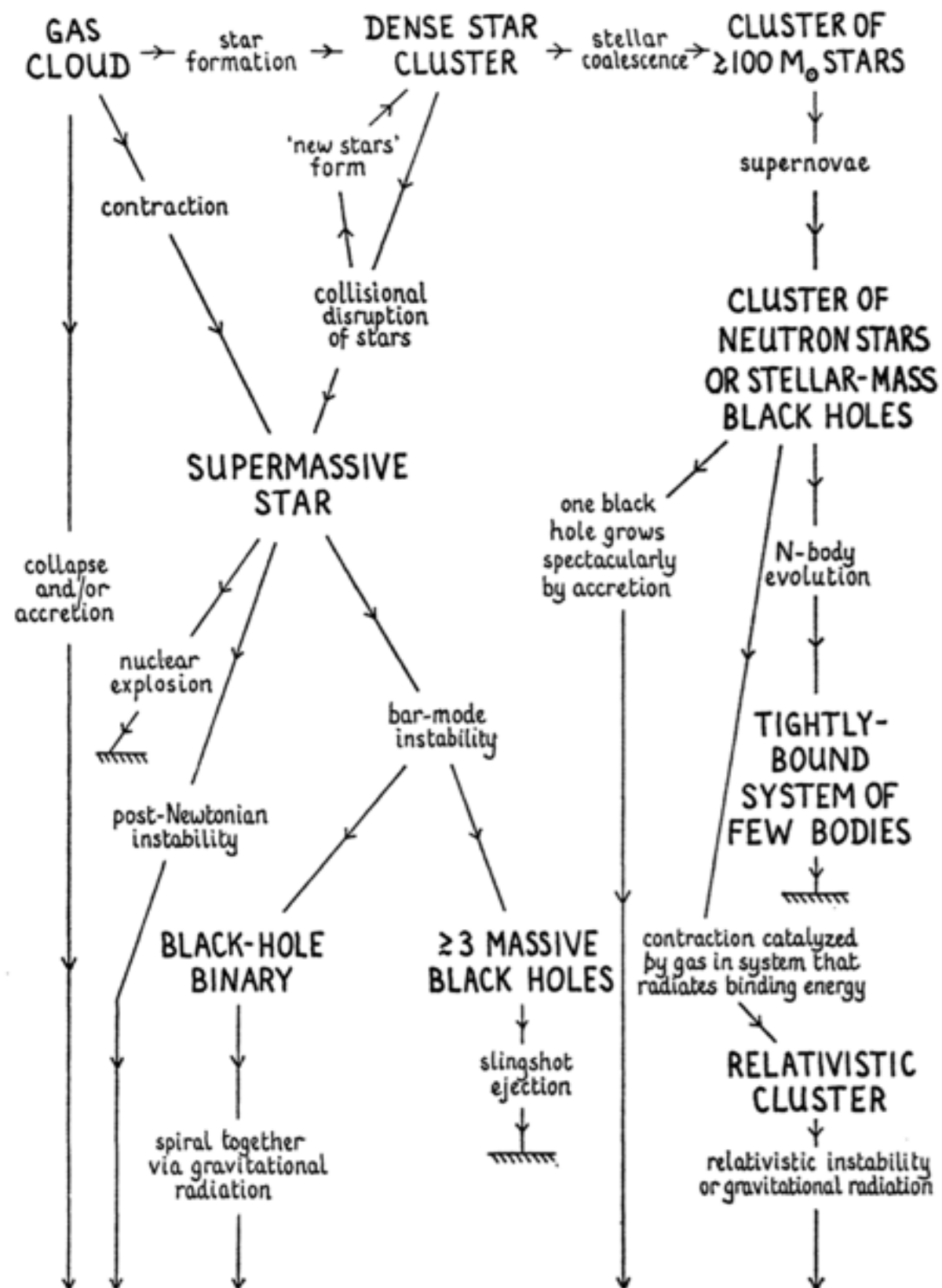


Figure 1 | Evolution of seed black holes. Schematic of the evolution of seed black holes assuming two different formation mechanisms (the death of the first generation of massive stars versus the direct collapse of gas into a black hole). Dark matter halos and the galaxies in them grow through merging. Black holes grow both via merging and by accreting gas. One additional complication is that after merging, gravitational radiation 'recoil' (see text for details) may send the black hole out of the galaxy. At present, we can distinguish between the two scenarios based on the fraction of small galaxies that contain massive black holes (we call this the 'occupation fraction').

2. Models of SMBH



massive black hole

Halo

Massive
Stars

Globular
Cluster

Galaxy

Gas Cloud

BHs

$\exists 60 M_{\odot}$

IMBHs

$10^2 – 10^4 M_{\odot}$

SMBHs

$\exists 10^6 M_{\odot}$

Starburst galaxy M82 has 1000M BH

Matsushita+, ApJ, 545, L107 (2000)

Matsumoto+, ApJ, 547, L25 (2001)

HLX-1 has 20,000M BH!

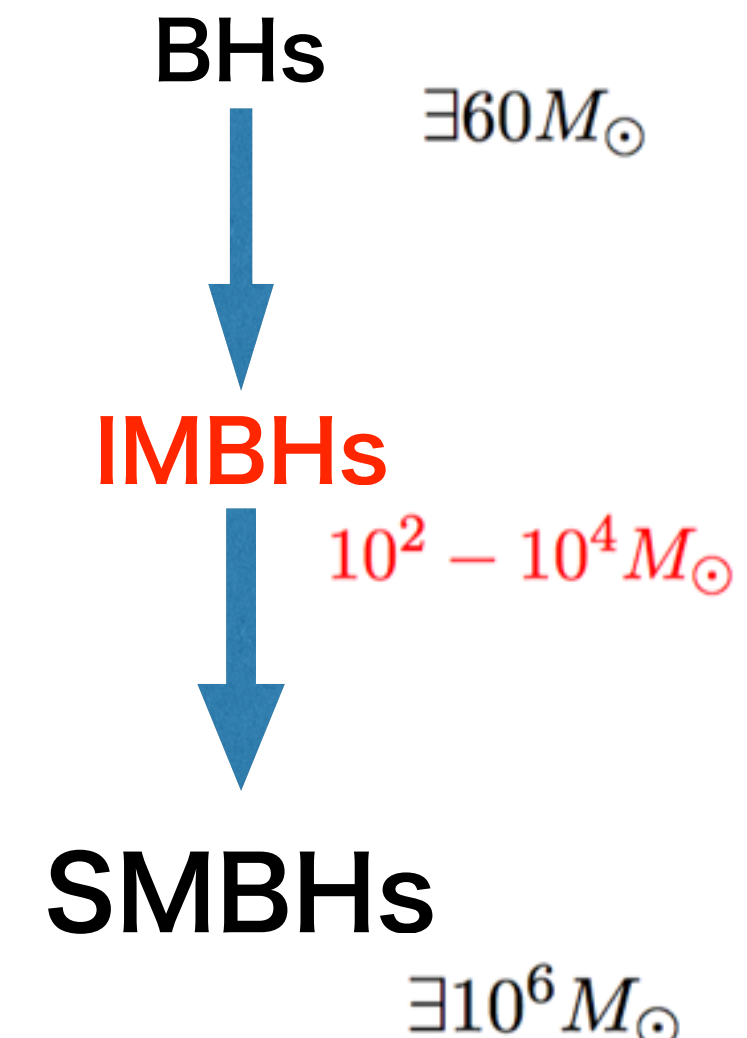
<http://hubblesite.org/newscenter/archive/releases/2012/2012/11/full/>

Table 2. The distances and velocity dispersions of galactic globular clusters. Possible masses of IMBHs, if they exist, are obtained from $M - \sigma$ relation [112].

NGC No.	distance (kpc) [63]	vel. disp. σ (km/s) [111]	BH mass (M_{\odot})
104	4.5	10.0	794.7
362	8.5	6.2	116.3
1851	12.1	11.3	1299
1904	12.9	3.9	18.04
5272	10.4	4.8	41.57
5286	11.0	8.6	433.4
5694	34.7	6.1	108.9
5824	32.0	11.1	1209
5904	7.5	6.5	140.6
5946	10.6	4.0	19.97
6093	10.0	14.5	3539
6266	6.9	15.4	4508
6284	15.3	6.8	168.6
6293	8.8	8.2	357.9
6325	8.0	6.4	132.4
6342	8.6	5.2	57.35
6441	11.7	19.5	11645
6522	7.8	7.3	224.3
6558	7.4	3.5	11.68
6681	9.0	10.0	794.7
7099	8.0	5.8	88.96

Yagi, CQG 29 075005 (2012)
[arXiv:1202.3512]

Ebisuzaki +, ApJ, 562, L19 (2001)





1602.05325

Letter

0.15pc from SgrA*

Galactic center mini-spiral by ALMA: Possible origin of the central cluster

1-2 $\times 10^4$ Msun

Masato TSUBOI,^{1,2,*} Yoshimi KITAMURA,¹ Makoto MIYOSHI,³ Kenta UEHARA,²
Takahiro TSUTSUMI,⁴ and Atsushi MIYAZAKI^{3,5}

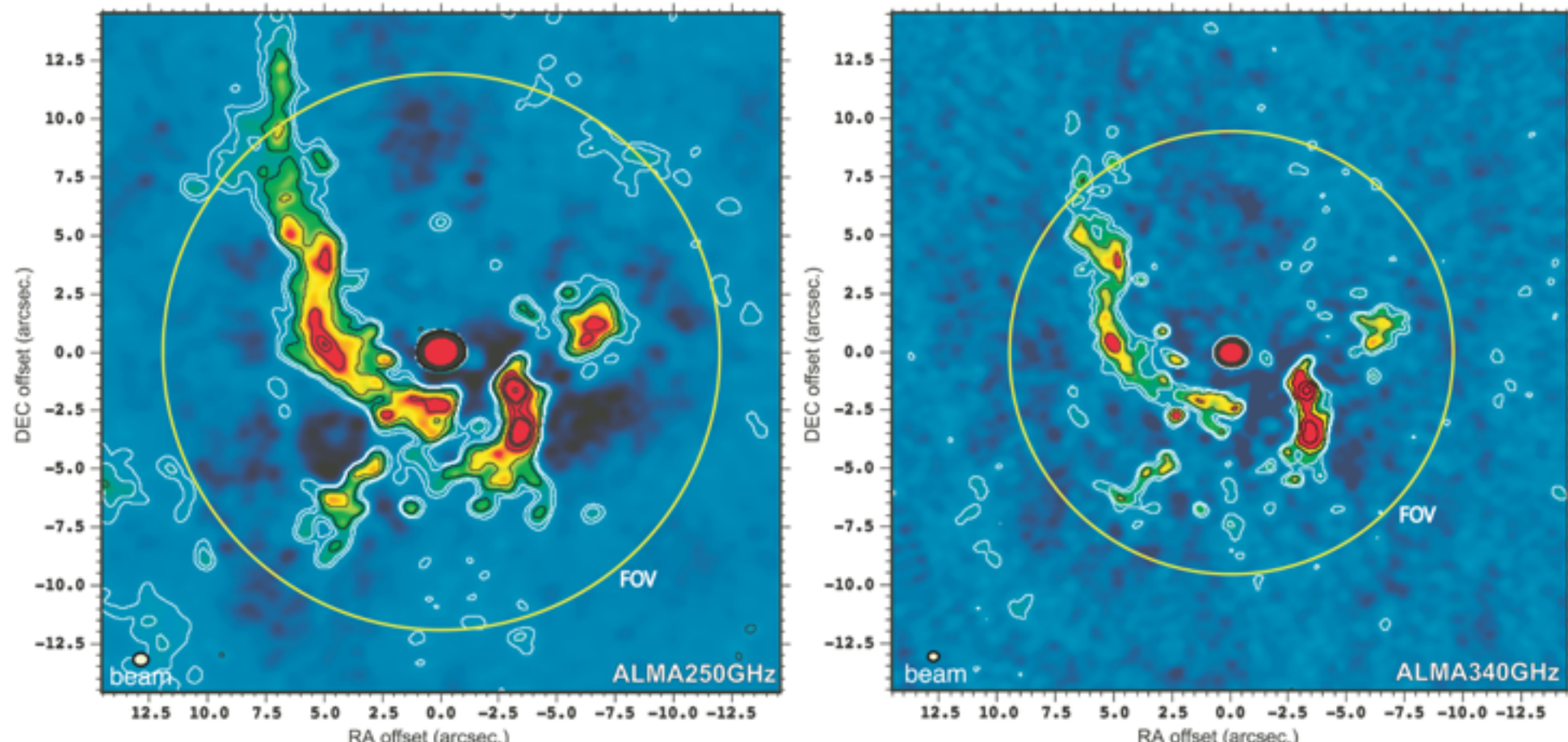


Fig. 2. Left panel: ALMA map in the 250 GHz band of the “mini-spiral” including Sgr A*. The four spectral windows of $f_c = 245, 247, 257$, and 259 GHz are combined to improve the sensitivity. The diameter of the FOV is 24'' (circle). The angular resolution is $0''.63 \times 0''.53$ at $PA = -84^\circ$, which is shown as an oval in the lower left corner. The RMS noise level is $0.13 \text{ mJy beam}^{-1}$, and the contour levels are $0.31, 0.63, 1.3, 2.5, 5.0, 10, 20, 30, 40, 50$, and 75 mJy beam^{-1} . The flux density of Sgr A* is $S_v = 3.55 \pm 0.35 \text{ Jy}$ at 250 GHz. Right panel: ALMA map in the 340 GHz band of the same region as the left panel. The four spectral windows of $f_c = 336, 338, 348$, and 350 GHz are combined to improve the sensitivity. The diameter of the FOV is 18'' (circle). The angular resolution is $0''.44 \times 0''.38$ at $PA = -89^\circ$, which is shown as an oval in the lower left corner. The RMS noise level is $0.33 \text{ mJy beam}^{-1}$, and the contour levels are the same as in the left panel. The flux density of Sgr A* is $S_v = 3.44 \pm 0.51 \text{ Jy}$ at 340 GHz. (Color online)

THE ECOLOGY OF STAR CLUSTERS AND INTERMEDIATE-MASS BLACK HOLES IN THE GALACTIC BULGE

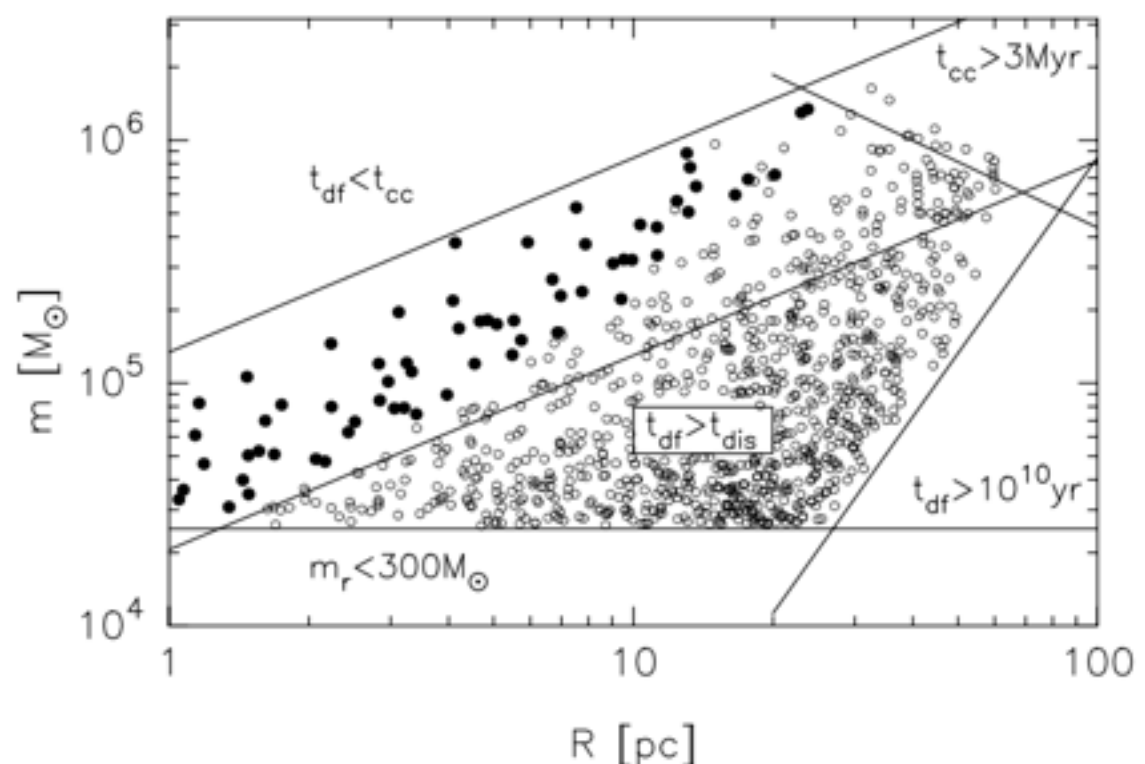
SIMON F. PORTEGIES ZWART,^{1,2} HOLGER BAUMGARDT,³ STEPHEN L. W. McMILLAN,⁴
JUNICHIRO MAKINO,⁵ PIET HUT,⁶ AND TOSHI EBISUZAKI⁷

Received 2005 November 11; accepted 2005 December 5

ABSTRACT

We simulate the inner 100 pc of the Milky Way to study the formation and evolution of the population of star clusters and intermediate-mass black holes (IMBHs). For this study we perform extensive direct N -body simulations of the star clusters that reside in the bulge, and of the inner few tenth of parsecs of the supermassive black hole in the Galactic center. In our N -body simulations the dynamical friction of the star cluster in the tidal field of the bulge are taken into account via semianalytic solutions. The N -body calculations are used to calibrate a semianalytic model of the formation and evolution of the bulge. We find that $\sim 10\%$ of the clusters born within ~ 100 pc of the Galactic center undergo core collapse during their inward migration and form IMBHs via runaway stellar merging. After the clusters dissolve, these IMBHs continue their inward drift, carrying a few of the most massive stars with them. We predict that a region within ~ 10 pc of the supermassive black hole (SMBH) is populated by ~ 50 IMBHs of $\sim 1000 M_{\odot}$. Several of these are still expected to be accompanied by some of the most massive stars from the star cluster. We also find that within a few milliparsecs of the SMBH there is a steady population of several IMBHs. This population drives the merger rate between IMBHs and the SMBH at a rate of about one per 10 Myr, sufficient to build the accumulated majority of mass of the SMBH. Mergers of IMBHs with SMBHs throughout the universe are detectable by *LISA* at a rate of about two per week.

PortegiesZwart+, ApJ 641(2006)319



'Missing link' founded

Ebisuzaki +, ApJ, 562, L19 (2001)

(1) formation of IMBHs by runaway mergers of massive stars in dense star clusters,

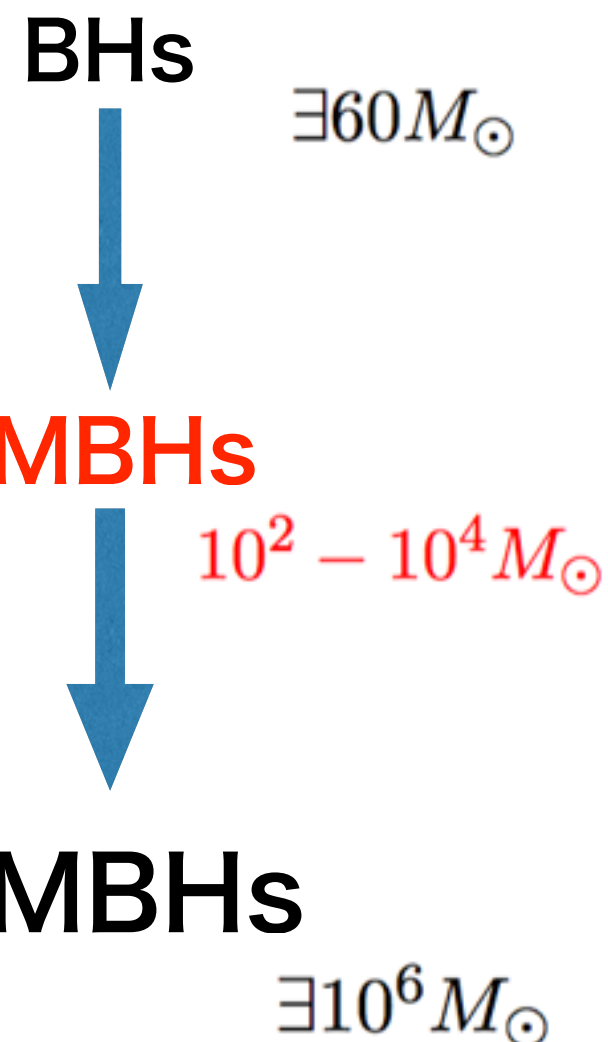
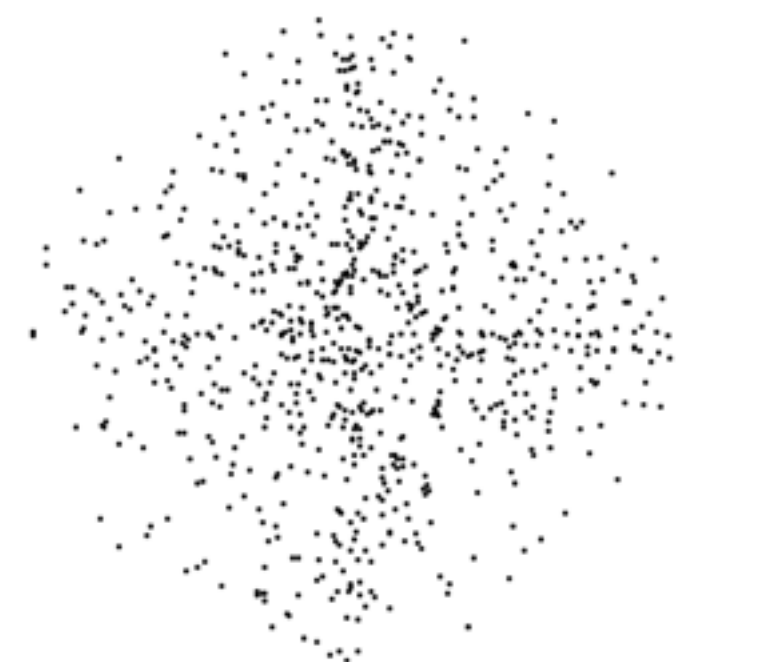
Marchant & Shapiro 1980; Portegies Zwart et al. 1999;
Portegies Zwart & McMillan 2002;
Portegies Zwart et al. 2004;
Holger & Makino 2003

(2) accumulations of IMBHs at the center region of a galaxy due to sinkages of clusters by dynamical friction

Matsubayashi et al. 2007

(3) mergings of IMBHs by multi-body interactions and gravitational radiation.

Iwasawa et. al. 2010



DETECTION OF IMBHs WITH GROUND-BASED GRAVITATIONAL WAVE OBSERVATORIES: A BIOGRAPHY OF A BINARY OF BLACK HOLES, FROM BIRTH TO DEATH

PAU AMARO-SEOANE^{1,2} AND LUCÍA SANTAMARÍA¹

¹ Max-Planck-Institut für Gravitationsphysik (Albert-Einstein-Institut), D-14476 Potsdam, Germany;

Pau.Amaro-Seoane@aei.mpg.de, Lucia.Santamaria@aei.mpg.de

² Institut de Ciències de l’Espai, IEEC/CSIC, Campus UAB, Torre C-5, parells, 2^{na} planta, ES-08193 Bellaterra, Barcelona, Spain

Received 2009 January 10; accepted 2010 August 16; published 2010 September 28

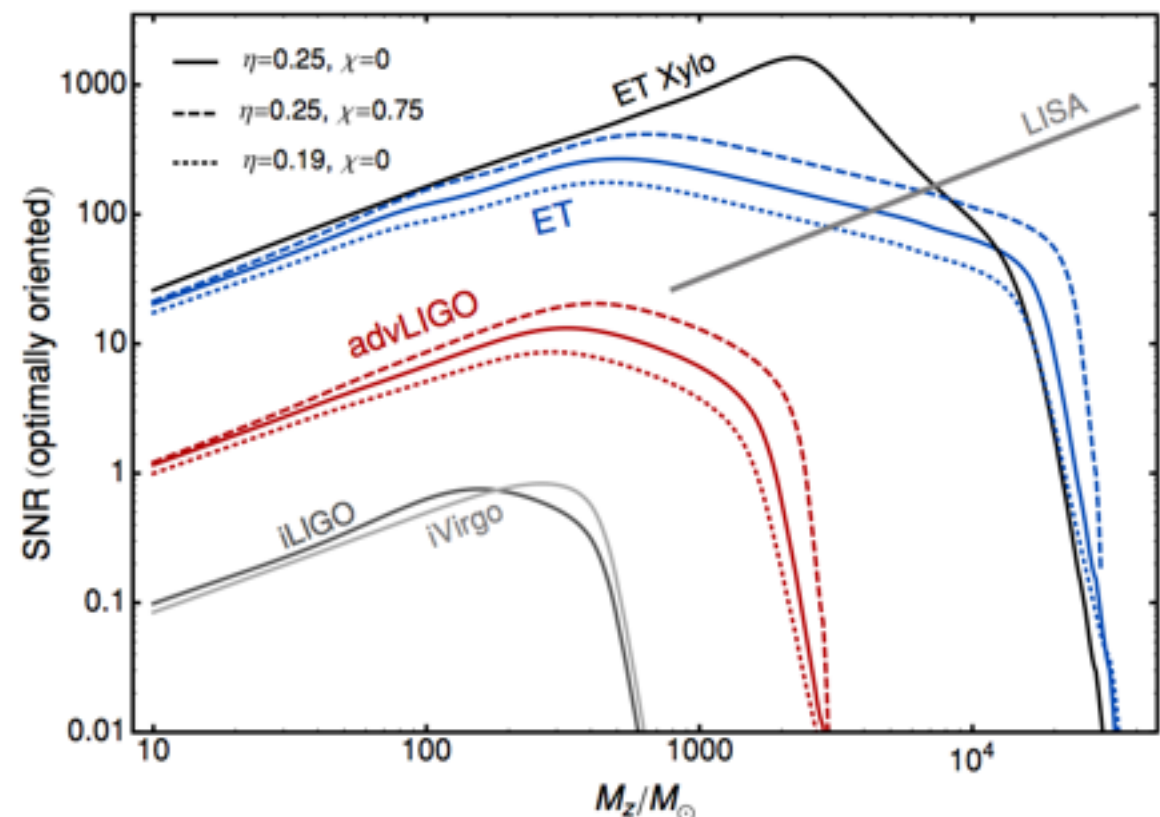


Figure 7. S/N as a function of the redshifted total mass of the BBH for the present and future generations of GW detectors and *LISA*. The sources are placed at a distance of 6.68 Gpc ($z = 1$) and the S/Ns correspond to sources optimally oriented and located. Solid lines indicate S/Ns for the equal-mass, non-spinning configuration (1); for Advanced LIGO and ET we have included the S/Ns produced by configurations (2) and (3) as well, indicated with dashed and dotted lines, respectively.

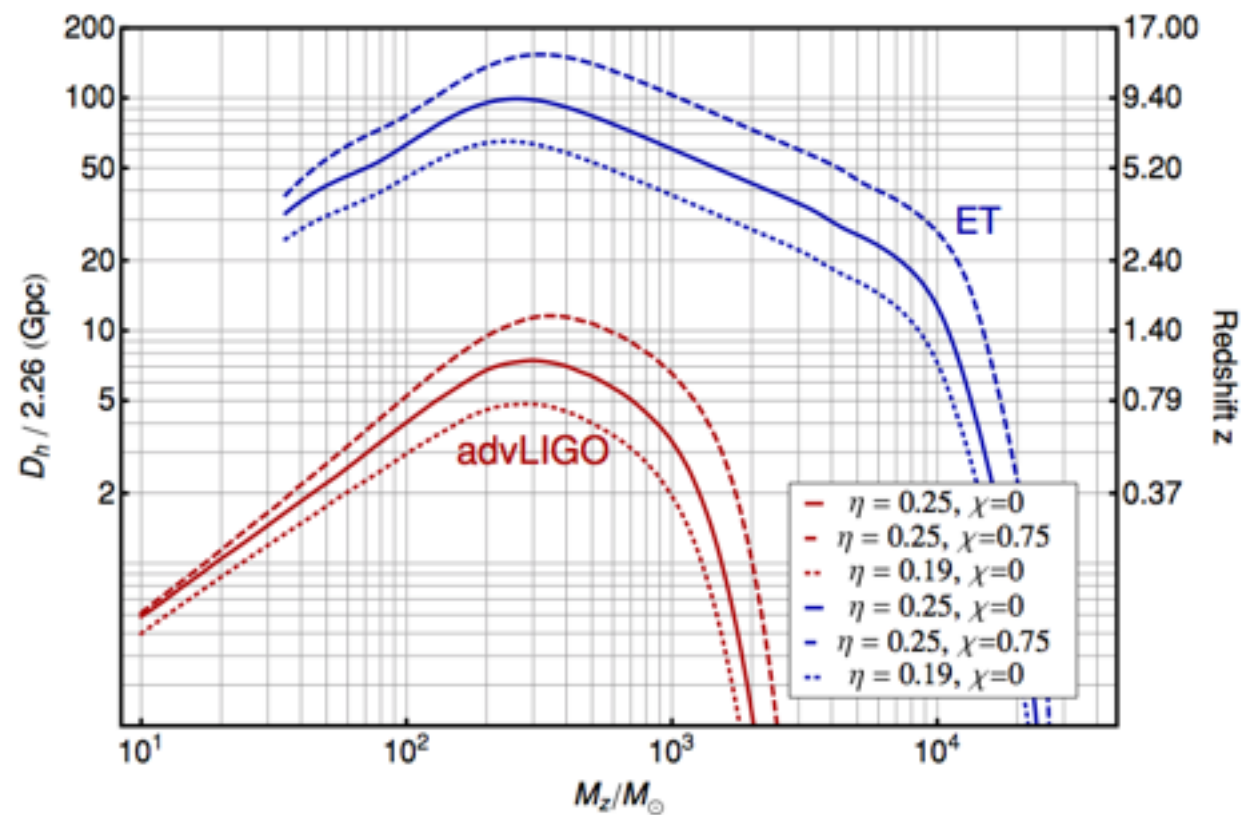


Figure 8. Orientation-averaged distance vs. redshifted mass for three binary configurations obtained with the design sensitivity curves of Advanced LIGO and the ET. The solid, dashed, and dotted lines correspond to the configurations denoted in the text as (1), (2), and (3), respectively. Note the ~40% increase in reach given by the hang-up configuration with $\chi = 0.75$ with respect to the non-spinning case.

DETECTION OF IMBHs WITH GROUND-BASED GRAVITATIONAL WAVE OBSERVATORIES: A BIOGRAPHY OF A BINARY OF BLACK HOLES, FROM BIRTH TO DEATH

PAU AMARO-SEOANE^{1,2} AND LUCÍA SANTAMARÍA¹

¹ Max-Planck-Institut für Gravitationsphysik (Albert-Einstein-Institut), D-14476 Potsdam, Germany;

Pau.Amaro-Seoane@aei.mpg.de, Lucia.Santamaria@aei.mpg.de

² Institut de Ciències de l’Espai, IEEC/CSIC, Campus UAB, Torre C-5, parells, 2^{na} planta, ES-08193 Bellaterra, Barcelona, Spain

Received 2009 January 10; accepted 2010 August 16; published 2010 September 28

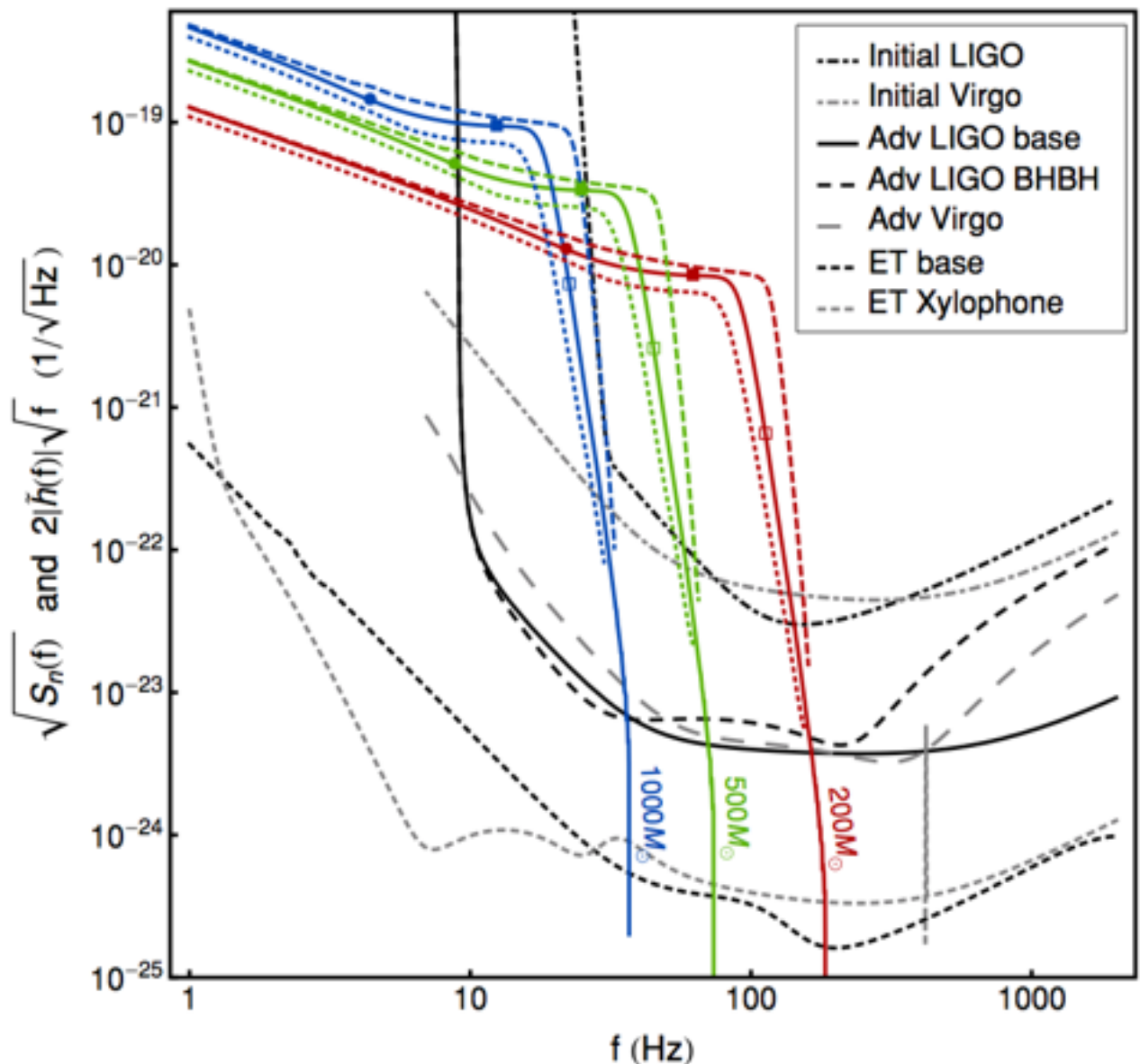


Figure 6. Hybrid waveform for three BBH configurations scaled to various IMBH masses. From top to bottom, we show BBH systems with total mass 1000 , 500 , and $200 M_{\odot}$ in blue, green, and red, respectively. Solid lines correspond to the equal-mass, non-spinning configuration (1), dashed lines to the equal-mass, $\chi = 0.75$ configuration (2), and dotted lines to the non-spinning, $q = 3$ configuration (3). The sources are optimally oriented and placed at 100 Mpc of the detectors. The symbols on top of configuration (1) mark various stages of the BBH evolution: solid circles represent the ISCO frequency, squares the light ring frequency, and open squares the Lorentzian ringdown frequency (corresponding to 1.2 times the fundamental ringdown frequency f_{FRD}), when the BBH system has merged and the final BH is ringing down. Currently operating and planned ground-based detectors are drawn as well: plotted are the sensitivity curves of initial LIGO and Virgo, two possible configurations for Advanced LIGO (zero detuning and $30-30 M_{\odot}$ BBH optimized), Advanced Virgo, and the proposed ET in both its broadband and xylophone configurations.

IMBH-IMBH mergers produce low freq. GW

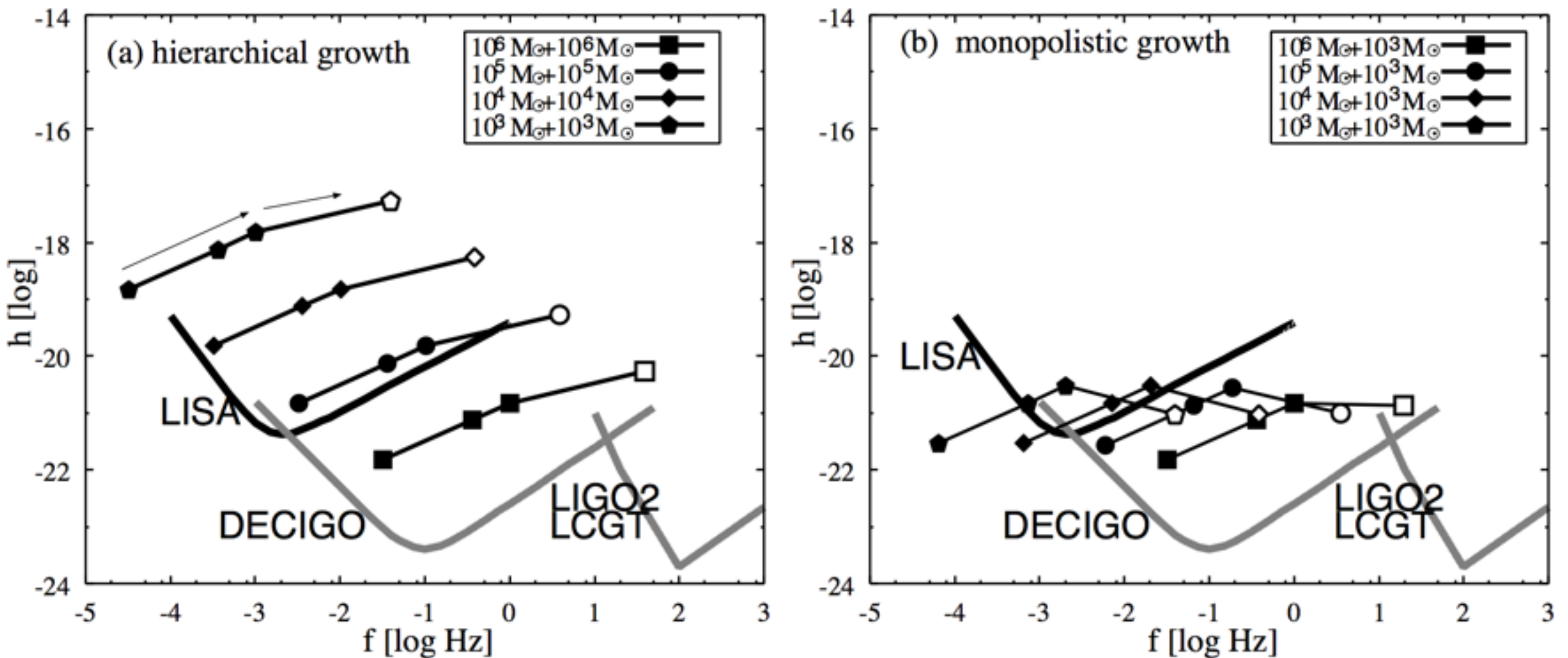
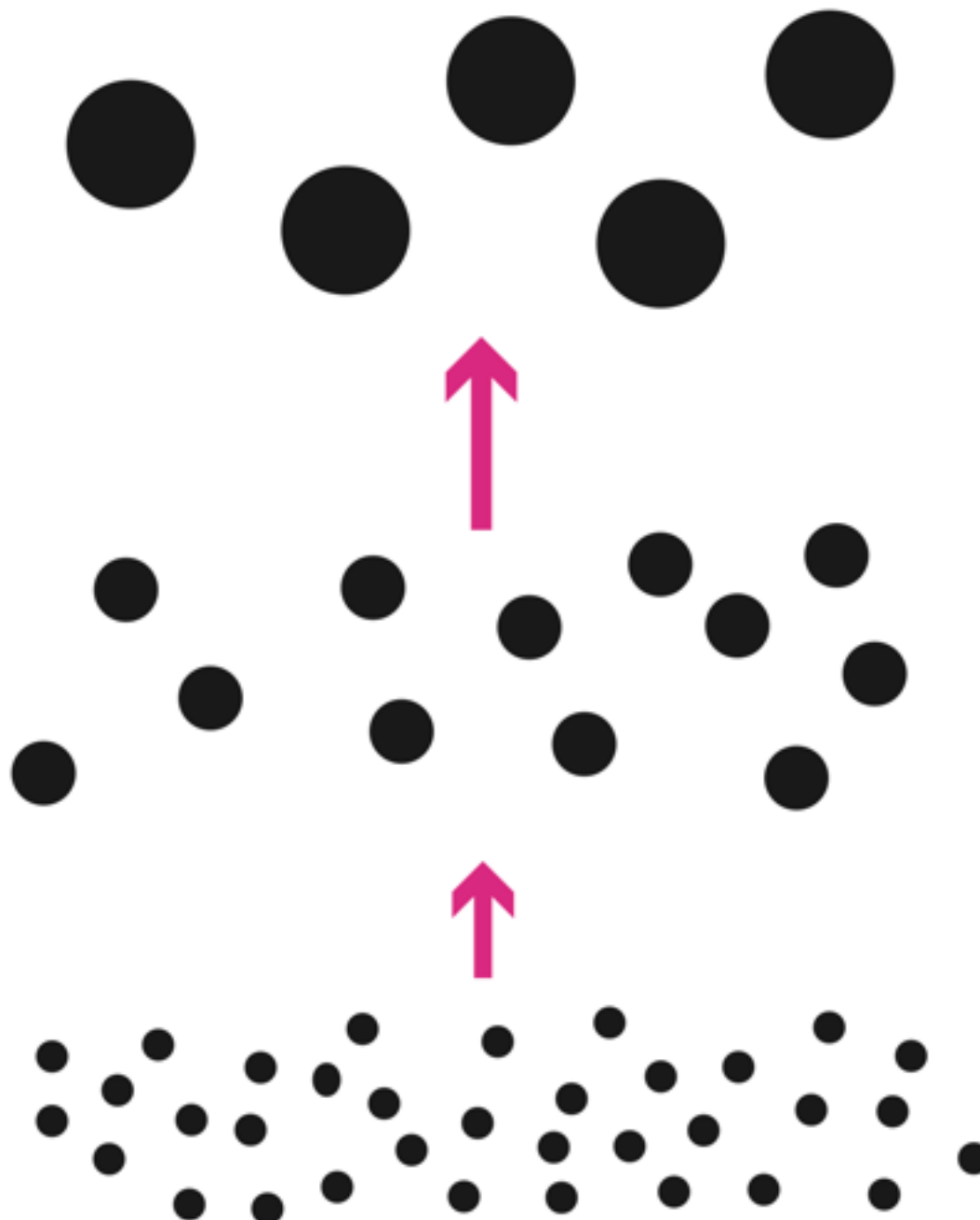
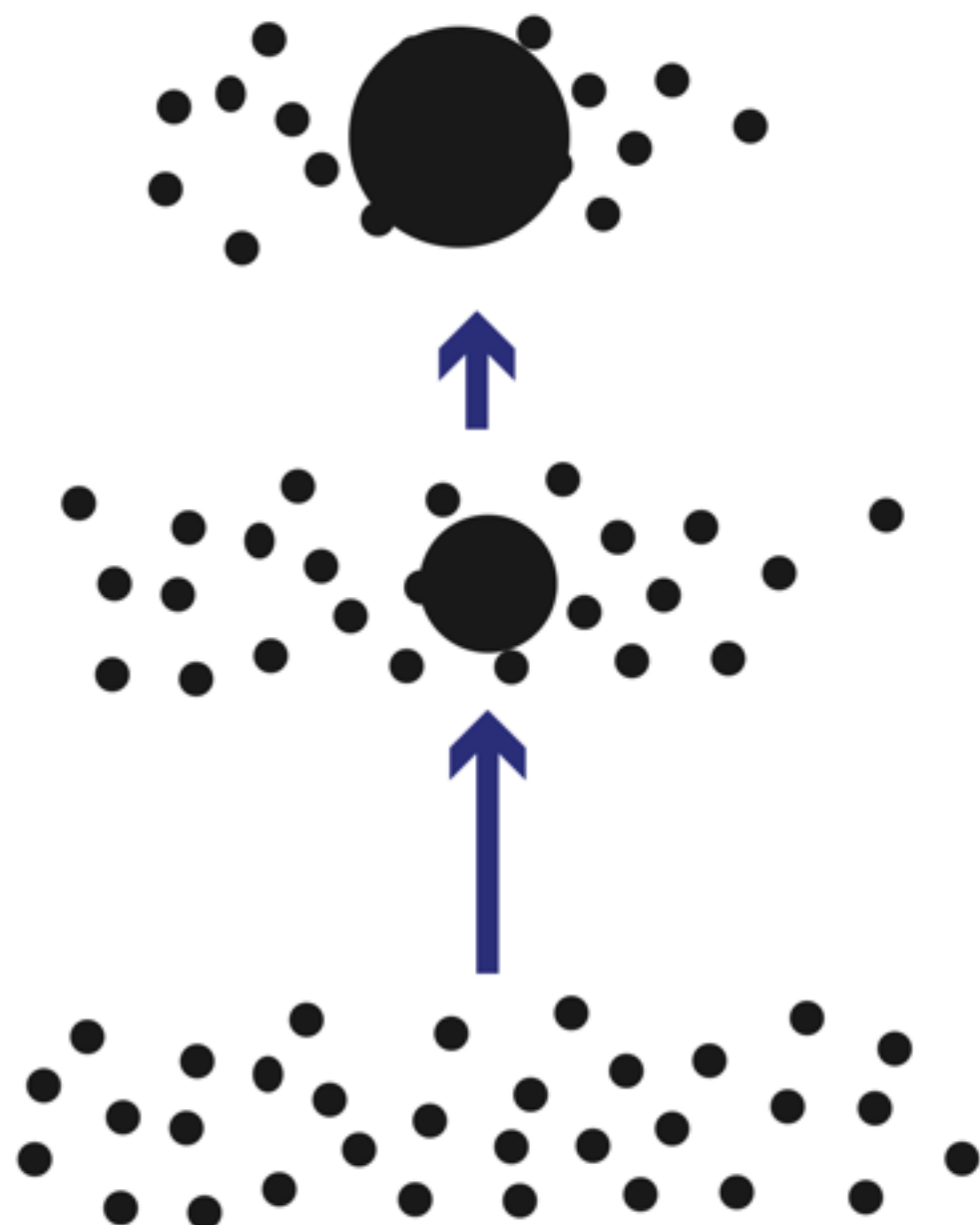


Fig. 1.— Expected gravitational radiation amplitude from merging IMBHs of (a) hierarchical growth model, and (b) monopolistic growth model. We plotted both the inspiral phase ($f_{\text{insp}}, h_{\text{insp}}$), [eqs. (2) and (3)], and the ringdown phase ($f_{\text{QNM}}, h_{\text{coal}}$), [eqs. (4) and (6)], for various mass combinations. The open and closed circle and square in the inspiral phase are of $a = 50, 10$ and $5 R_{\text{grav}}$. The final burst frequency, f_{QNM} , depends on the efficiency, ϵ , which we fix $\epsilon \simeq 10^{-2}$ for plots. Lines are the sensitivity of the future detectors; LISA, DECIGO, LIGO 2, and LCGT, taken from Fig. 1 in Seto et al. (2001). The data are evaluated at the distance $R = 4$ Gpc.

Hierarchical growth model



Monopolistic growth model



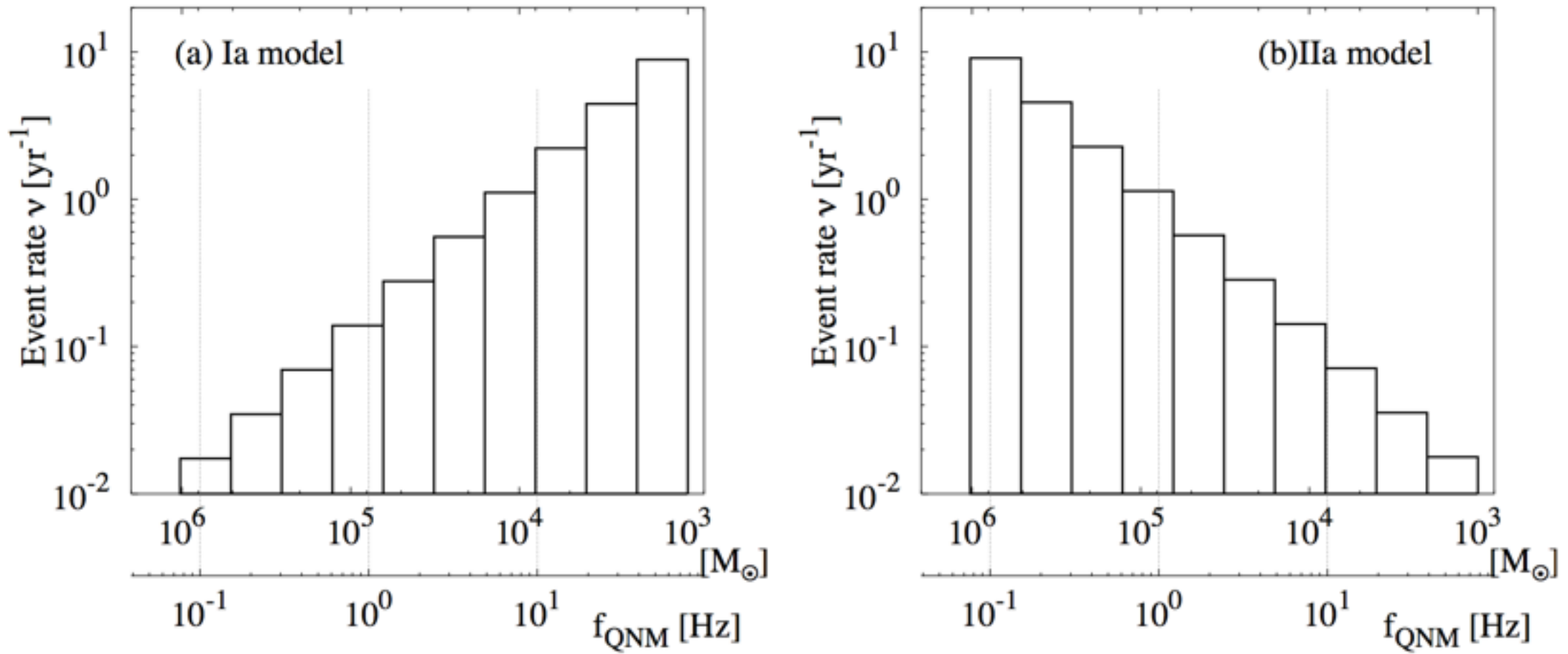
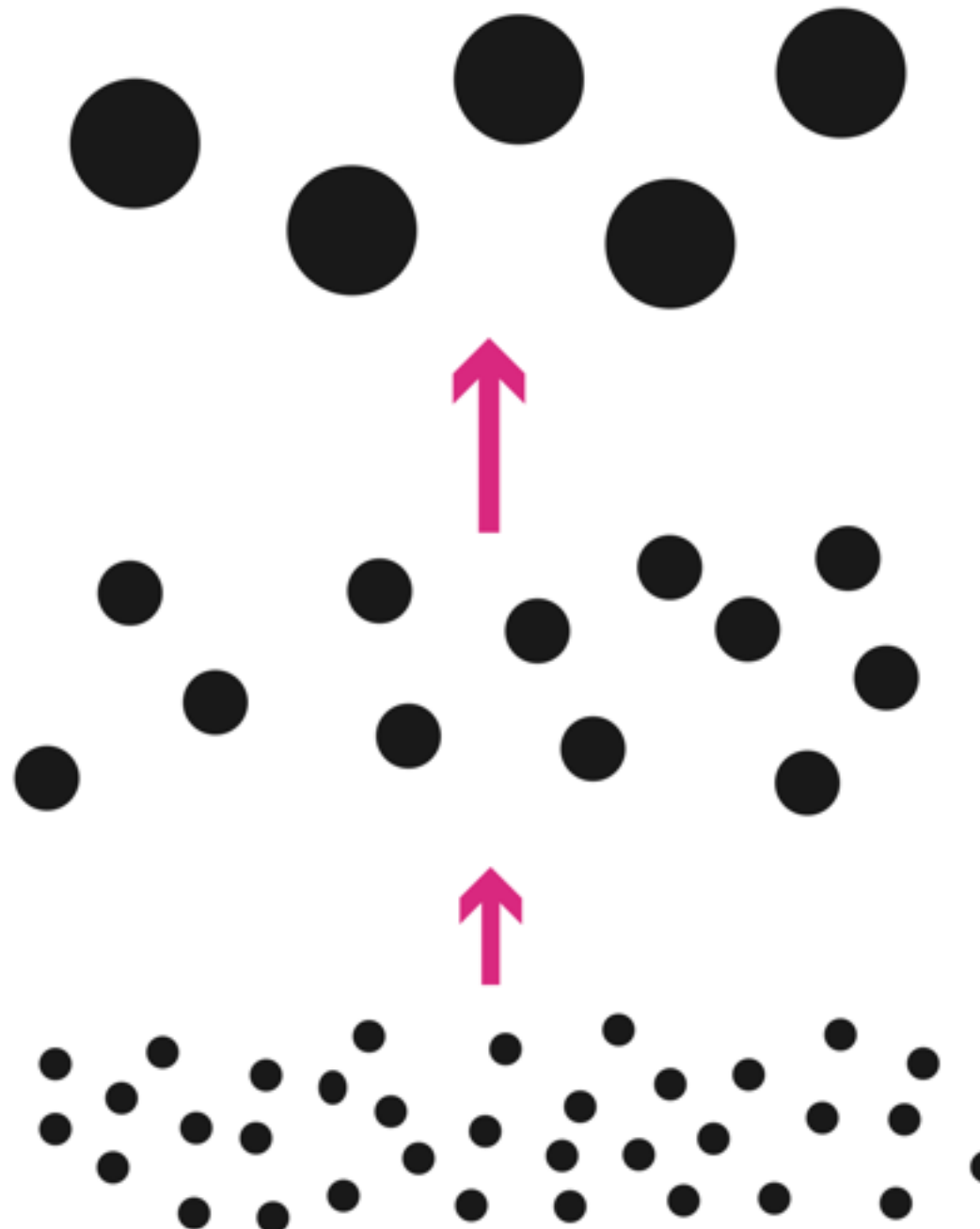


Fig. 2.— Event numbers of mergers starting from a thousand of $10^3 M_\odot$ IMBHs. The vertical axis is the event rate ν [yr $^{-1}$], eqs. (12) and (14). The horizontal axis is the mass of the post-merger BH, M_T , which is also interpreted in the final gravitational radiation frequency f_{QNM} . Fig. (a) and (b) are for the hierarchical growth model and for the monopolistic growth model, respectively. Both plots are for the homogeneous distribution model, while we just multiply three for each event rate for the thin-shell galaxy distribution model. If a SMBH grows up hierarchically, then the bursts of gravitational radiation appear in higher frequency region. In the monopolistic model, the bursts appear in lower frequency region. We fix the increasing-mass rate, α , as unity for the plots.

Hierarchical growth model



How many BHs in a galaxy?
How many galaxies in the Universe?

**How many BH mergers
in the Universe?**

**How many BH mergers
we observe in a year?**

Detectable Distance ?
KAGRA/aLIGO/aVIRGO

Cosmological model?
BH spin? Signal-to-Noise?

contents

1. Gravitational Waves

Detectors, GW events

2. Models of SMBH

hierarchical growth model, or others

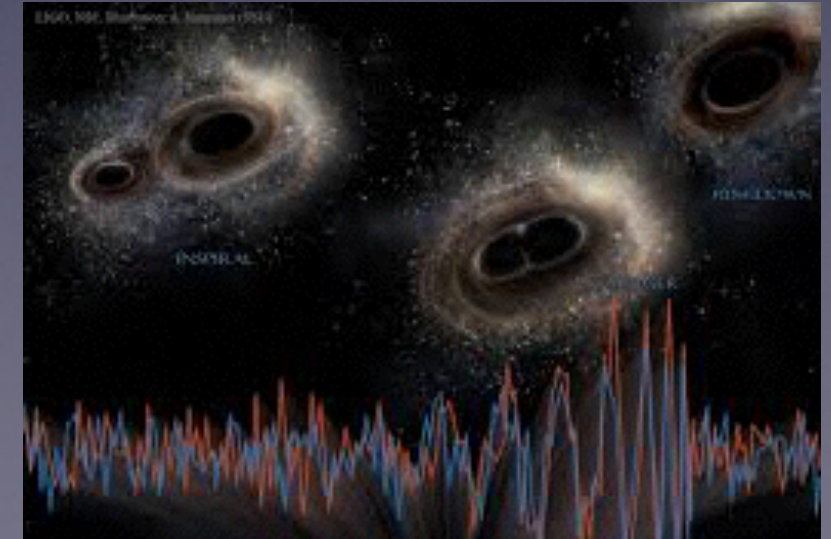
3. Counting BHs

How many BHs in a galaxy?

How many galaxies in the Universe?

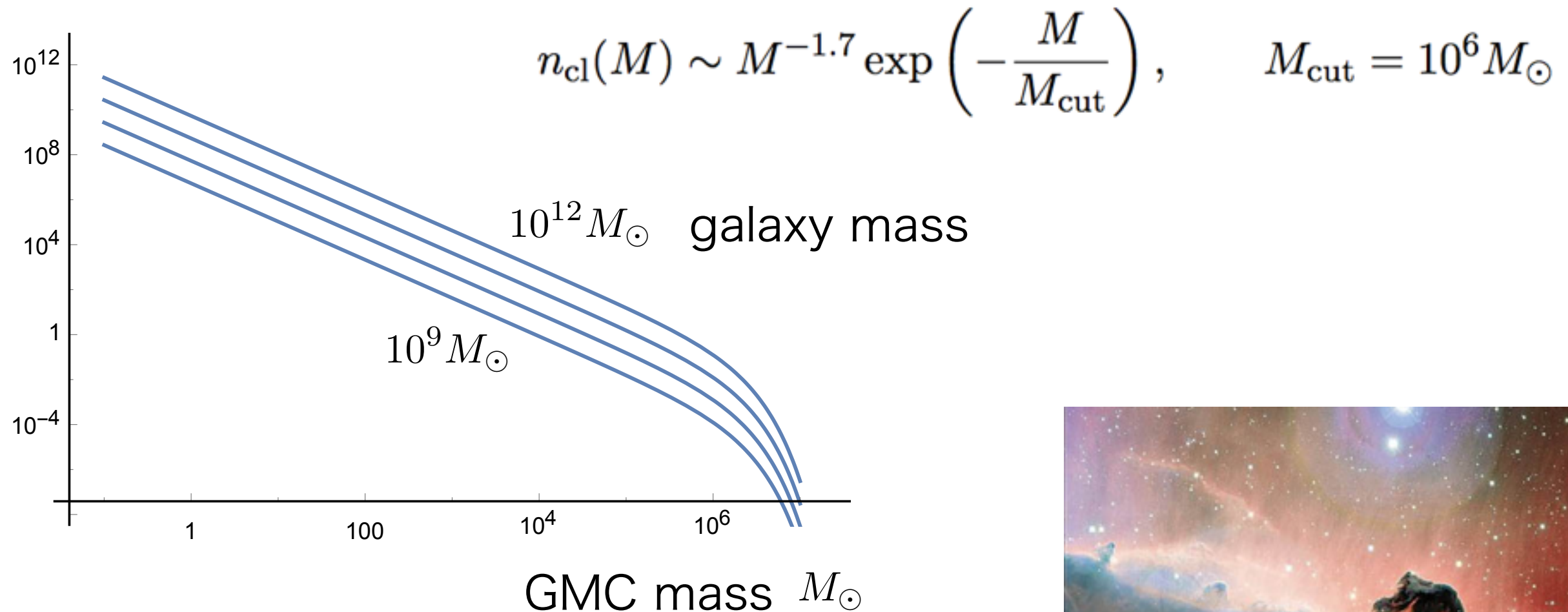
4. Event Rates at aLIGO/KAGRA/DECIGO/LISA

How many BH mergers in the Universe?



How many BHs in a Galaxy?

Mass Function of Giant Molecular Clouds



The Formation and Destruction of Molecular Clouds and Galactic Star Formation

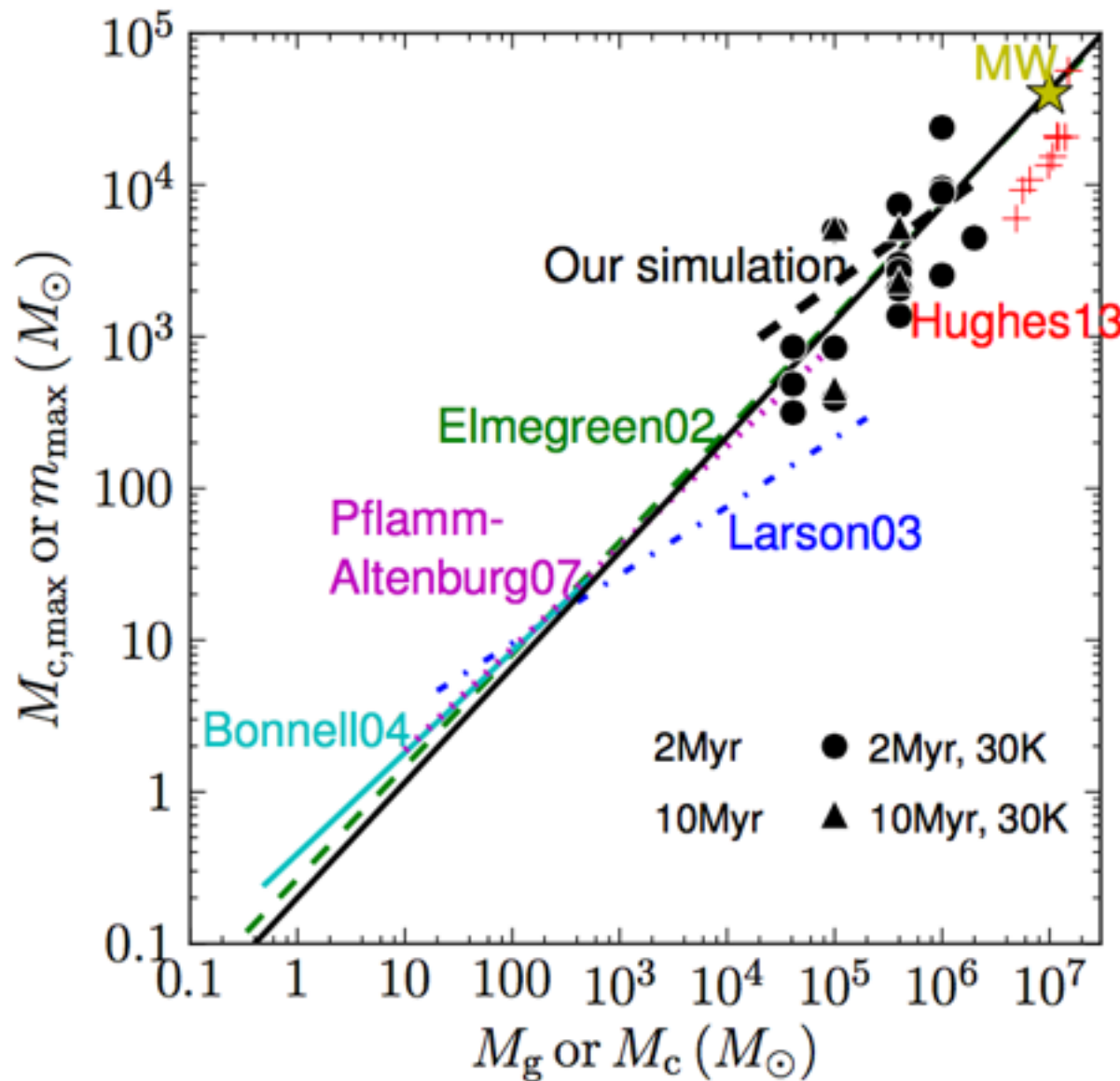
An Origin for The Cloud Mass Function and Star Formation Efficiency

Shu-ichiro Inutsuka¹, Tsuyoshi Inoue,², Kazunari Iwasaki^{1,3}, and Takashi Hosokawa⁴

A&A 580, A49 (2015) [arXiv:1505.04696]

How many BHs in a Galaxy?

Molecular Clouds Maximum Core



The initial mass function of star clusters that form in turbulent molecular clouds

M. S. Fujii¹ * and S. Portegies Zwart²*

¹Division of Theoretical Astronomy, National Astronomical Observatory of Japan 2-21-1 Osawa, Mitaka, Tokyo 181-8588, Japan

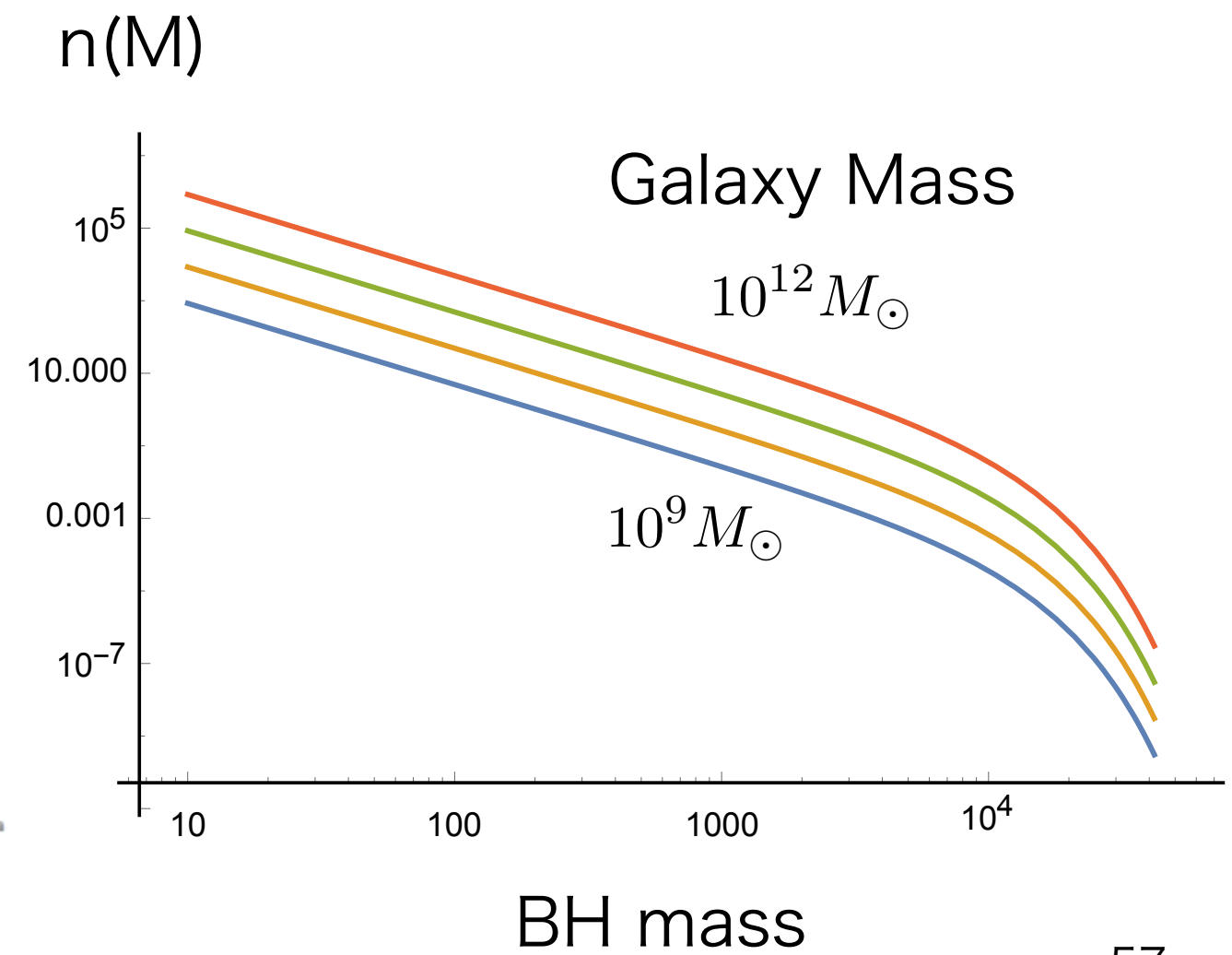
²Leiden Observatory, Leiden University, NL-2300RA Leiden, The Netherlands

1309.1223v3

$$M_{c,\text{max}} = 0.20 M_c^{0.76}$$



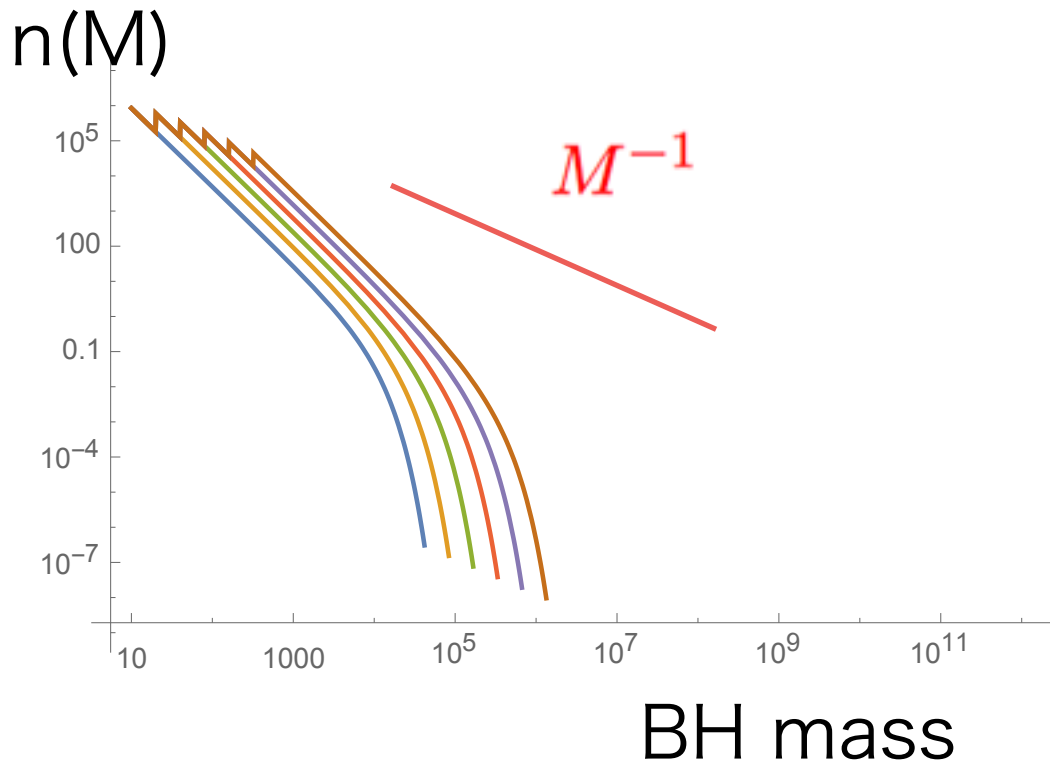
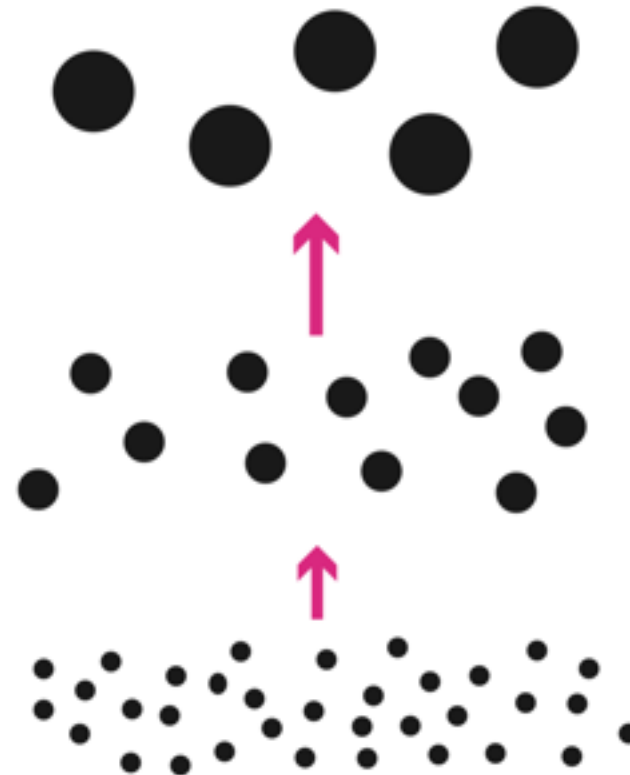
Building Block BH



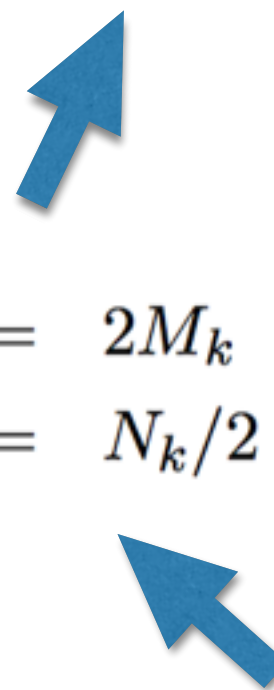
How many BHs in a Galaxy?

Count BHs to form a SMBH

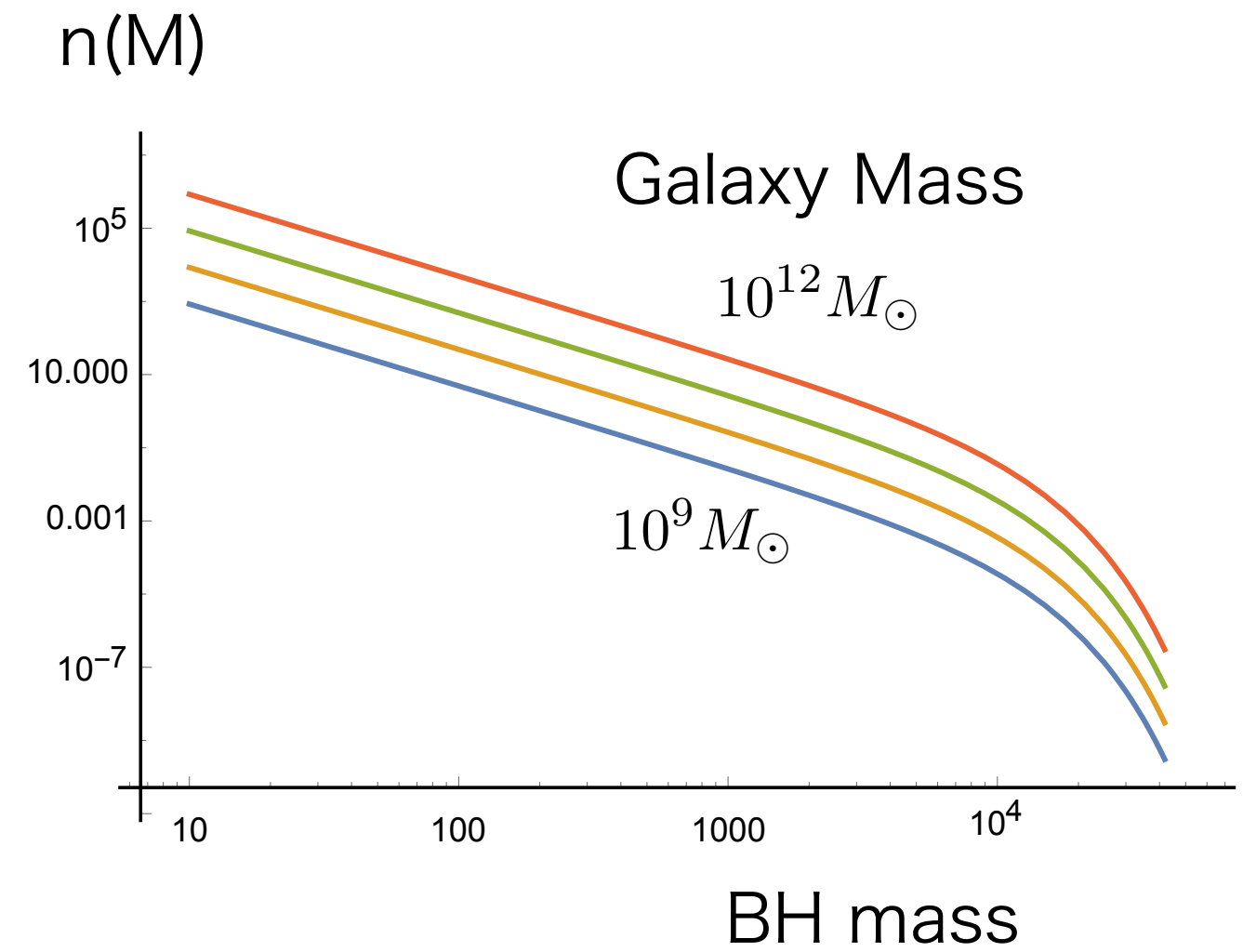
Hierarchical growth model



$$\begin{aligned}M_{k+1} &= 2M_k \\N_{k+1} &= N_k/2\end{aligned}$$

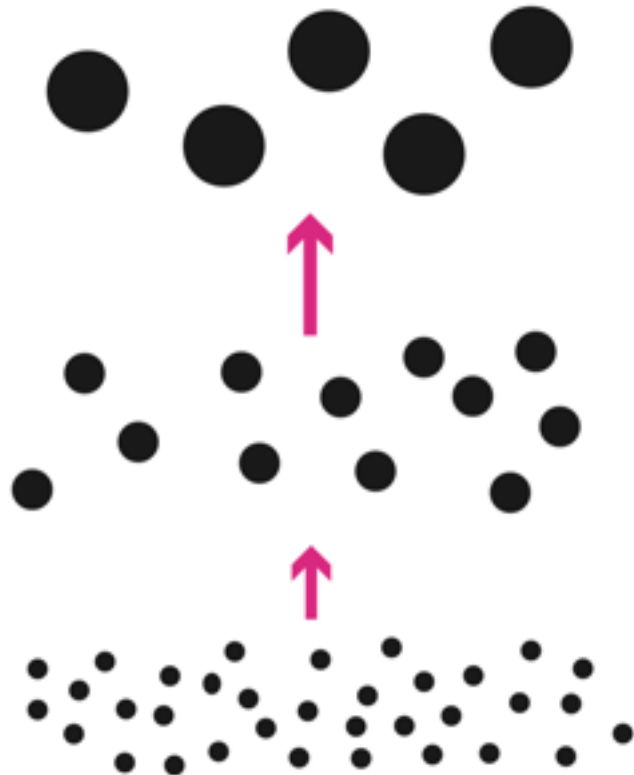


Building Block BH



How many BHs in a Galaxy?

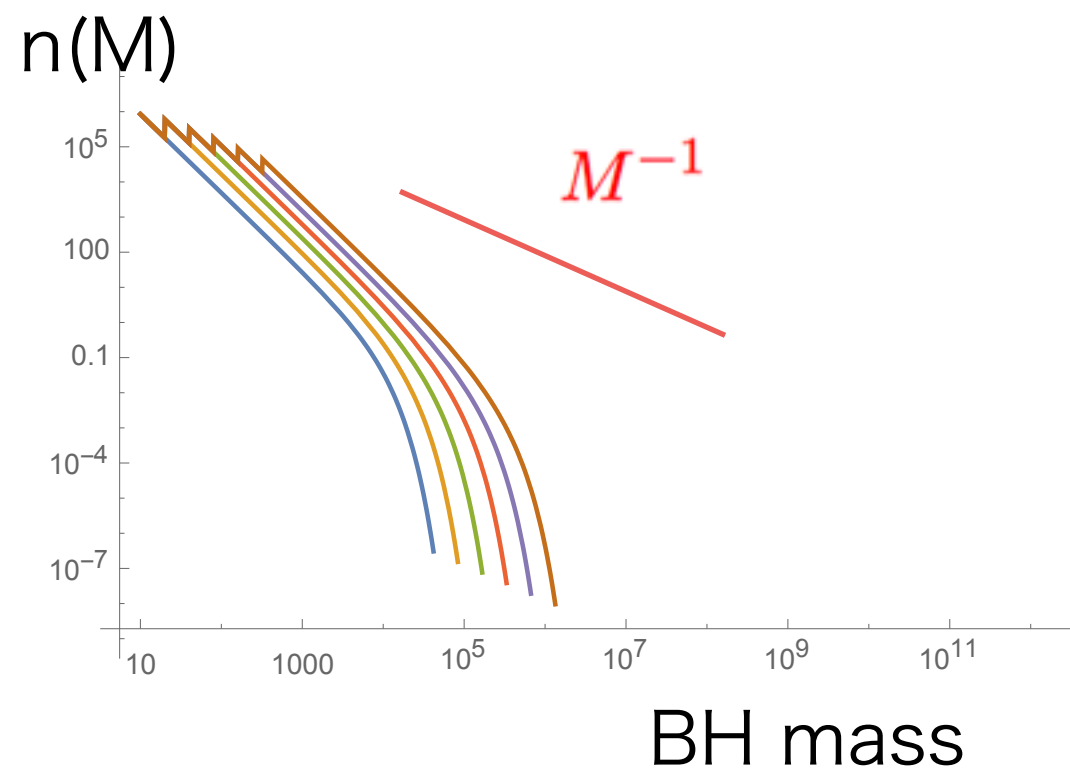
Hierarchical growth model



$$M_{k+1} = 2M_k$$
$$N_{k+1} = N_k/2$$



dynamical friction



How many Galaxies in the Universe?

Count BHs to form a SMBH

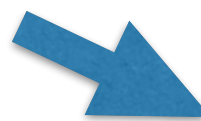


$$\begin{aligned}M_{\text{SMBH}} &= 2 \times 10^{-4} M_{\text{galaxy}} \\&= 10^{-3} M_{\text{bulge}}\end{aligned}$$

(sub-)Galaxy
from Halo model

Mon. Not. R. Astron. Soc. 371, 1173–1187 (2006)

doi:10



The non-parametric model for linking galaxy luminosity
with halo/subhalo mass

A. Vale¹* and J. P. Ostriker^{1,2}

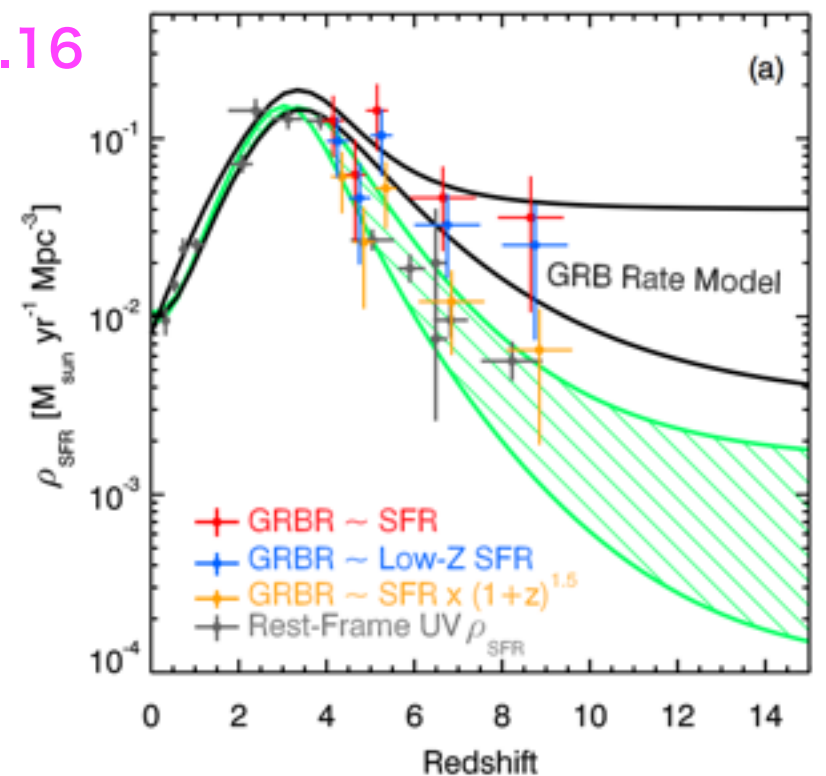
¹Institute of Astronomy, University of Cambridge, Madingley Road, Cambridge CB3 0HA

²Princeton University Observatory, Princeton University, Princeton, NJ 08544, USA

THE ASTROPHYSICAL JOURNAL, 744:95 (13pp), 2012 January 10
© 2012. The American Astronomical Society. All rights reserved. Printed in the U.S.A.

Star Formation Rate

peak z=3.16



CONNECTING THE GAMMA RAY BURST RATE AND THE COSMIC STAR FORMATION HISTORY:
IMPLICATIONS FOR REIONIZATION AND GALAXY EVOLUTION

BRANT E. ROBERTSON^{1,2,3} AND RICHARD S. ELLIS¹

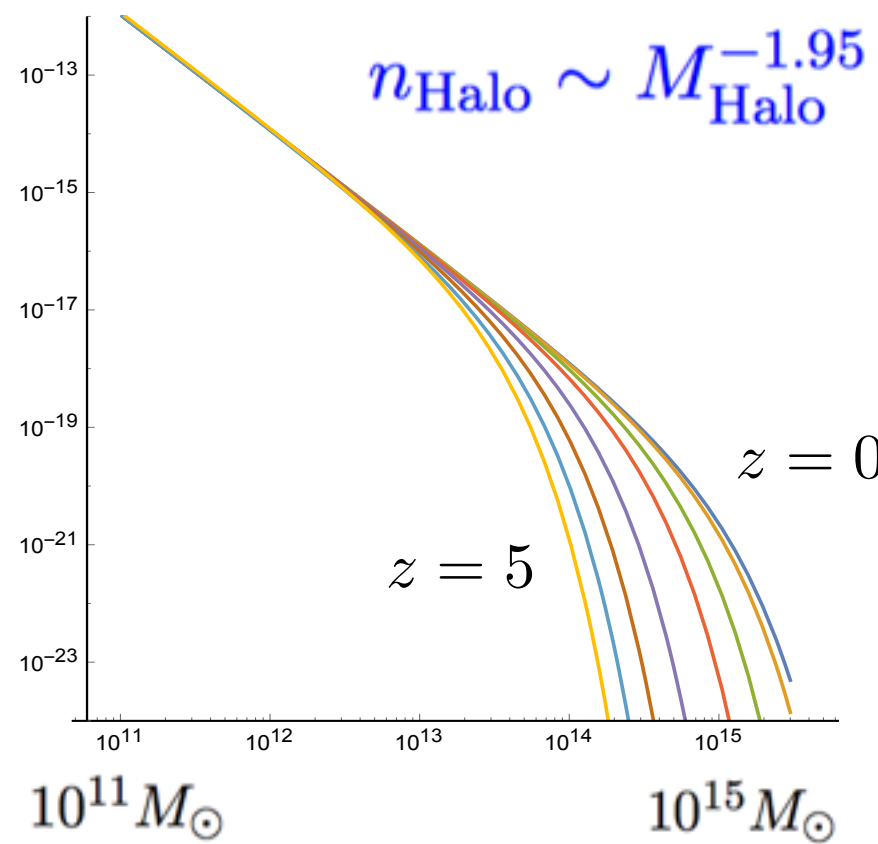
¹ Astronomy Department, California Institute of Technology, MC 249-17, 1200 East California Boulevard, Pasadena, CA 91125, USA; brant@astro.caltech.edu

² Steward Observatory, University of Arizona, 933 North Cherry Avenue, Tucson, AZ 85721, USA

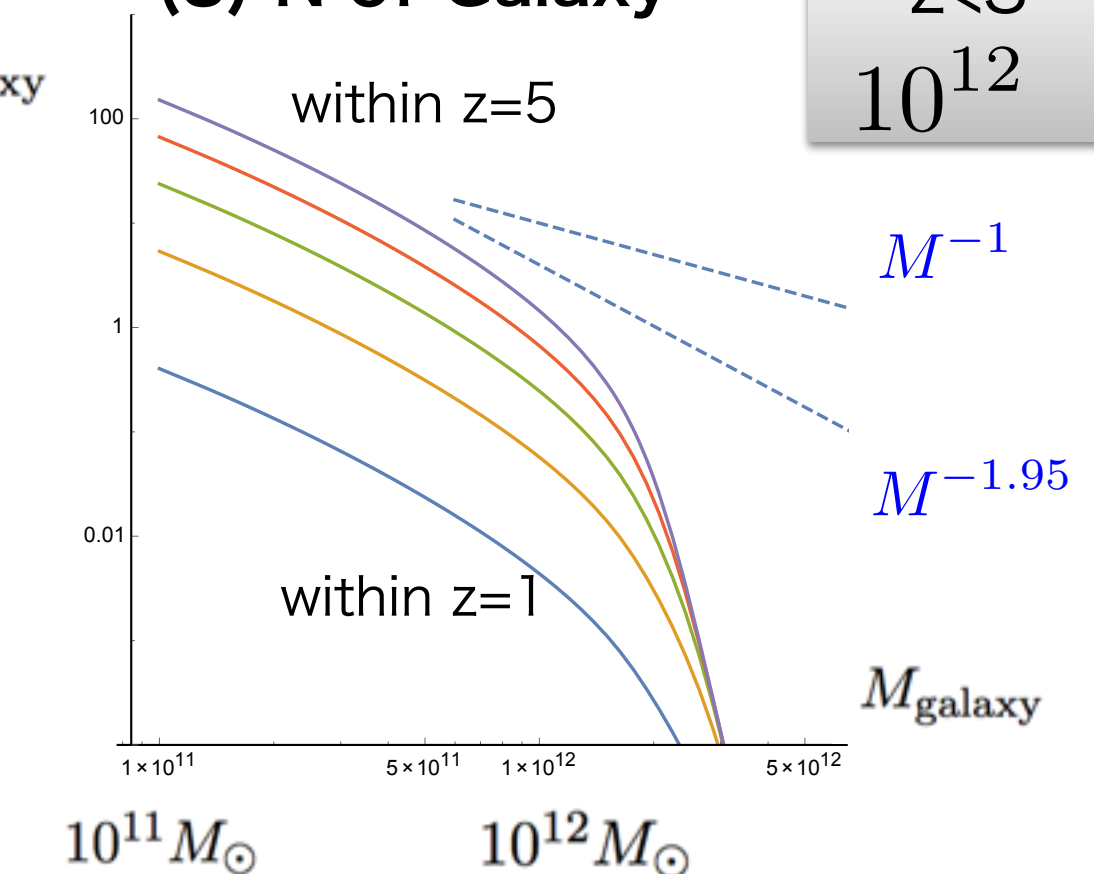
Received 2011 September 5; accepted 2011 November 18; published 2011 December 19

How many Galaxies in the Universe?

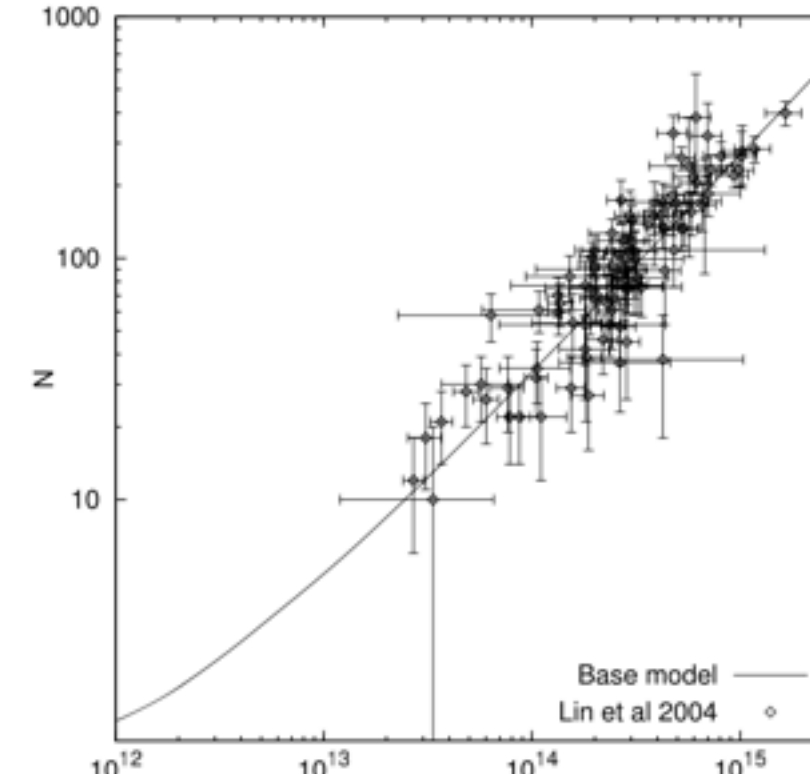
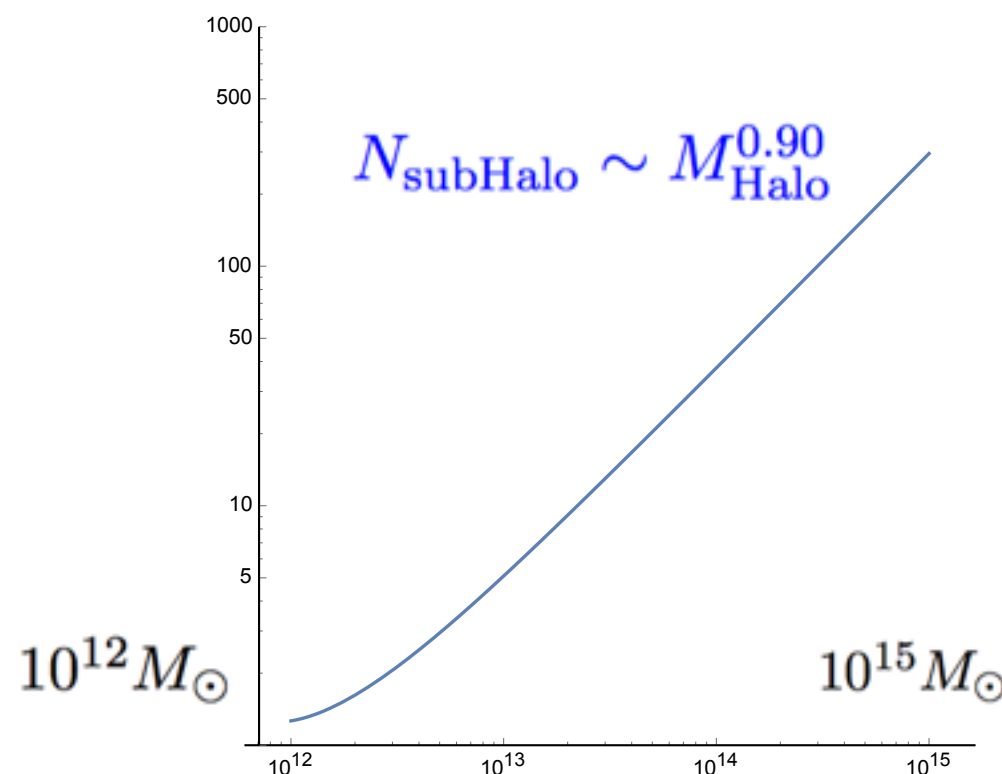
(1) Halo number density



(3) N of Galaxy



(2) N of seeds of Galaxy (subHalo)



Mon. Not. R. Astron. Soc. 371, 1173–1187 (2006)

The non-parametric model for z vs M_{Halo}

A. Vale¹★ and J. P. Ostriker^{1,2}

¹Institute of Astronomy, University of Cambridge, Madingley Road, Cambridge, CB3 0HA, UK

²Princeton University Observatory, Princeton University, Princeton, NJ 08544, USA



YOU ARE HERE: Home > News & Press > A universe of two trillion galaxies

RAS@200

NAM 2017

Home

Search

News & Press

News archive

News for kids

NEWS & PRESS

A universe of two trillion galaxies

Last Updated on Monday, 24 October 2016 11:26

Published on Thursday, 13 October 2016 14:00

An international team of astronomers, led by Christopher Conselice, Professor of Astrophysics at the University of Nottingham, have found that the universe contains at least two trillion galaxies, ten times more than previously thought. The team's work, which began with seed-corn funding from the Royal Astronomical Society, appears in the *Astrophysical Journal* today.

<http://iopscience.iop.org/article/10.3847/0004-637X/830/2/83>

<https://www.ras.org.uk/news-and-press/2910-a-universe-of-two-trillion-galaxies>

x10 more than before

of galaxy (z<8) : 2×10^{12}

of galaxy $10^6 > M_{\odot}$
reduces in evolution

THE EVOLUTION OF GALAXY NUMBER DENSITY AT $z < 8$ AND ITS IMPLICATIONS

Christopher J. Conselice, Aaron Wilkinson, Kenneth Duncan¹, and Alice Mortlock²

Published 2016 October 14 • © 2016. The American Astronomical Society. All rights reserved.

The Astrophysical Journal, Volume 830, Number 2

Metrics ▾

+ Article information

Abstract

The evolution of the number density of galaxies in the universe, and thus also the total number of galaxies, is a fundamental question with implications for a host of astrophysical problems including galaxy evolution and cosmology. However, there has never been a detailed study of this important measurement, nor a clear path to answer it. To address this we use observed galaxy stellar mass functions up to $z \sim 8$ to determine how the number densities of galaxies change as a function of time and mass limit. We show that the increase in the total number density of galaxies (ϕ_T), more massive than $M_* = 10^6 M_\odot$, decreases as $\phi_T \sim t^{-1}$,

How many Galaxies in the Universe?

Count BHs to form a SMBH

(sub-)Galaxy
from Halo model

Mon. Not. R. Astron. Soc. 371, 1173–1187 (2006)

doi:10

The non-parametric model for linking galaxy luminosity
with halo/subhalo mass

A. Vale^{1*} and J. P. Ostriker^{1,2}

¹Institute of Astronomy, University of Cambridge, Madingley Road, Cambridge CB3 0HA

²Princeton University Observatory, Princeton University, Princeton, NJ 08544, USA

THE ASTROPHYSICAL JOURNAL, 744:95 (13pp), 2012 January 10
© 2012. The American Astronomical Society. All rights reserved. Printed in the U.S.A.

doi:10.1088/0004-637X/744/2/95

CONNECTING THE GAMMA RAY BURST RATE AND THE COSMIC STAR FORMATION HISTORY:
IMPLICATIONS FOR REIONIZATION AND GALAXY EVOLUTION

BRANT E. ROBERTSON^{1,2,3} AND RICHARD S. ELLIS¹

¹ Astronomy Department, California Institute of Technology, MC 249-17, 1200 East California Boulevard, Pasadena, CA 91125, USA; brant@astro.caltech.edu

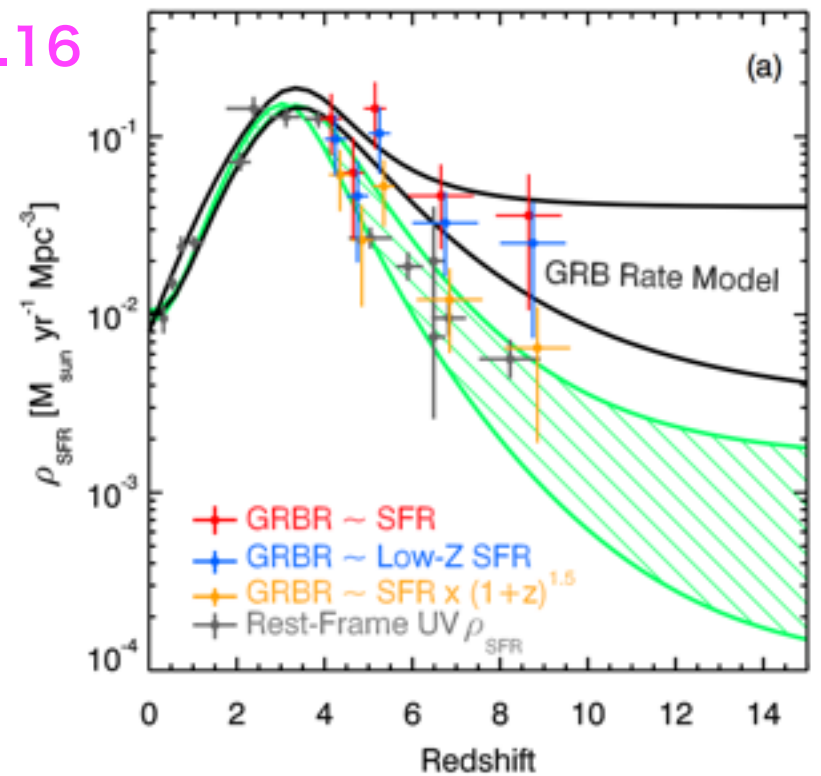
² Steward Observatory, University of Arizona, 933 North Cherry Avenue, Tucson, AZ 85721, USA

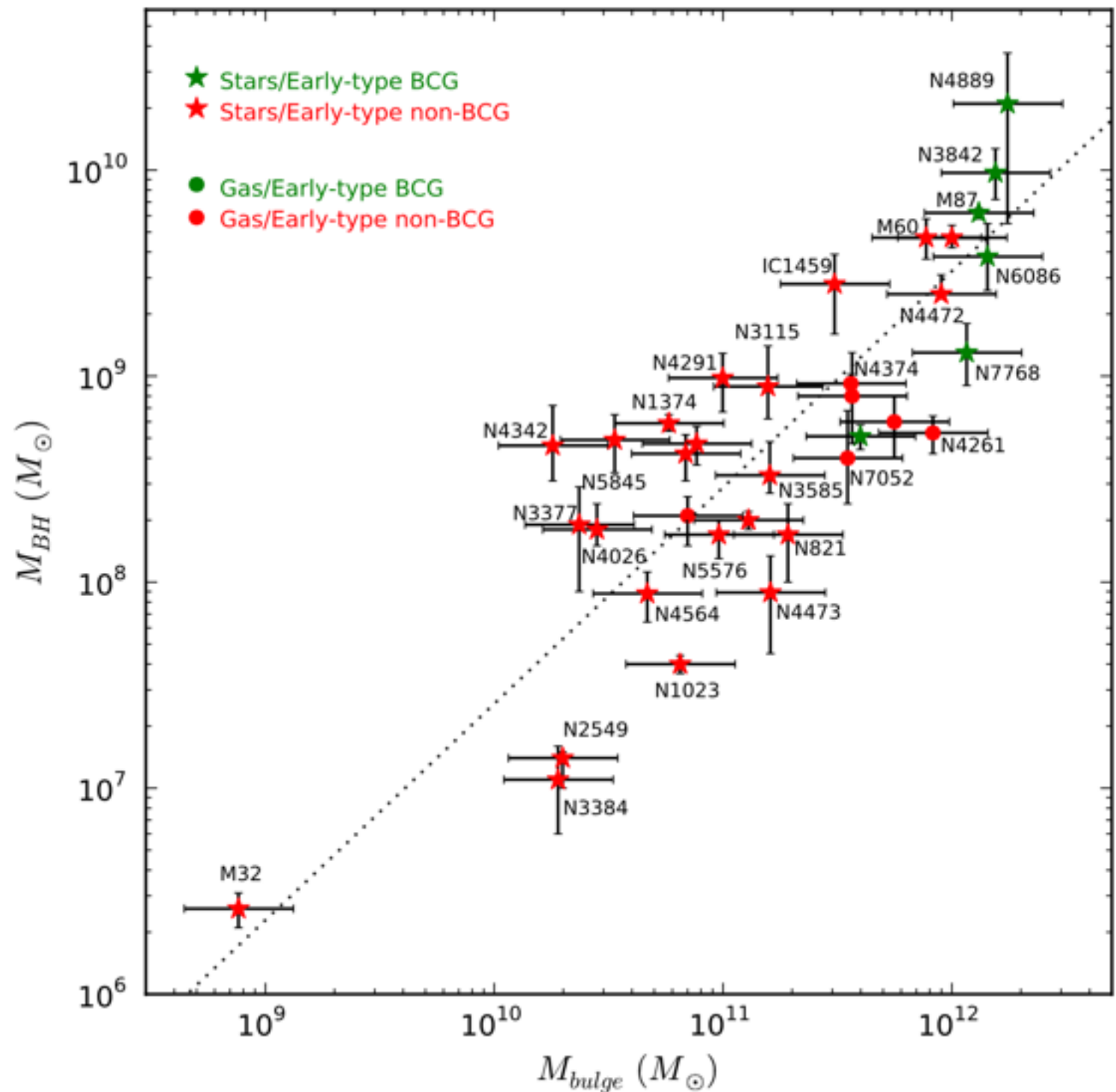
Received 2011 September 5; accepted 2011 November 18; published 2011 December 19

$$\begin{aligned} M_{\text{SMBH}} &= 2 \times 10^{-4} M_{\text{galaxy}} \\ &= 10^{-3} M_{\text{bulge}} \end{aligned}$$

Star Formation Rate

peak z=3.16





$$M_{\text{SMBH}} = 2 \times 10^{-4} M_{\text{galaxy}}$$

$$= 10^{-3} M_{\text{bulge}}$$

McConnell-Ma
ApJ 764(2013)184

Figure 3. M_\bullet - M_{bulge} relation for the 35 early-type galaxies with dynamical measurements of the bulge stellar mass in our sample. The symbols are the same as in Figure 1. The black line represents the best-fitting power-law $\log_{10}(M_\bullet / M_\odot) = 8.46 + 1.05 \log_{10}(M_{\text{bulge}} / 10^{11} M_\odot)$.

contents

1. Gravitational Waves

Detectors, GW events

2. Models of SMBH

hierarchical growth model, or others

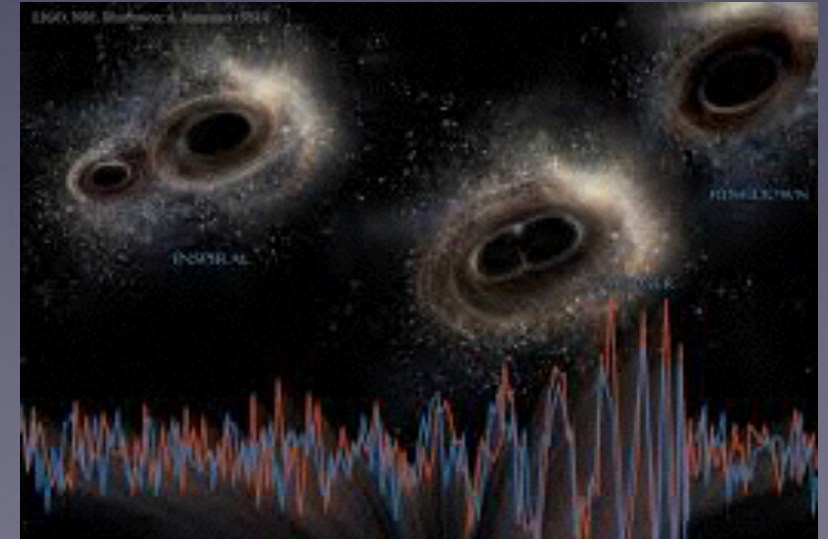
3. Counting BHs

How many BHs in a galaxy?

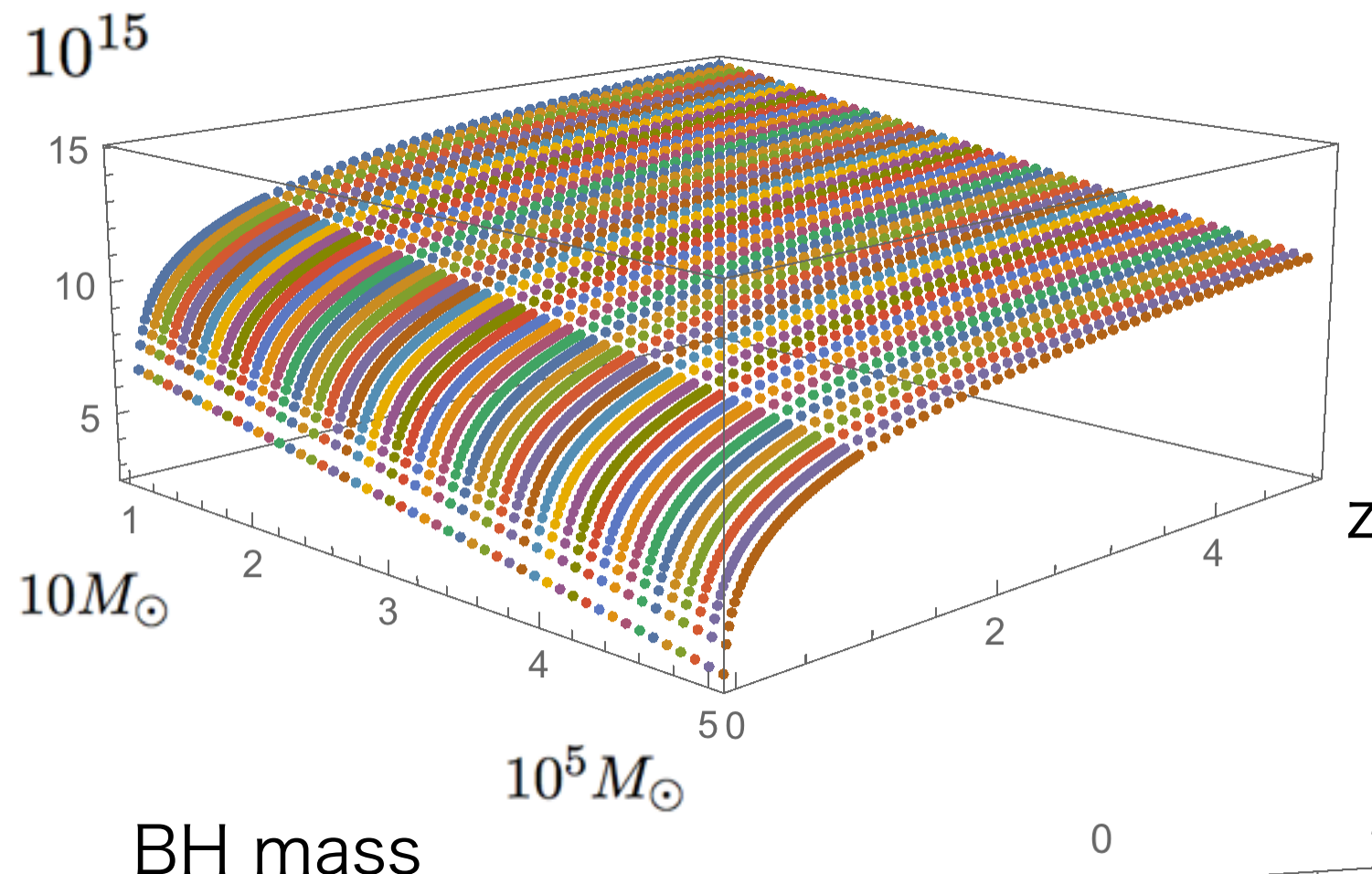
How many galaxies in the Universe?

4. Event Rates at aLIGO/KAGRA/DECIGO/LISA

How many BH mergers in the Universe?



How many BH mergers in the Universe?

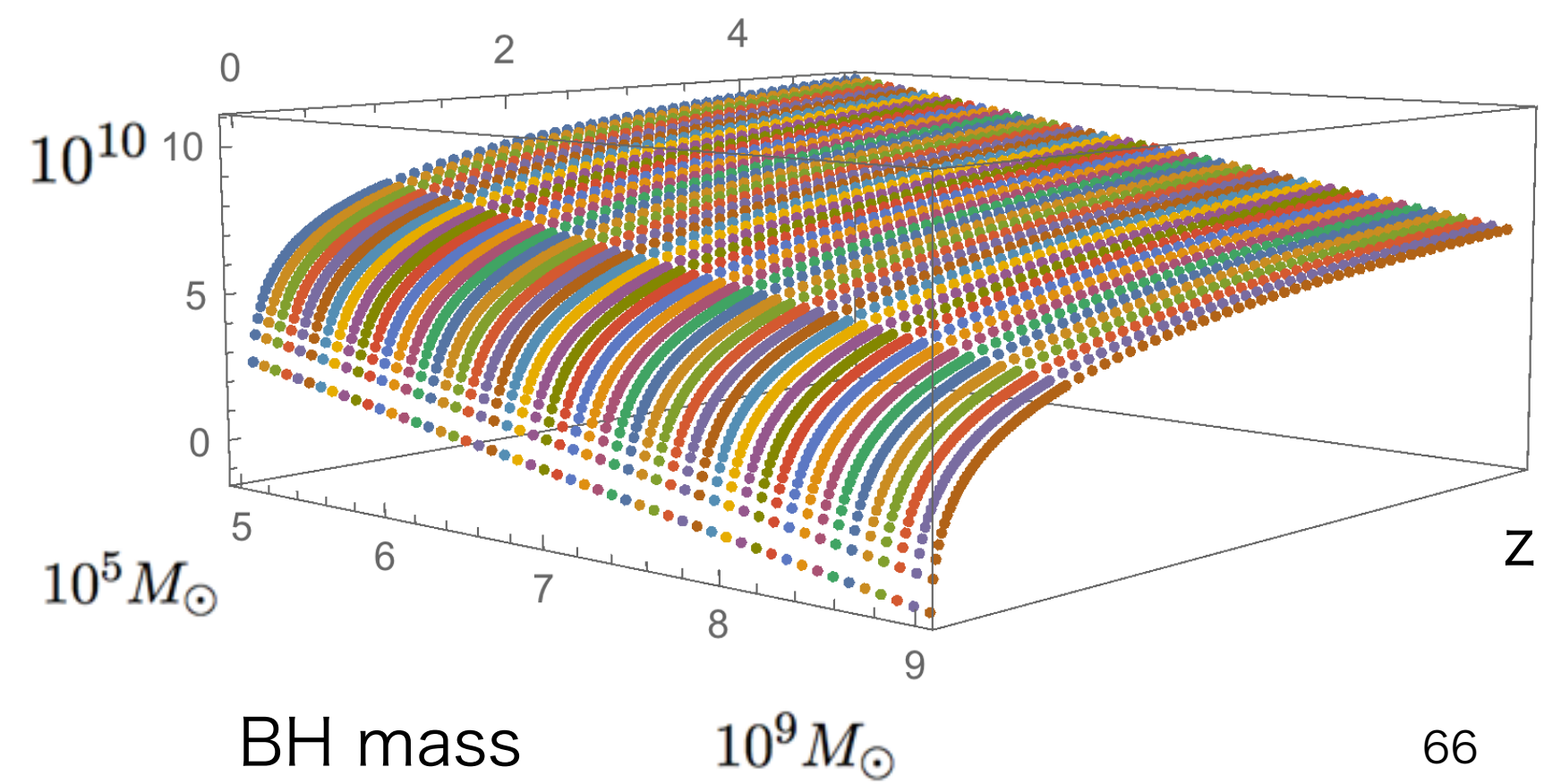


in Standard Cosmology

$$\text{Event Rate } R[\text{yr}^{-1}] = \frac{N_{\text{merger}}(z)}{V(D/2.26)}$$

Standard Cosmology

averaging distances
for all directions



Signal-to-Noise Ratio (SNR)

Let the true signal $h(t)$, the function of time, is detected as a signal, $s(t)$, which also includes the unknown noise, $n(t)$:

$$s(t) = h(t) + n(t). \quad (17)$$

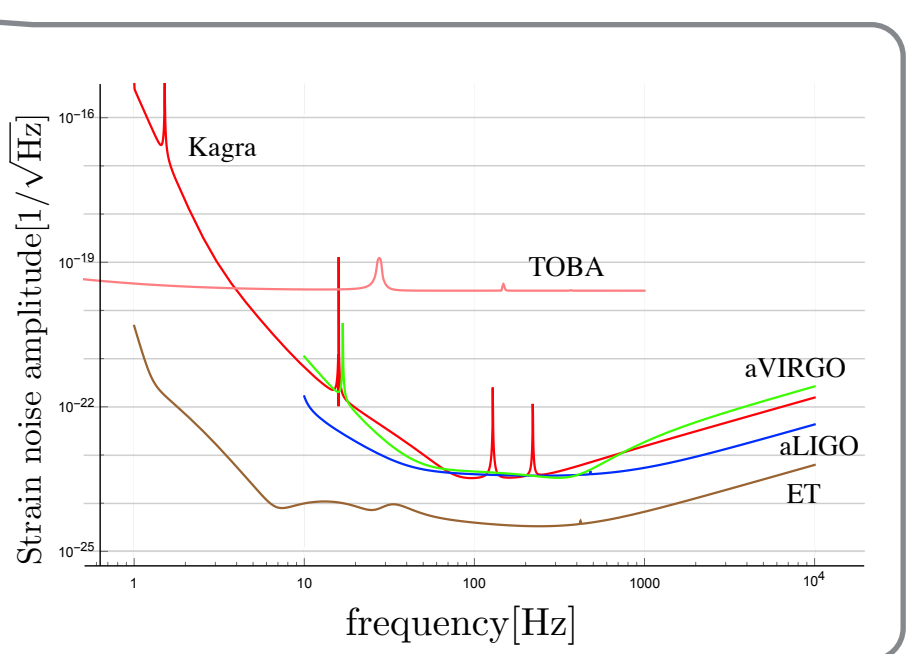
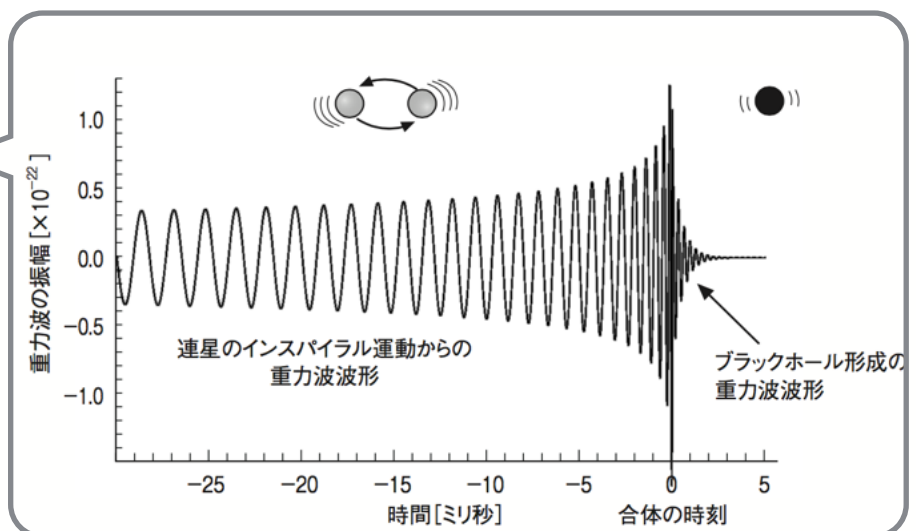
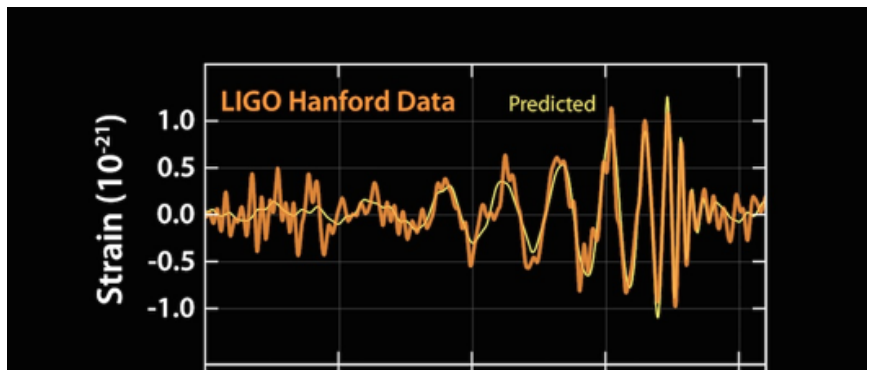
The standard procedure for the detection is judged by the optimal signal-to-noise ratio (SNR), ρ , which is given by

$$\rho = 2 \left[\int_0^\infty \frac{\tilde{h}(f) \tilde{h}^*(f)}{S_n(f)} df \right]^{1/2}, \quad (18)$$

where $\tilde{h}(f)$ is the Fourier-transformed quantity of the wave,

$$\tilde{h}(f) = \int_{-\infty}^{\infty} e^{2\pi i f t} h(t) dt, \quad (19)$$

and $S_n(f)$ the (one-sided) power spectral density of strain noise of the detector, as we showed in Fig. 1.



Detectable Distances at bKAGRA

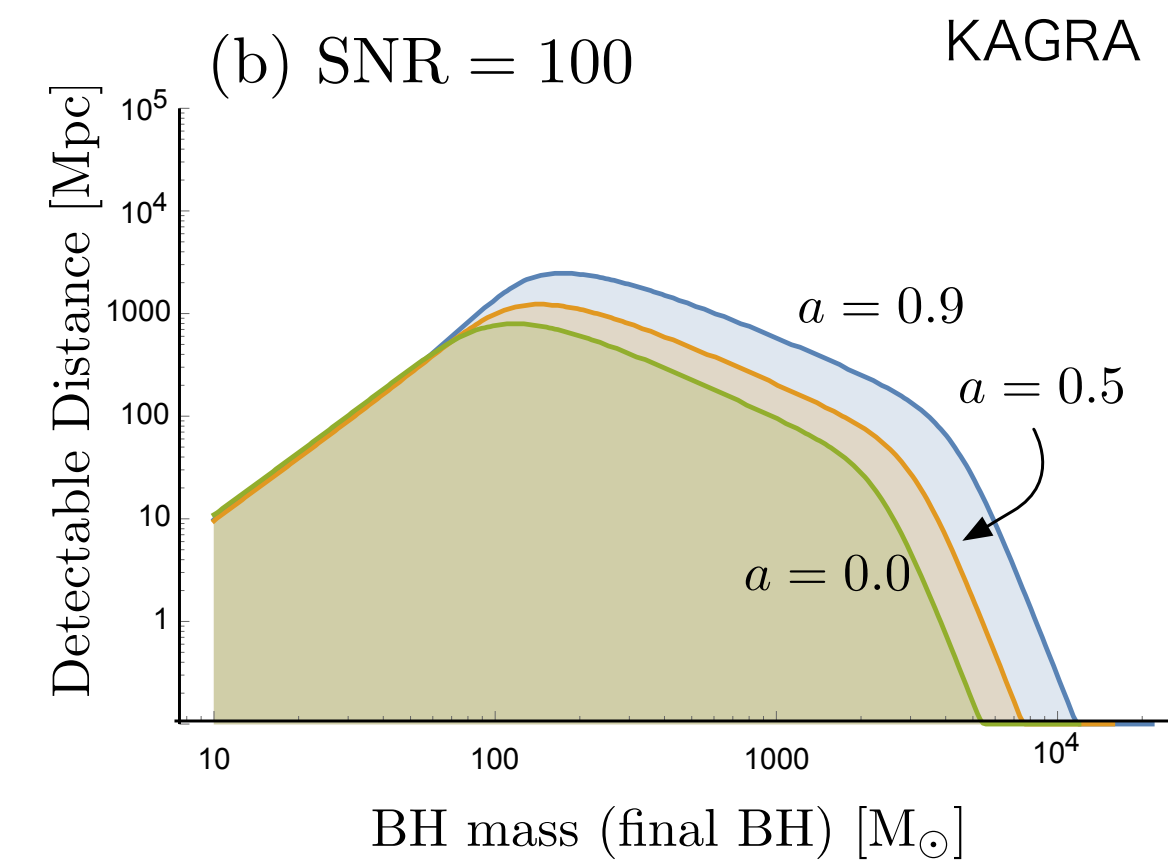
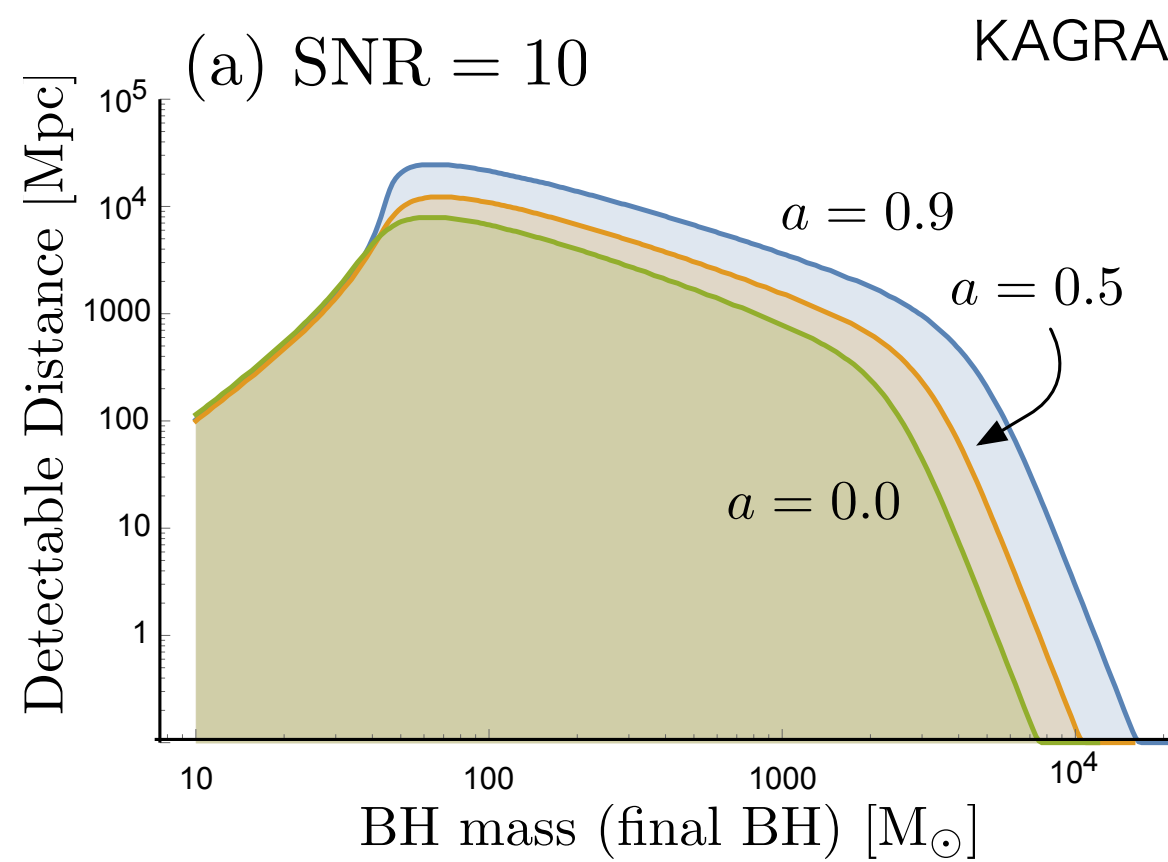
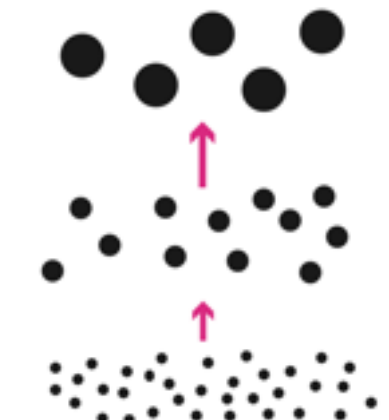
Flanagan&Hughes, PRD57(1998)4535

$$\text{SNR} \quad \rho^2 = \frac{8}{5} \frac{\epsilon_r(a)}{f_R^2} \frac{(1+z)M}{S_h(f_R/(1+z))} \left(\frac{(1+z)M}{d_L(z)} \right)^2 \left(\frac{4\mu}{M} \right)^2$$

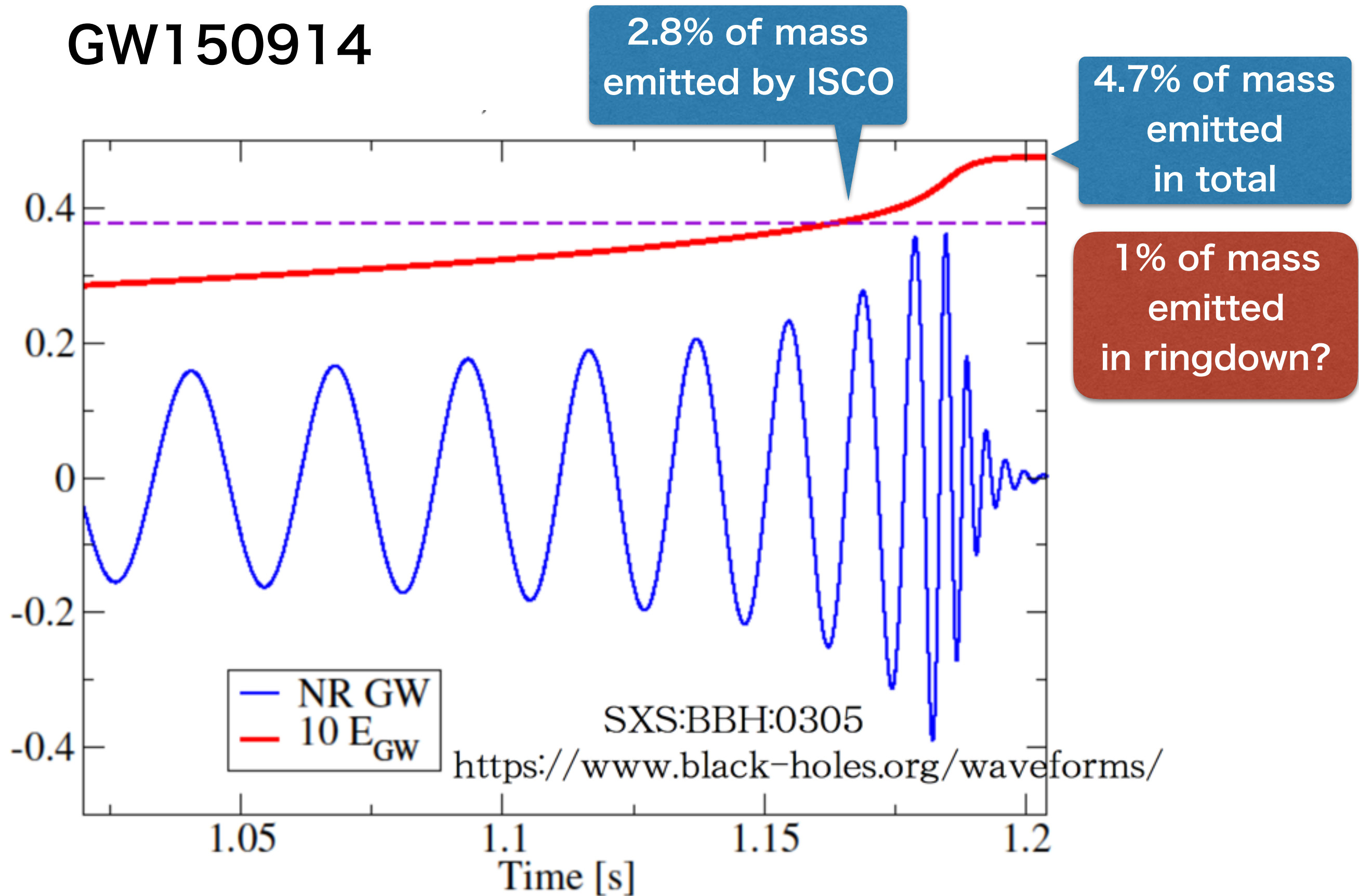
Standard Cosmology

Energy emission=4% of total M, 1% at ringdown

Hierarchical Growth

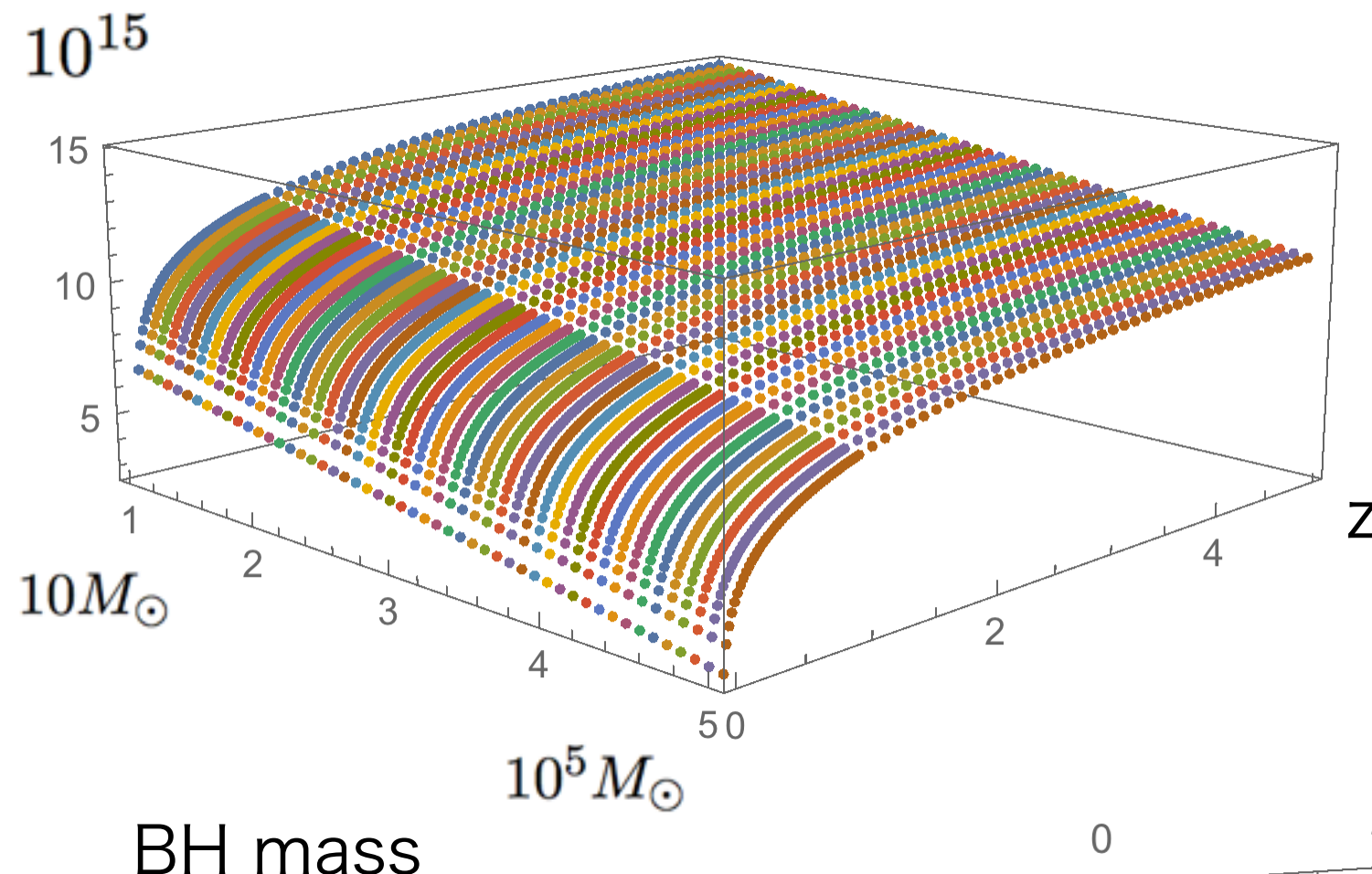


GW150914



Slide copy from Hiroyuki Nakano

How many BH mergers in the Universe?

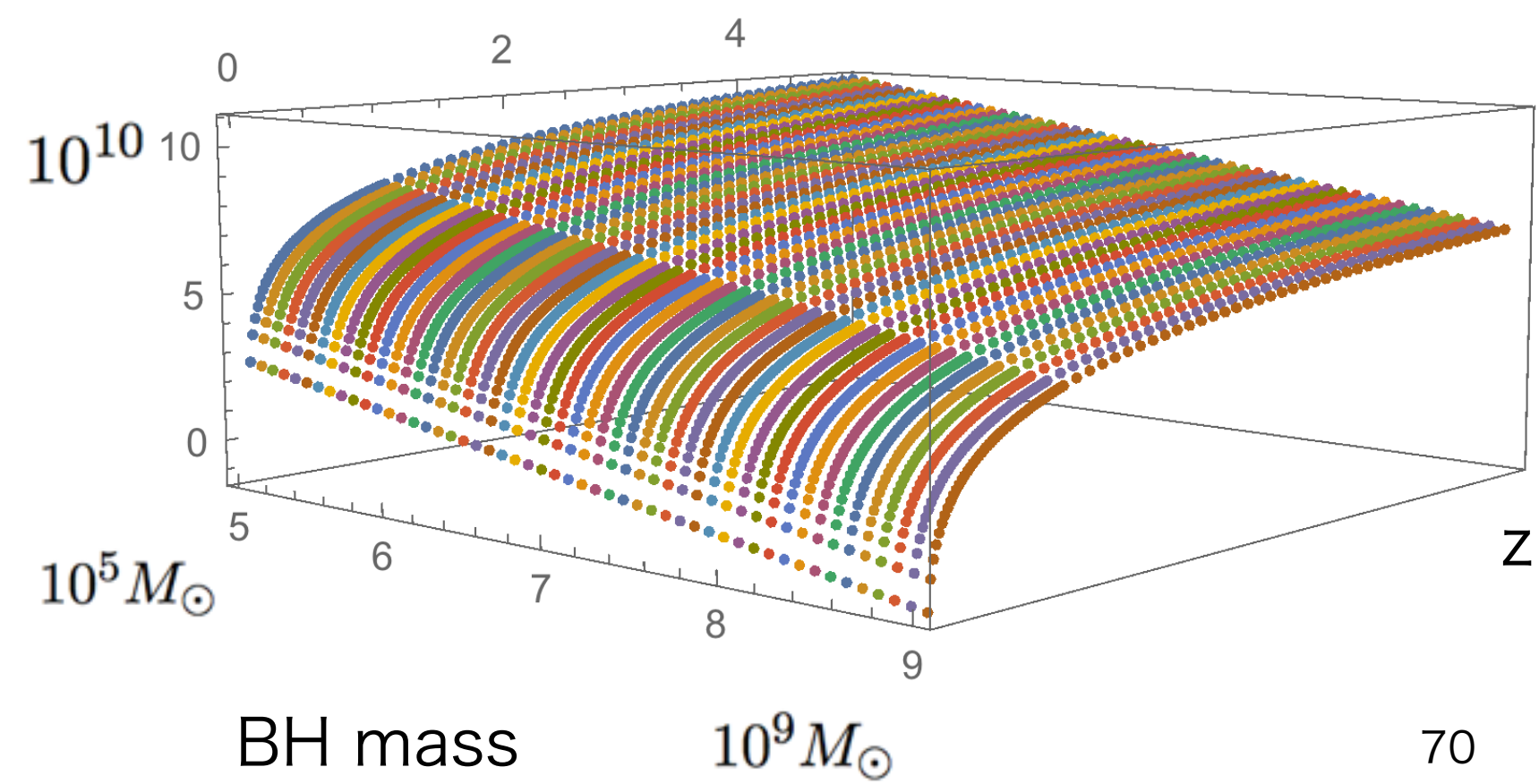


in Standard Cosmology

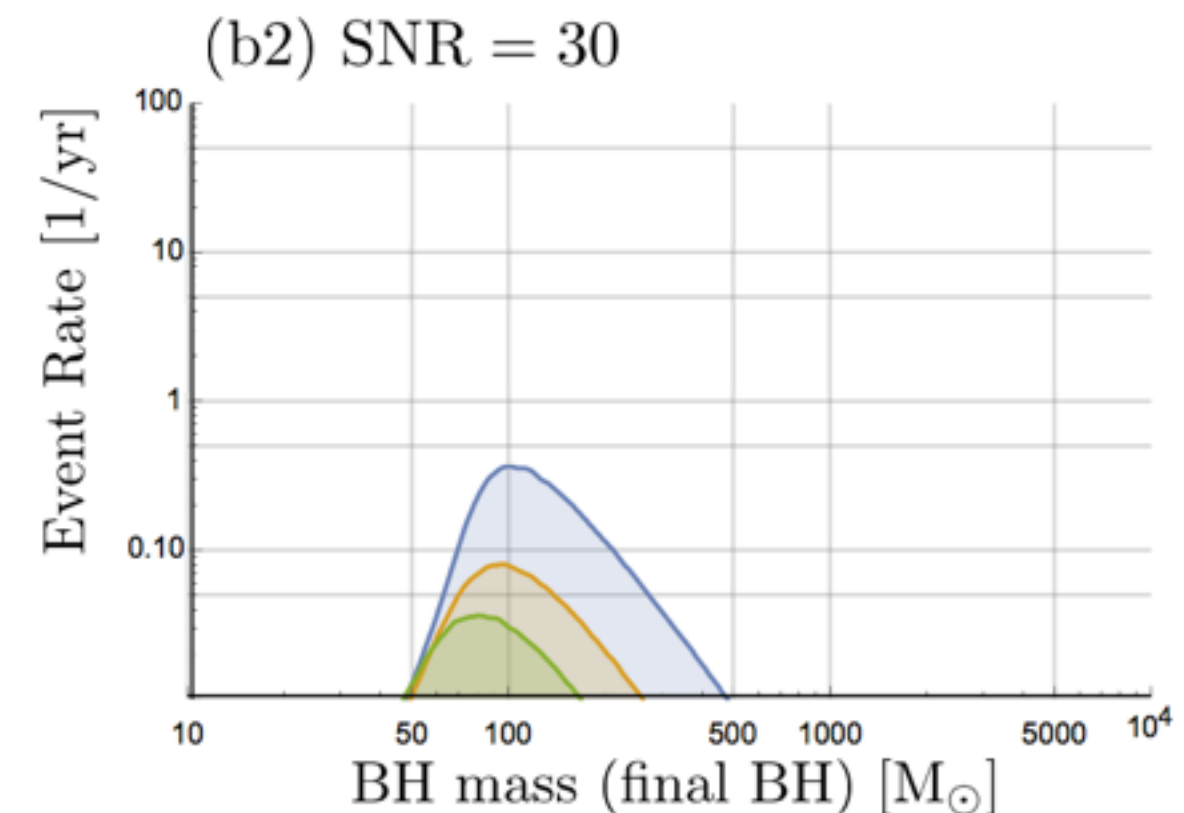
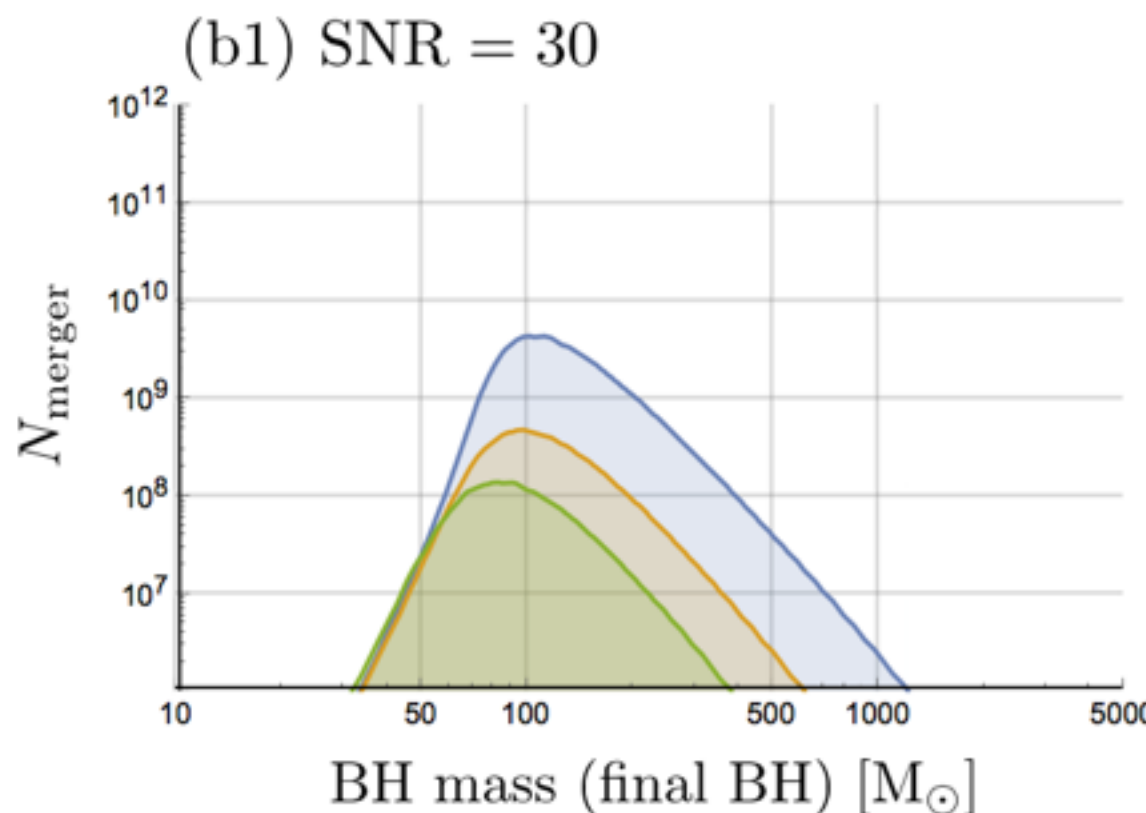
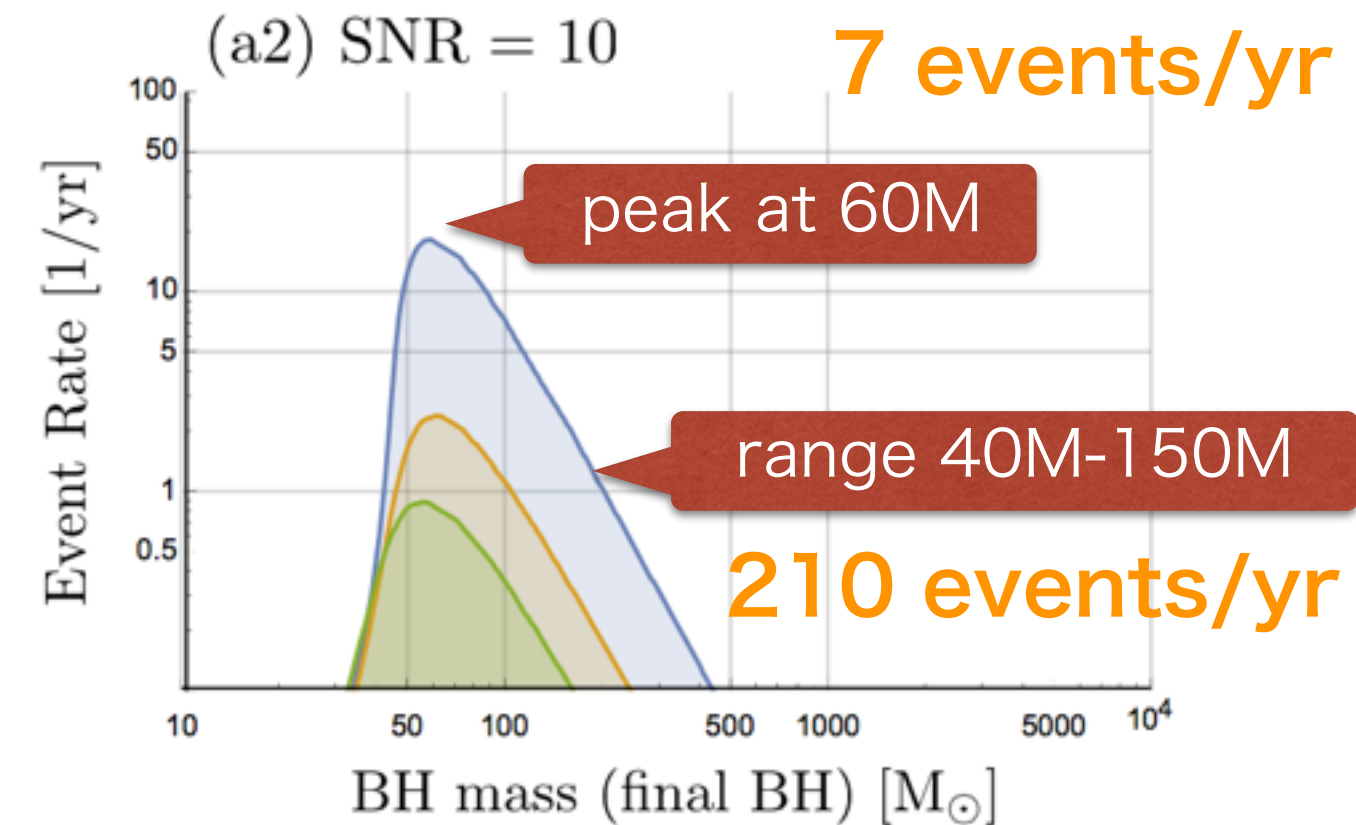
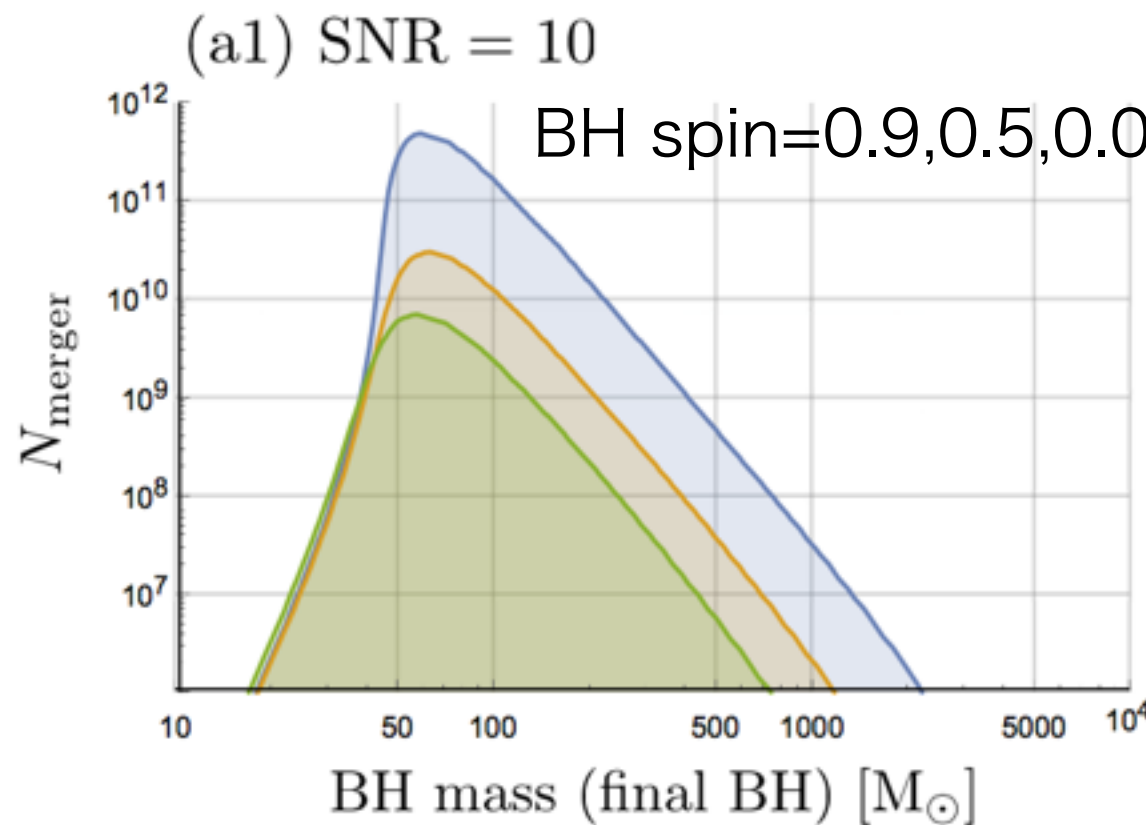
$$\text{Event Rate } R[\text{yr}^{-1}] = \frac{N_{\text{merger}}(z)}{V(D/2.26)}$$

Standard Cosmology

averaging distances
for all directions



Event Rates at bKAGRA



Event Rates at bKAGRA/aLIGO

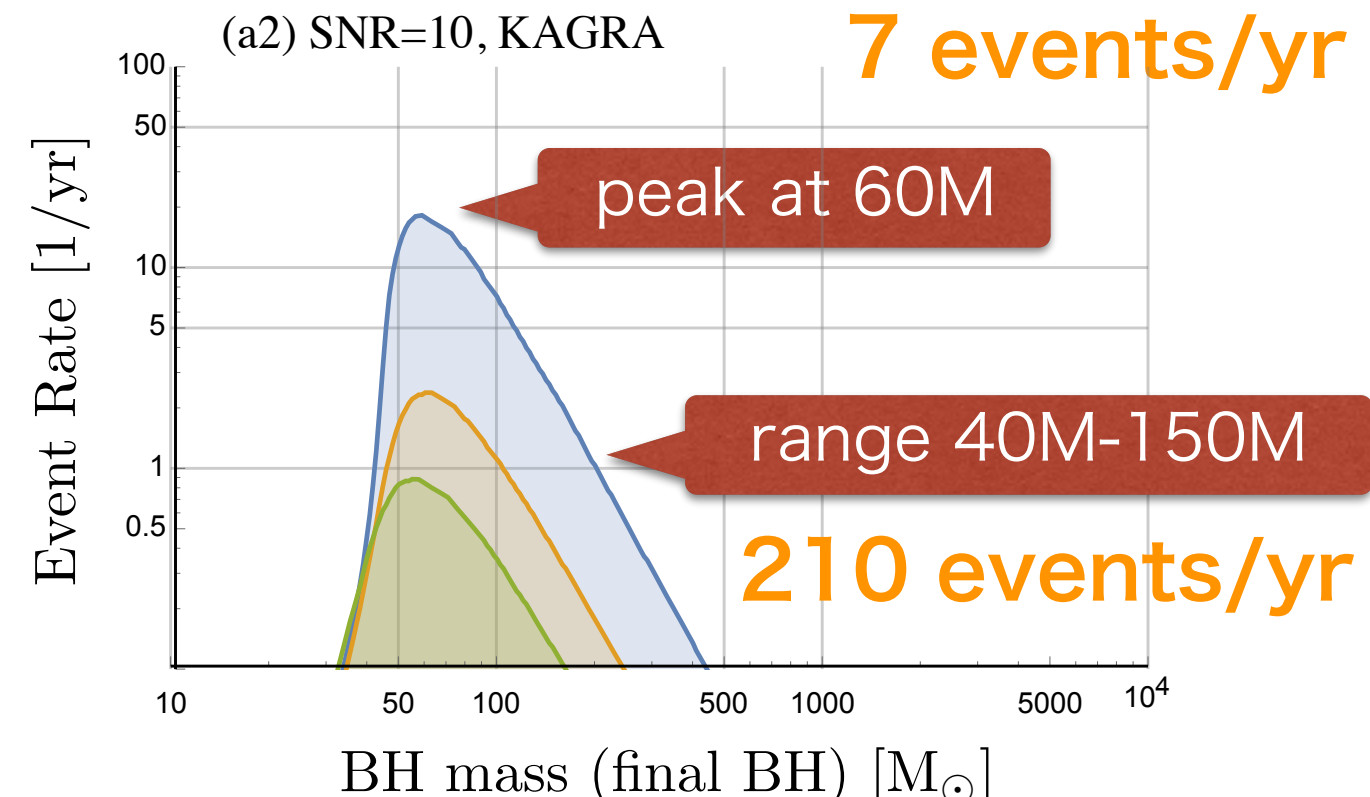
LIGO group [1602.03842]

THE ASTROPHYSICAL JOURNAL LETTERS, 833:L1 (8pp), 2016 December 10

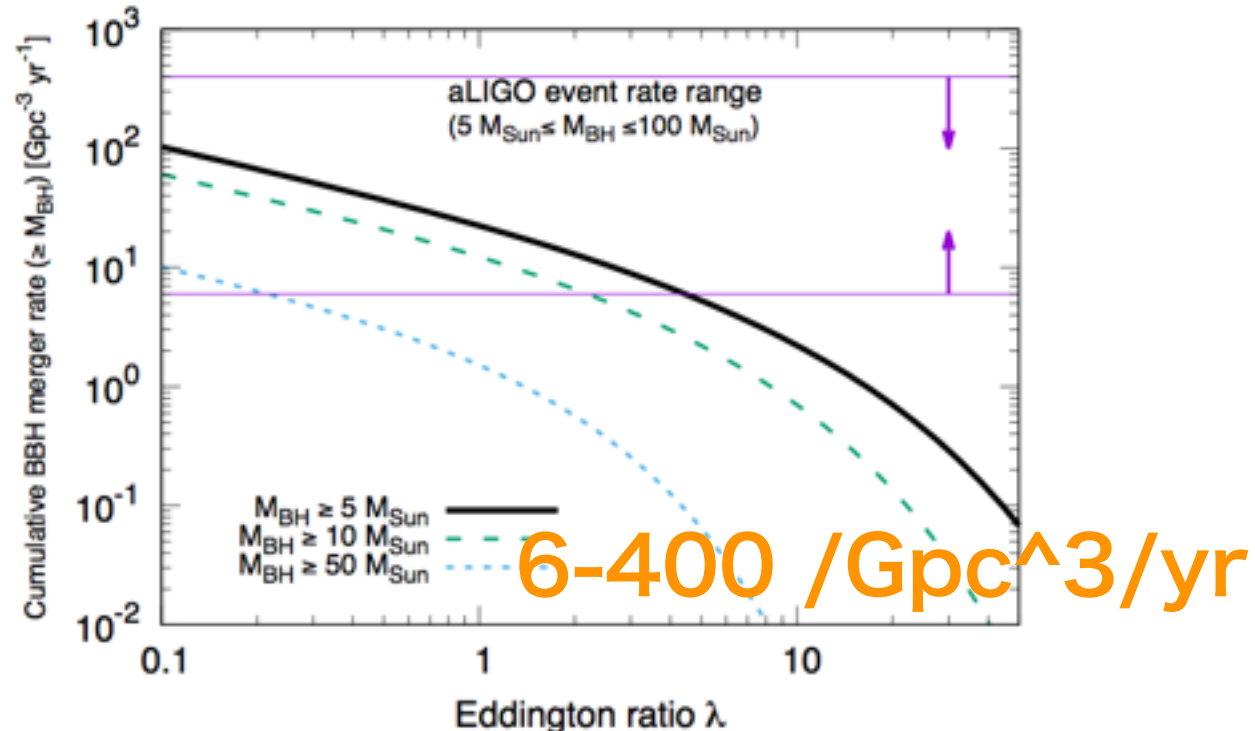
Table 1

Rates of BBH Mergers Estimated under Various Assumptions

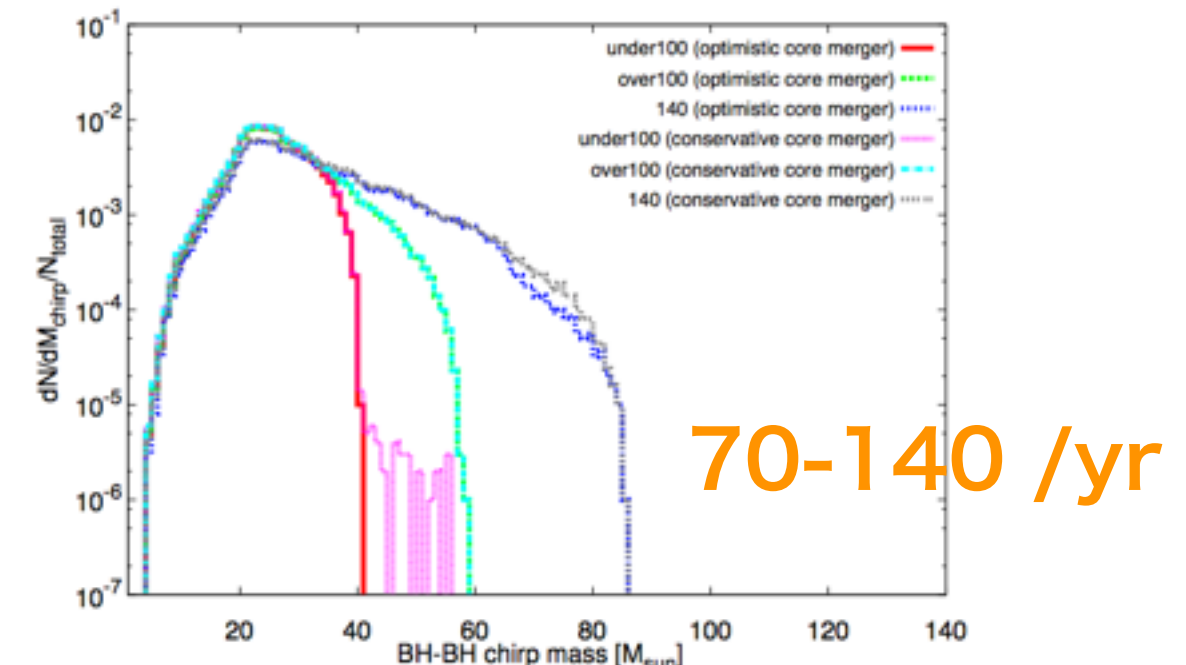
Mass Distribution	$R/(Gpc^{-3} yr^{-1})$		
	pycbc	gstlal	Combined
GW150914	16^{+38}_{-13}	17^{+39}_{-14}	17^{+39}_{-13}
LVT151012	61^{+152}_{-53}	62^{+164}_{-55}	62^{+165}_{-54}
Both	82^{+155}_{-61}	84^{+172}_{-64}	83^{+168}_{-63}
Astrophysical			
Flat in log mass	63^{+121}_{-49}	60^{+122}_{-48}	61^{+124}_{-50}
Power Law (-2.35)	200^{+390}_{-160}	200^{+410}_{-160}	200^{+400}_{-160}



Inoue+ MNRAS461(16)4329



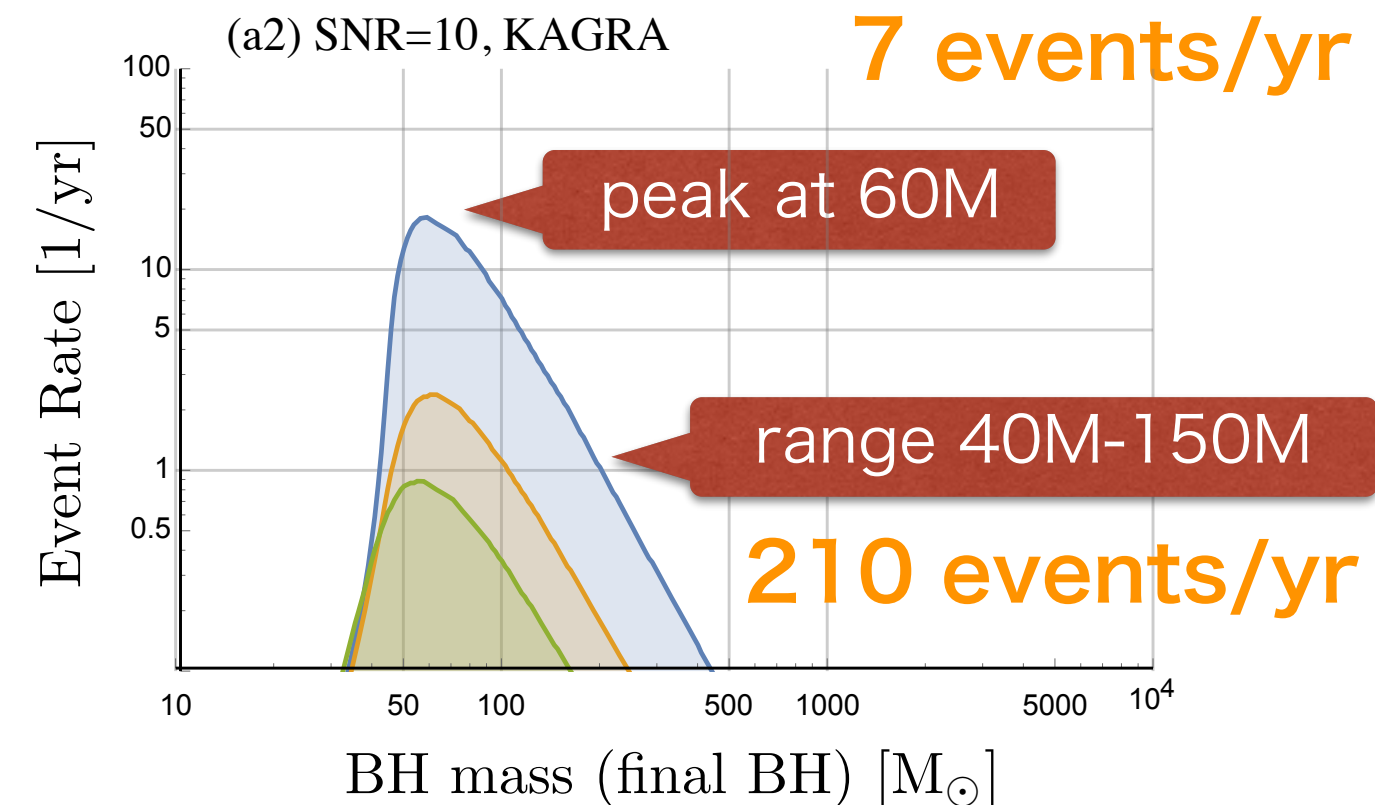
Kinugawa+ MNRAS456(15)1093



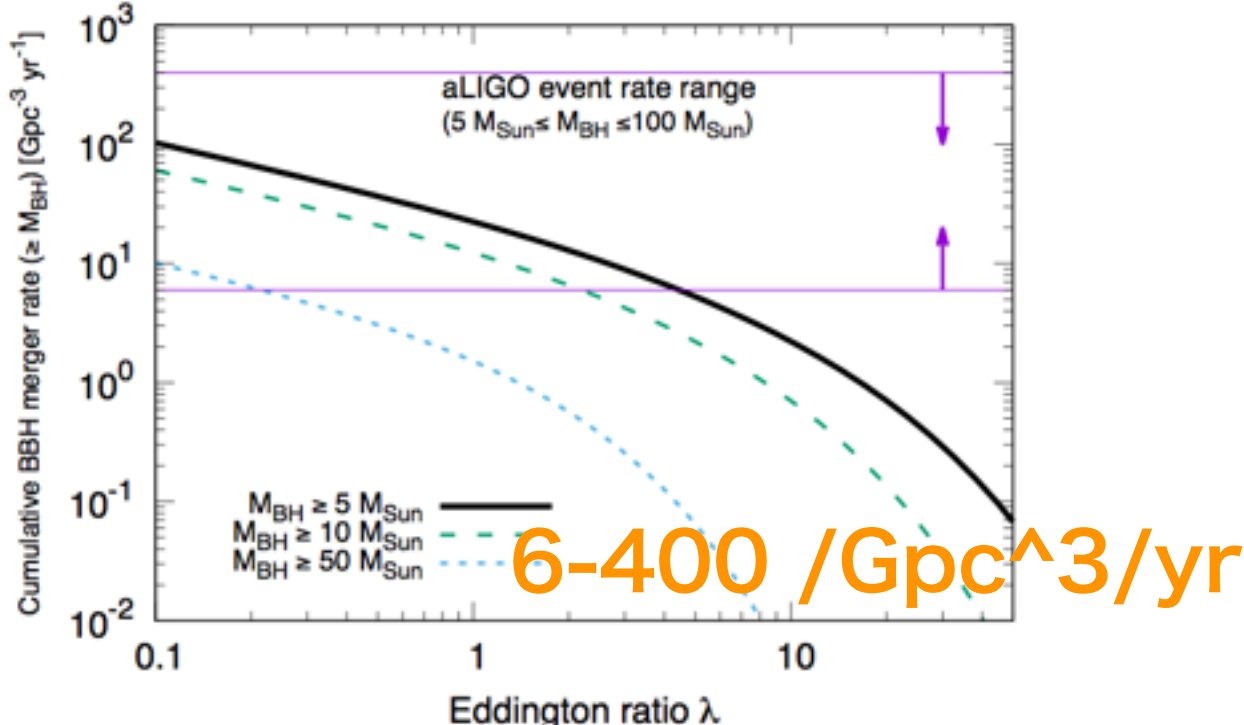
Event Rates at bKAGRA/aLIGO

LIGO group PRX6(2016)041015

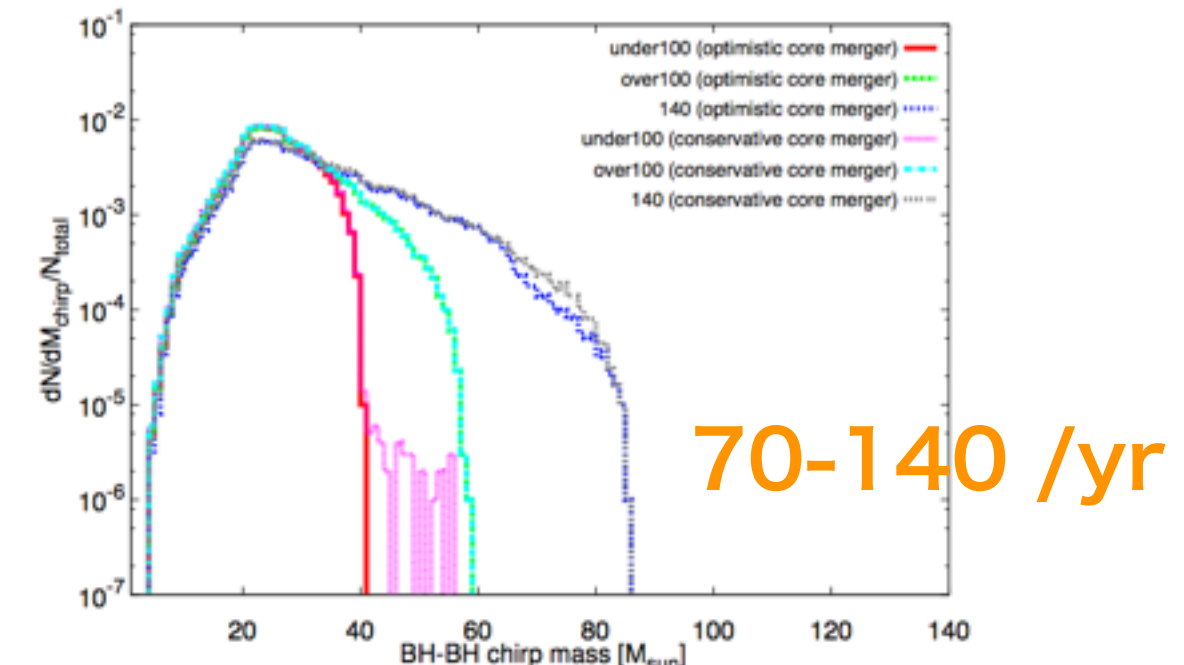
Mass distribution	PyCBC	GstLAL	$R/(Gpc^{-3} yr^{-1})$	Combined
Event based				
GW150914	$3.2^{+8.3}_{-2.7}$	$3.6^{+9.1}_{-3.0}$	$3.4^{+8.8}_{-2.8}$	
LVT151012	$9.2^{+30.3}_{-8.5}$	$9.2^{+31.4}_{-8.5}$	$9.1^{+31.0}_{-8.5}$	
GW151226	35^{+92}_{-29}	37^{+94}_{-31}	36^{+95}_{-30}	
All	53^{+100}_{-40}	56^{+105}_{-42}	55^{+103}_{-41}	
Astrophysical				
Flat in log mass	31^{+43}_{-21}	29^{+43}_{-21}	31^{+42}_{-21}	
Power law (-2.35)	100^{+136}_{-69}	94^{+137}_{-66}	97^{+135}_{-67}	



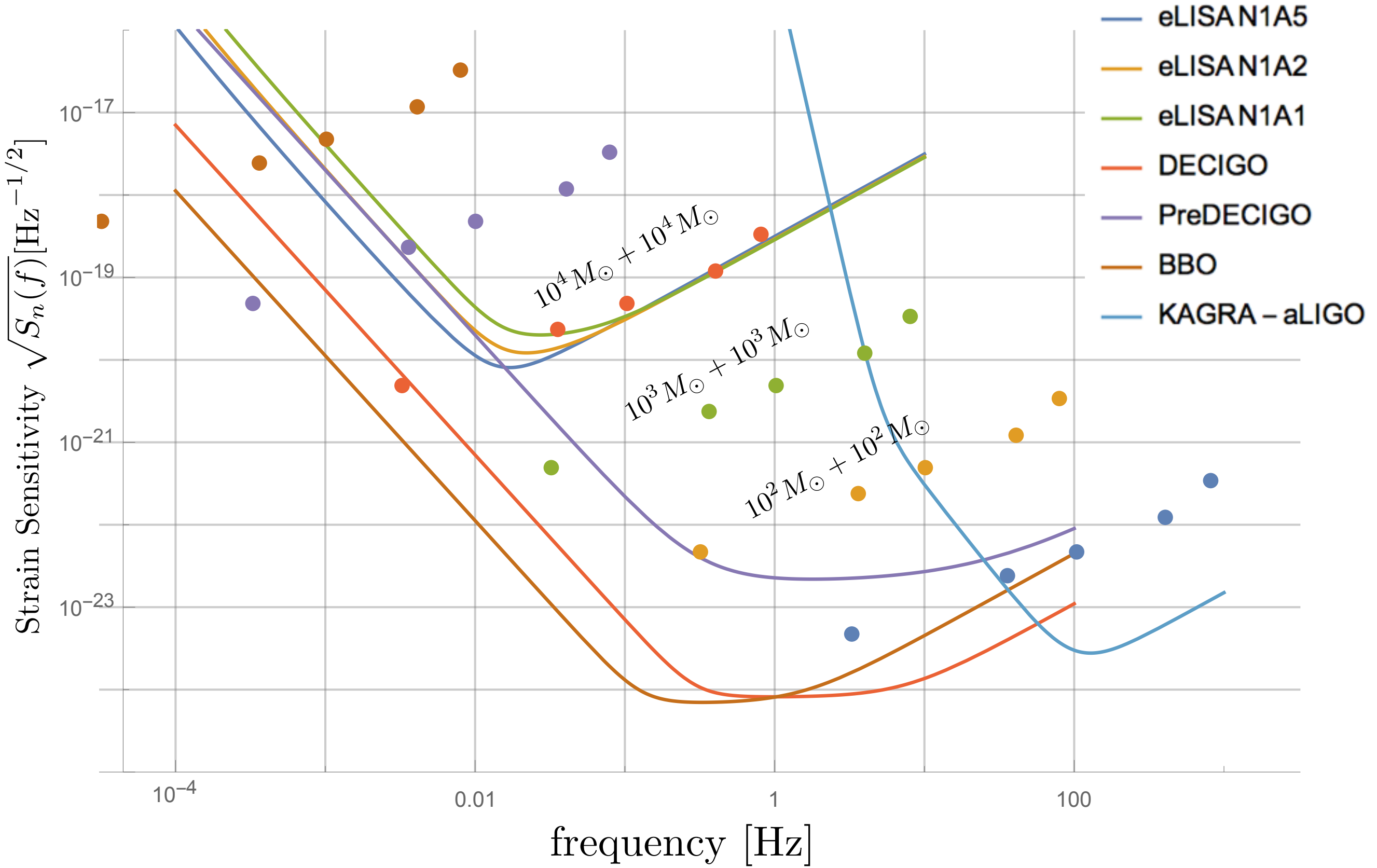
Inoue+ MNRAS461(16)4329



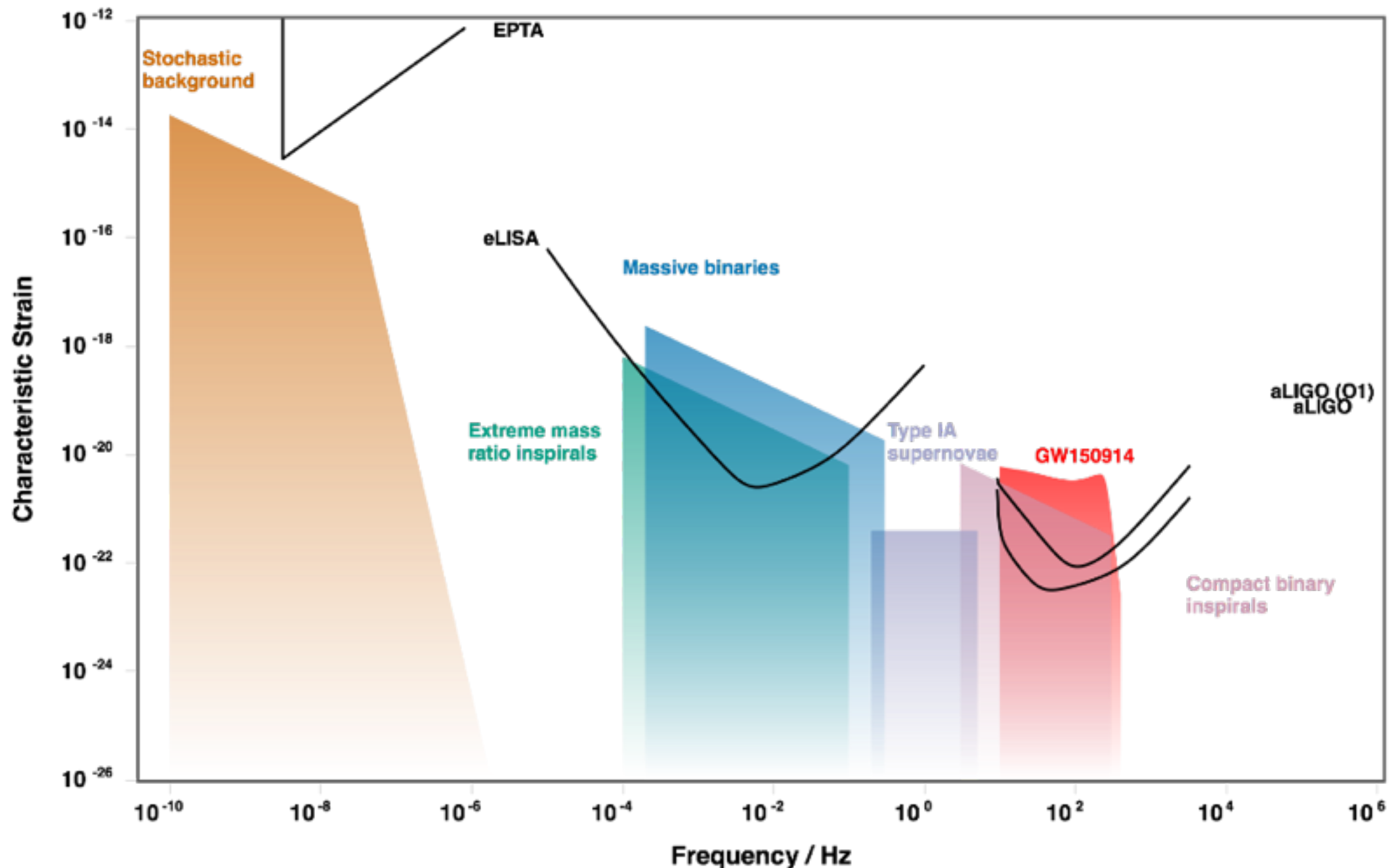
Kinugawa+ MNRAS456(15)1093



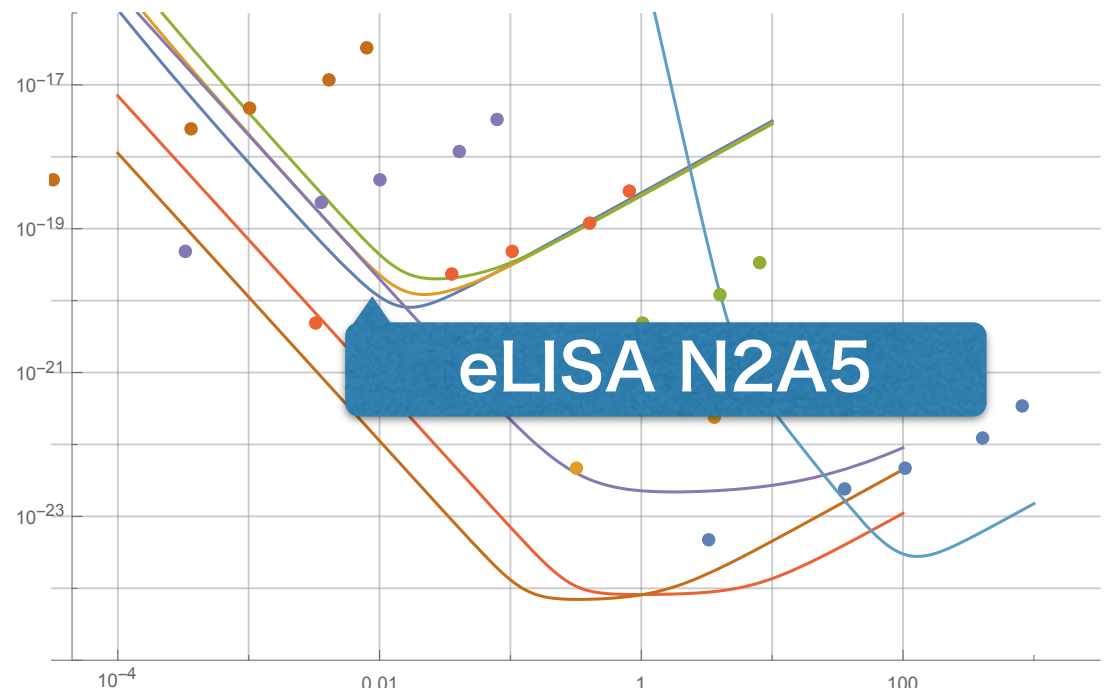
Sensitivity of Space GW Interferometers



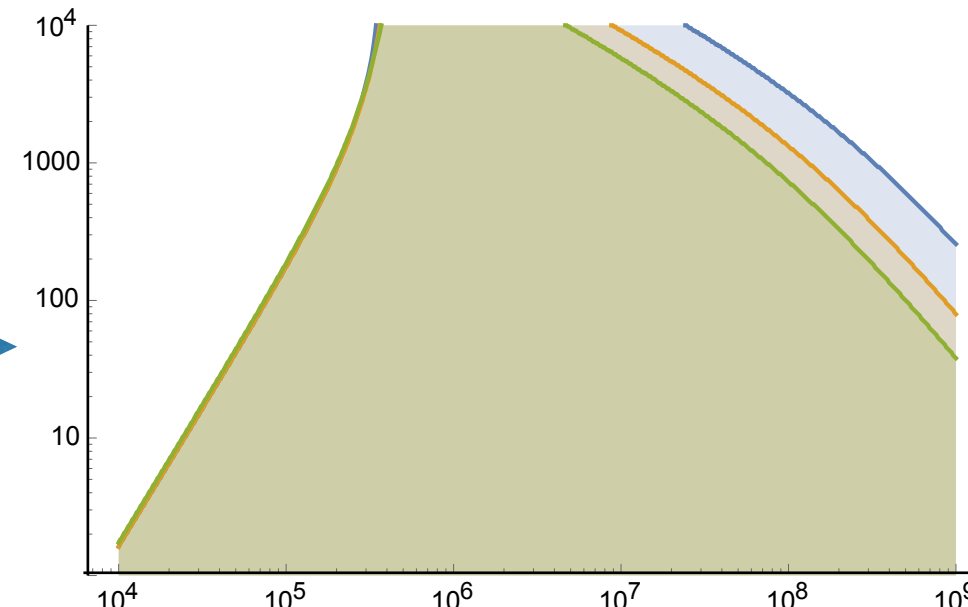
これは遊べる GWplotter
<http://rhcole.com/apps/GWplotter/>



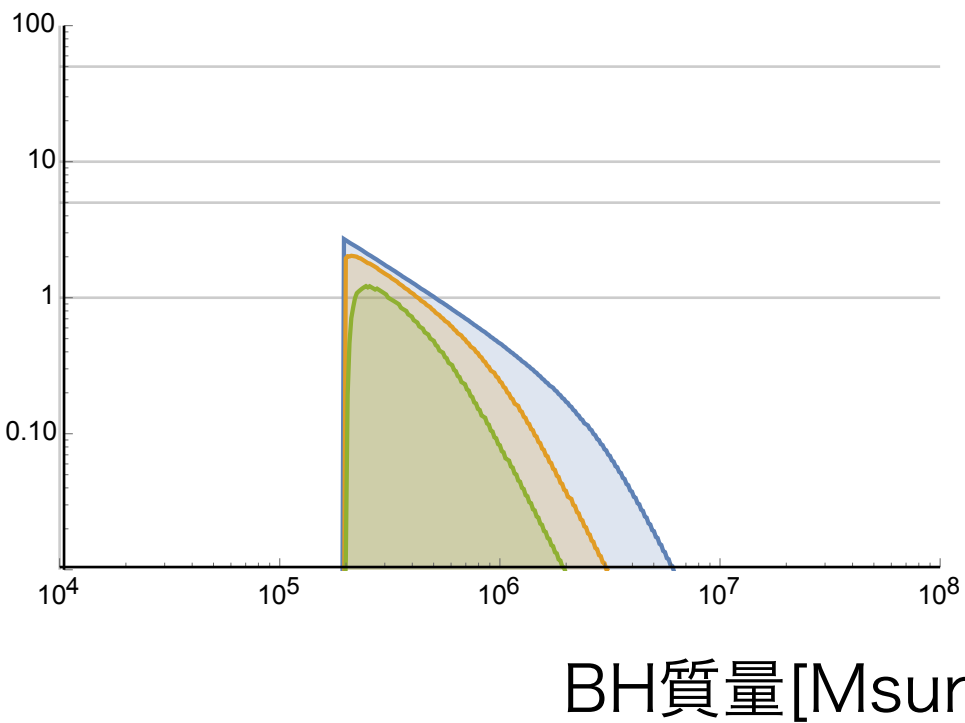
Event Rates at eLISA



観測できるBH合体距離
[Mpc] (S/N=10)

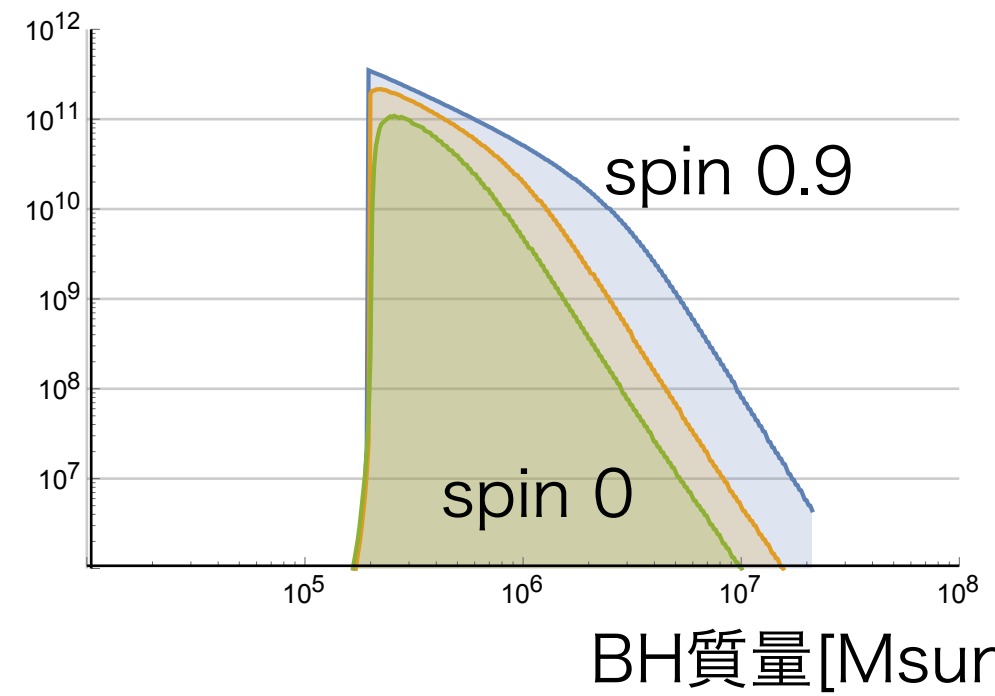


1年間で観測できるBH数分布
(S/N=10) 年55個



BH質量 [Msun]

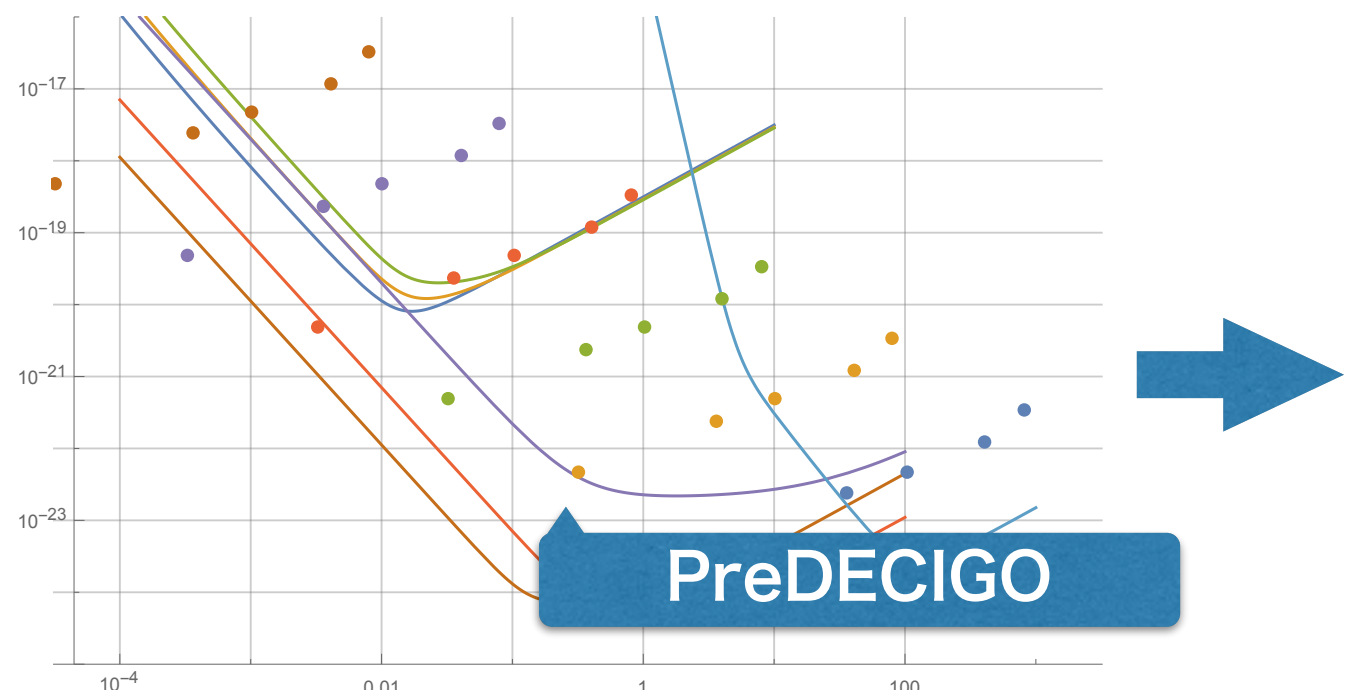
観測できるBH数分布



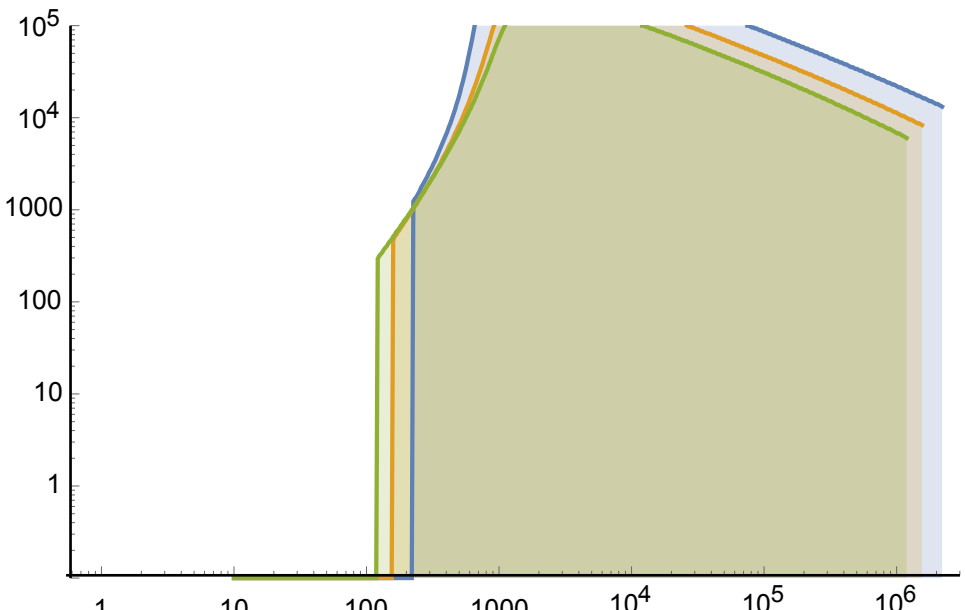
Event Rates at PreDECIGO

観測できるBH合体距離
(S/N=10)

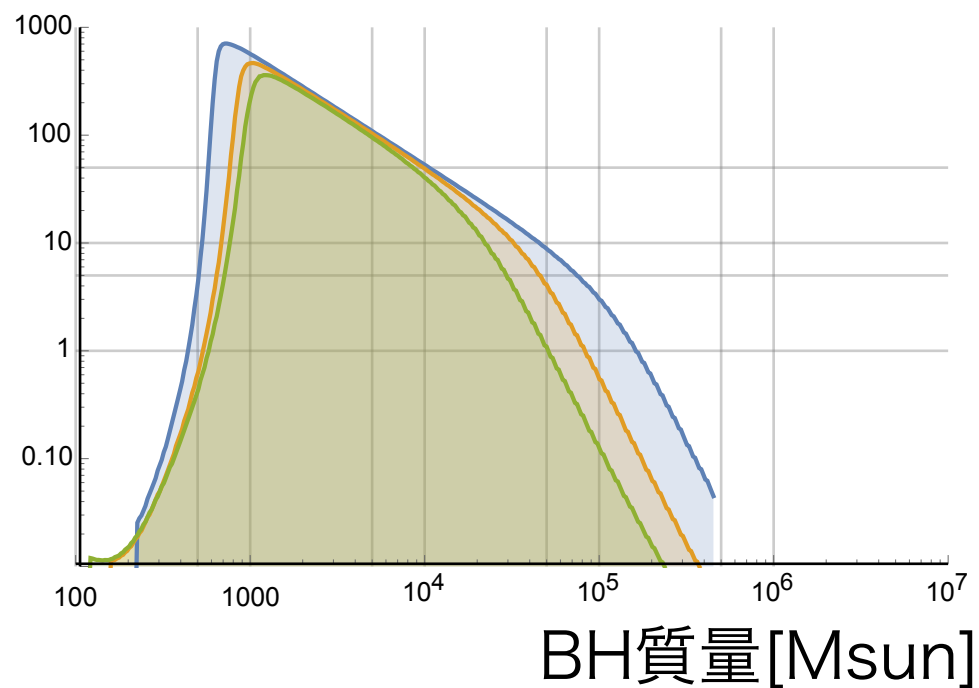
[Mpc]



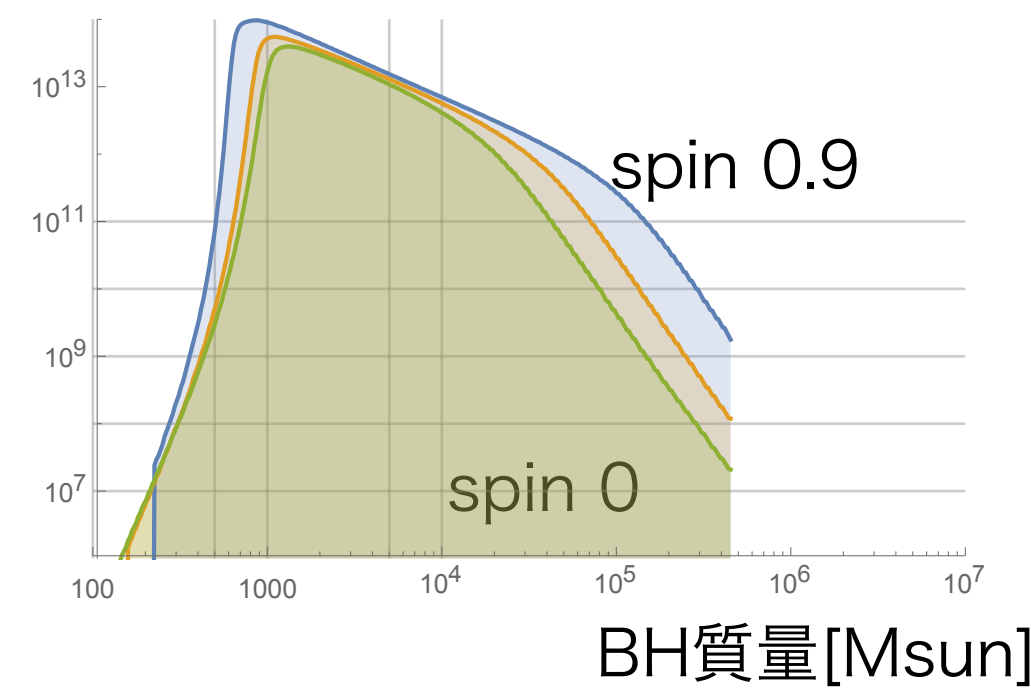
PreDECIGO



1年間で観測できるBH数分布
(S/N=10)

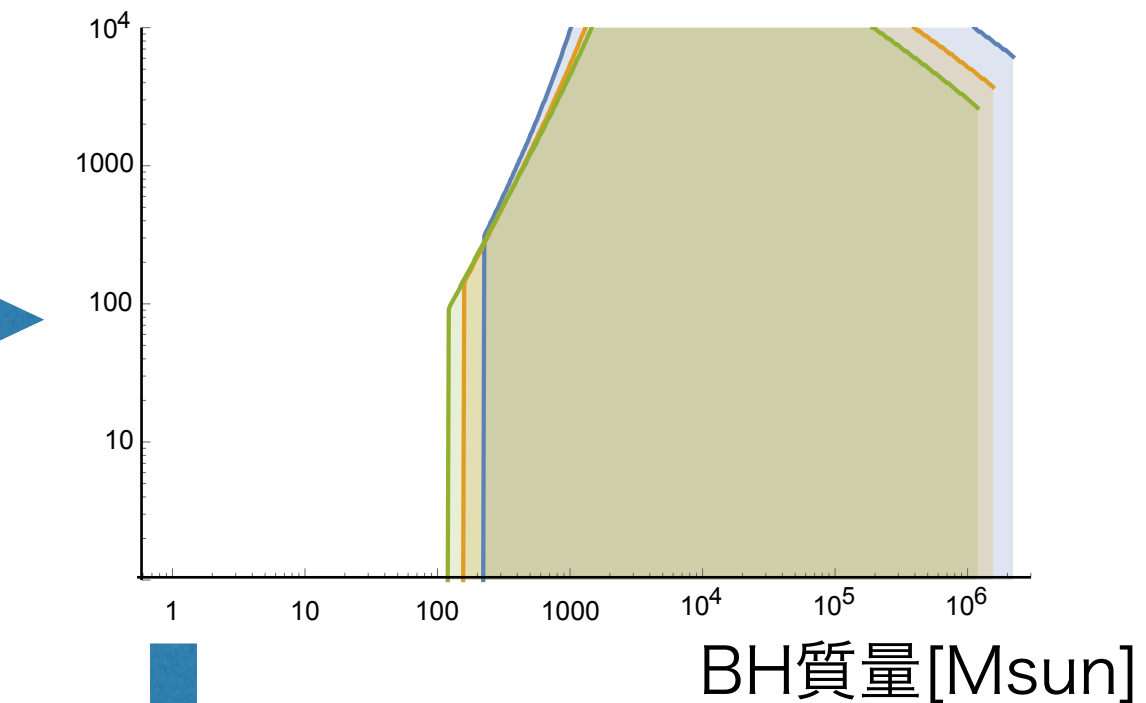
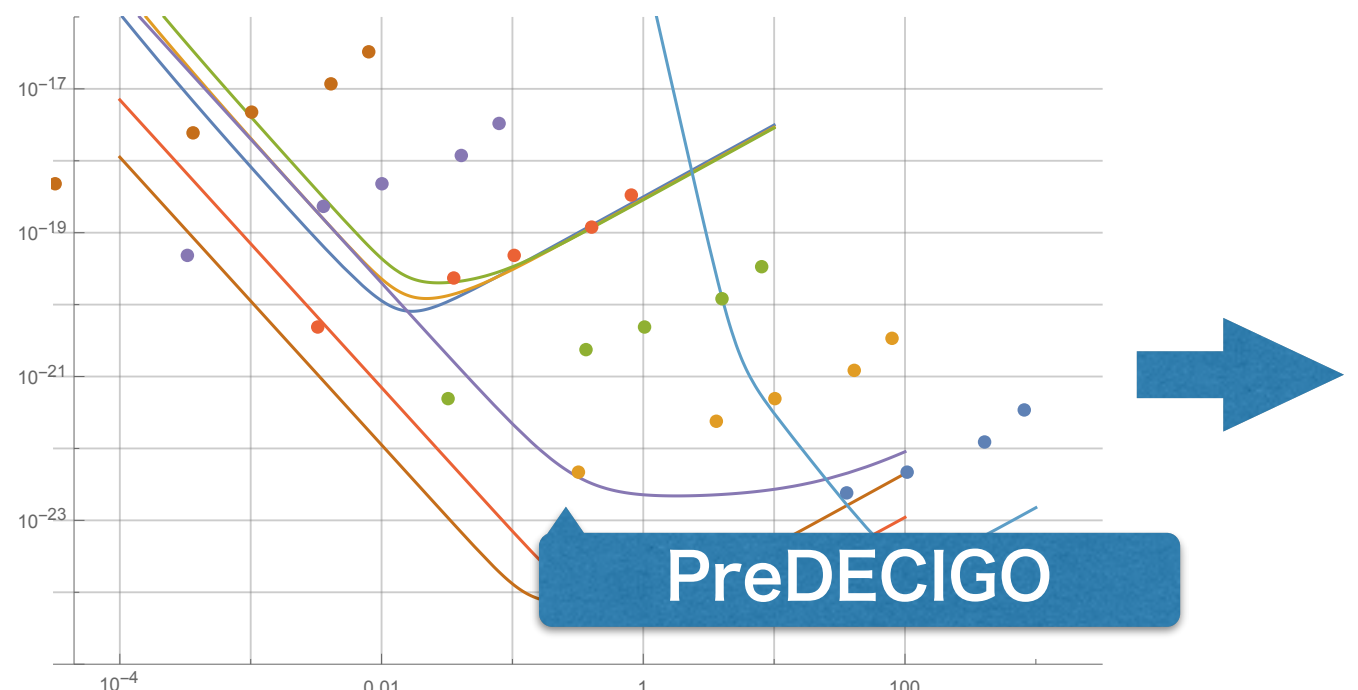


観測できるBH数分布

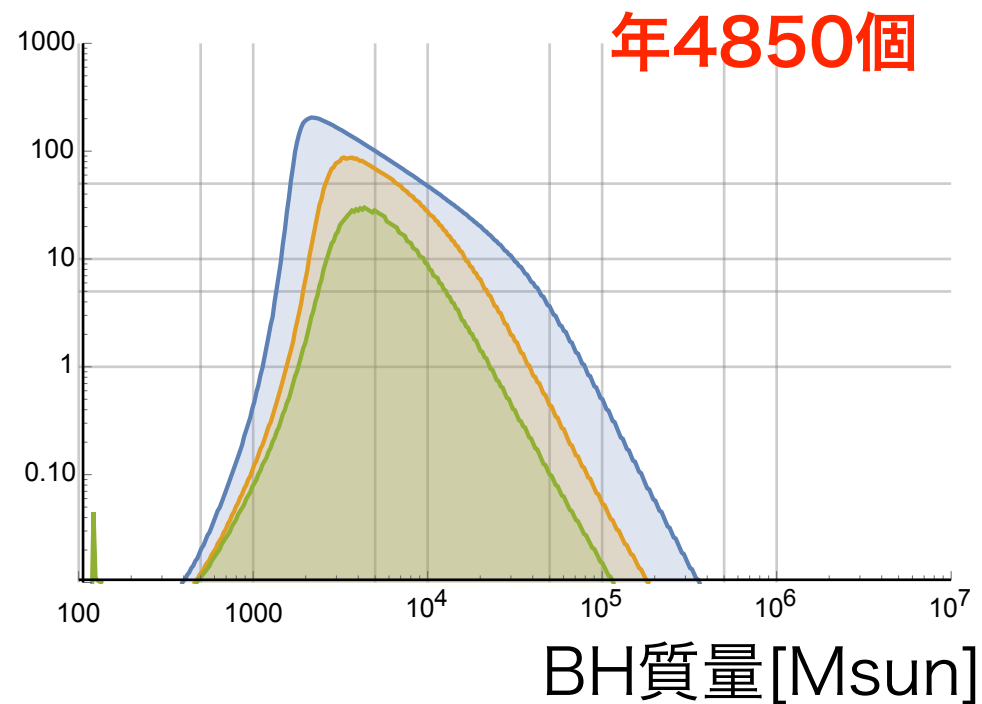


Event Rates at PreDECIGO

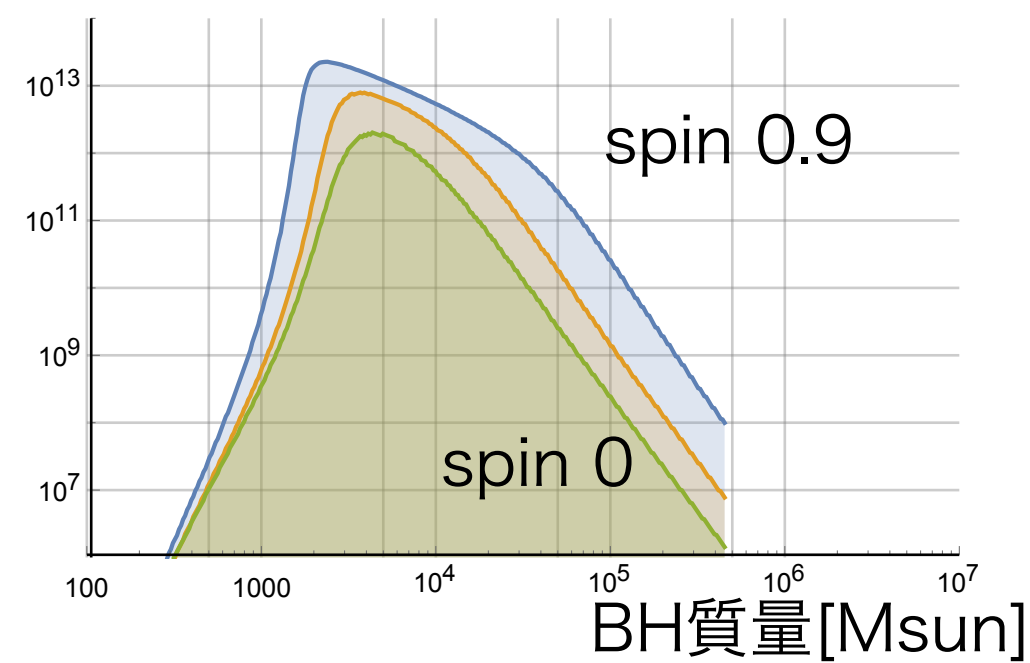
観測できるBH合体距離
[Mpc] (S/N=30)



1年間で観測できるBH数分布
(S/N=30)



観測できるBH数分布



まとめ

SMBHの形成シナリオとして、IMBHsの合体を経由するボトムアップシナリオを仮定して、重力波検出頻度を計算した。

モデルの仮定：

分子雲のコアが $10M_{\odot}$ 以上になったら、BHになると仮定した。

BHは等質量同士のものが次々に合体して成長していくものと仮定した。

BHが形成された後、ガス降着で太ることは考慮していない。

銀河数分布は、サブハロー モデルと、星形成率を乗じたものから計算した。

SMBHは、宇宙初期のガスのdirect collapseによって生じたという説もあるが、そのような形成仮定があれば、このモデルで得た検出頻度は減る。

リングダウン部分の重力波を直接検出できる、と仮定した。

重力波検出のデータを蓄積することによって、銀河分布やSMBH形成シナリオを特定したり、宇宙膨張モデルの検証や、重力理論の検証が可能になる。